University of Windsor
Scholarship at UWindsor

Electronic Theses and Dissertations

1984

Static and dynamic analysis of sandwich beams.

Darwis. Darmali
University of Windsor

Follow this and additional works at: http://scholar.uwindsor.ca/etd

Recommended Citation
Darmali, Darwis., "Static and dynamic analysis of sandwich beams." (1984). *Electronic Theses and Dissertations.* Paper 3576.

This online database contains the full-text of PhD dissertations and Masters' theses of University of Windsor students from 1954 forward. These documents are made available for personal study and research purposes only, in accordance with the Canadian Copyright Act and the Creative Commons license—CC BY-NC-ND (Attribution, Non-Commercial, No Derivative Works). Under this license, works must always be attributed to the copyright holder (original author), cannot be used for any commercial purposes, and may not be altered. Any other use would require the permission of the copyright holder. Students may inquire about withdrawing their dissertation and/or thesis from this database. For additional inquiries, please contact the repository administrator via email (scholarship@uwindsor.ca) or by telephone at 519-253-3000ext. 3208.

National Library of Canada
Canadian Theses Service
Ottawa, Canada
K1A 0N4

Bibliothèque nationale du Canada
Services des thèses canadiennes

CANADIAN THESES

THÈSES CANADIENNES

NOTICE

The quality of this microfiche is heavily dependent upon the quality of the original thesis submitted for microfilming. Every effort has been made to ensure the highest quality of reproduction possible.

If pages are missing, contact the university which granted the degree.

Some pages may have indistinct print especially if the original pages were typed with a poor typewriter ribbon or if the university sent us an inferior photocopy.

Previously copyrighted materials (journal articles, published tests, etc.) are not filmed.

Reproduction in full or in part of this film is governed by the Canadian Copyright Act, R.S.C. 1970, c. C-30. Please read the authorization forms which accompany this thesis.

AVIS

La qualité de cette microfiche dépend grandement de la qualité de la thèse soumise au microfilmage. Nous avons tout fait pour assurer une qualité supérieure de reproduction.

S'il manque des pages, veuillez communiquer avec l'université qui a conféré le grade.

La qualité d'impression de certaines pages peut laisser à désirer, surtout si les pages originales ont été dactylographiées à l'aide d'un ruban usé ou si l'université nous a fait parvenir une photocopie de qualité inférieure.

Les documents qui font déjà l'objet d'un droit d'auteur (articles de revue, examens publiés, etc.) ne sont pas microfilmés.

La reproduction, même partielle, de ce microfilm est soumise à la Loi canadienne sur le droit d'auteur, SRC 1970, c. C-30. Veuillez prendre connaissance des formules d'autorisation qui accompagnent cette thèse.

THIS DISSERTATION
HAS BEEN MICROFILMED
EXACTLY AS RECEIVED

LA THÈSE A ÉTÉ
MICROFILMÉE TELLE QUE
NOUS L'AVONS REÇUE

Canada

STATIC AND DYNAMIC ANALYSIS OF SANDWICH BEAMS

by

Darwis Darmali

A Thesis
submitted to the Faculty of Graduate Studies through the
Department of Civil Engineering in Partial Fulfillment
of the requirements for the Degree of
Master of Applied Science at
The University of Windsor

Windsor, Ontario, Canada

© 1984

STATIC AND DYNAMIC ANALYSIS OF SANDWICH BEAMS

ABSTRACT

by

DARWIS DARMALI

The finite element technique is applied to the analysis of sandwich beams, including circular arches. Finite displacement formulations are developed and incorporated for geometric nonlinear analysis. Material nonlinearities are included for sandwich beams with faces having nonlinear stress-strain behaviour. Appropriate tangent moduli are used in the stress-strain relations of the faces and a combined iterative-incremental method is employed to predict strains in the faces. The dynamic formulation is limited to normal mode analysis, and natural frequencies are based on linearized strain-displacement relations.

The displacement functions necessary for describing the behaviour of the sandwich beams are represented by Oscullatory (first order Hermite) interpolation formulae. The Fletcher-Powell method is used as the algorithmic tool used to minimize the total potential energy. The static formulation is presented in terms of displacements, geometry and various stiffness constants associated with faces and core. The dynamic analysis is formulated in terms of various inertia constants for the faces and core together with the displacements and

geometry. Several numerical examples are presented to illustrate the potential and efficacy of the present analysis. In addition to the various references cited from published literature adopted for comparison, experimental studies were carried out on nine sandwich beams.

ACKNOWLEDGEMENTS

The author would like to express his sincere thanks and appreciation to Dr. G. R. Monforton, who as thesis advisor provided his suggestions and guidance in the completion of this project.

The author appreciates greatly the financial assistance provided during the study period (Grant No. A4126) by the Natural Science and Engineering Research Council of Canada.

Further acknowledgement is extended to Mr. Frank Kiss, technician in the Civil Engineering Laboratories at the University of Windsor, for his assistance in conducting the experiments.

Thanks are also due to Mrs. Zeleney for her patience and cooperation in typing this manuscript.

TABLE OF CONTENTS

ABSTRACT iii

ACKNOWLEDGEMENTS v

LIST OF SYMBOLS viii

LIST OF FIGURES xiii

LIST OF TABLES xv

CHAPTER

I. INTRODUCTION 1

1.1 Literature Review 3
1.2 Purpose and Scope 7

II. GENERAL FORMULATION 10

2.1 General 10
2.2 Face Considerations 10
2.2.1 Strain Energy 12
2.2.2 Kinetic Energy 13
2.3 Core Considerations 14
2.3.1 Strain Energy 16
2.3.2 Kinetic Energy 17
2.4 Potential Energy of the Applied Loads 17

III. DISCRETIZED FORMULATION 19

3.1 General 19
3.2 Discretized Strain Energy 21
3.3 Discretized Kinetic Energy 25
3.4 Gradient Vector for the Discretized Element . . 26

IV. METHOD OF ANALYSIS 31

4.1 General 31
4.2 Principle of Minimum Total Potential Energy . . 31
4.3 Fletcher-Powell Method 33
4.4 Hamilton's Principle 35
4.5 Combined Iterative-Incremental Method 36

V. IMPLEMENTATION AND NUMERICAL EVALUATION 38

5.1 General 38
5.2 Theoretical Comparisons 39
5.2.1 Example of Static Analysis 39

5.2.2 Example of Dynamic Analysis. 46
5.3 Experimental Programs. 48
5.3.1 Experimental Study of the Core Transverse Shear Modulus 49
5.3.2 Experimental Study of Simply Supported Sandwich Beams 51
5.4 Numerical Example on Fully Clamped Beam Under Bending 56

VI. SUMMARY, CONCLUSIONS AND RECOMMENDATIONS 59
6.1 Summary. 59
6.2 Conclusions. 60
6.3 Recommendations. 61

FIGURES 64

TABLES. 106

REFERENCES. 112

APPENDIX A. STIFFNESS AND INERTIA CONSTANTS OF SANDWICH BEAMS. . 117

A.1 Constitutive Equation 117
A.2 Force-Deformation Relations 120
A.3 Inertia Constants 121

APPENDIX B. STIFFNESS AND MASS MATRICES FOR CURVED SANDWICH BEAMS 124

VITA AUCTORIS 151

LIST OF SYMBOLS

a,b	length and width of the element, respectively
A,B,D	total membrane, coupling and bending stiffnesses of faces, respectively
A_f,B_f,D_f	membrane, coupling and bending stiffnesses of faces, respectively
$[A]$	transformation matrix
B_c	core transverse shear stiffness
c	subscript, identifying core
d	number of degrees of freedom of the assembled structure
E	modulus of elasticity
$E_{11}^{(k)}$, $E_{22}^{(k)}$	elastic moduli of the kth lamina
$\vec{e}_x,\vec{e}_n$	unit vectors in coordinate directions
f	subscript, identifying bottom and top faces (f=1,2)
G_c	core transverse shear moduli
G	face transverse shear moduli
K	symmetric positive definite matrix
$k_{ij}^{(2)}$, $k_{ij}^{(3)}$, $k_{ij}^{(4)}$	elements of stiffness matrices which involve quadratic, cubic and quartic contribution to the element strain energy, respectively
$[K^{(2)}]$, $[K^{(3)}]$, $[K^{(4)}]$	stiffness matrices which involve quadratic, cubic and quartic contribution to the element strain energy, respectively

$[\bar{K}^{(2)}]$	master stiffness matrix for assembled structure
L	total Lagrangian function; also denoting length of beam
l	step length along the direction $\vec{s}$
M_f	face moment resultant
$m_{ij}^{(2)}$	elements of mass matrix associated with quadratic contribution to the element kinetic energy
$\bar{M}_f$	applied moment on faces
$[M^{(2)}]$	mass matrix associated with quadratic contribution to the element kinetic energy
$[\bar{M}^{(2)}]$	master mass matrix for assembled structure
n	number of elements comprising the assembled structure
N_f	face longitudinal force resultant
$\bar{N}_f$	applied longitudinal force on faces
p,q	subscripts, denoting the end nodes of the element
$[P]$	work equivalent load vector
Q_s, J_s, I_s	translatory, rotary and coupling inertia constants for faces (s=f=1,2) and core (s=c)
R_s	principal radii of curvature for faces (s=f=1,2) and core (s=c)
s	subscript, identifying bottom and top faces (s=f=1,2) and core (s=c)
S_s	cross-sectional area of faces (s=f=1,2) and core (s=c)
$S_x(z_f), S_y(z_f), S_{xy}(z_f)$	depth dependent elastic constants for faces of the beam

$S_{ij}^{(k)}$	elastic constants in stress strain law for the kth lamina
$[S(z_f)]$	array of depth dependent elastic constants for face
$[S^{(k)}]$	matrix contains the elastic constants associated with the kth lamina
$\vec{s}$	conjugate direction
T_s	kinetic energy of faces (s=f=1,2) and core (s=c)
t_s	thickness of faces (s=f=1,2) and core (s=c)
$[T_\sigma^{(k)}]$	stress transformation matrix for kth lamina
$[T_\epsilon^{(k)}]$	strain transformation matrix for kth lamina
u_s, w_s	displacement components of reference axis for faces (s=f=1,2) and core (s=c)
$\tilde{u}_s, \tilde{w}_s$	displacement components of a point at distance z_s from reference axis for faces (s=f=1,2) and core (s=c)
U_s	strain energy of faces (s=f=1,2) and core (s=c)
$U_f^{(2)}$, $U_f^{(3)}$, $U_f^{(4)}$	face strain energy which involve quadratic, cubic and quartic terms in the displacement variables, respectively
V_s	transverse shear force resultants for faces (s=f=1,2) and core (s=c)
V_x	shear force between face and core
$\overline{V}_f$	applied transverse forces on faces
W_f	potential of applied loads
x_s	longitudinal axis of faces (s=f=1,2) and core (s=c)

$\{X\}$	vector of element generalized displacements
$\{\bar{X}\}$	vector of independent degrees of freedom
$\{\vec{X}_i\}$	vector of independent degrees of freedom in ith iteration
z_s	distance measured perpendicular to the reference axis of faces (s=f=1,2) and core (s=c)
$\{Z\}$	vector of the 10 possible multiples of the 4 degrees of freedom associated with w
$\sigma_{fx}, \sigma_{fy}, \tau_{fxy}$	normal and shear stresses of faces
$\sigma_1^{(k)}, \sigma_2^{(k)}, \tau_{12}^{(k)}, \sigma_x^{(k)}, \sigma_y^{(k)}, \tau_{xy}^{(k)}$	normal and shear stresses of the kth lamina
$\{\sigma_{fxy}\}$	vector of stresses for faces
$\{\sigma_{12}^{(k)}\}, \{\sigma_{xy}^{(k)}\}$	vector of stresses for the kth lamina
$\varepsilon_{fx}, \varepsilon_{fy}, \gamma_{fxy}$	normal and shear strains of faces
$\varepsilon_1^{(k)}, \varepsilon_2^{(k)}, \gamma_{12}^{(k)}, \varepsilon_x^{(k)}, \varepsilon_y^{(k)}, \gamma_{xy}^{(k)}$	normal and shear strains of the kth lamina
$\{\varepsilon_{fxy}\}$	vector of strains for faces
$\{\varepsilon_{12}^{(k)}\}, \{\varepsilon_{xy}^{(k)}\}$	vector of strains for the kth lamina

τ_c	core transverse shear stress
γ_c	core transverse shear strain
δ	deflection
ϕ_s	rotation of normal to reference axis for face (s=f=1,2) and core (s=c)
$\{\nabla T^{(2)}\}$	gradient vector associated with quadratic contribution to the kinetic energy with respect to vector {X}
$\{\nabla U^{(2)}\},\{\nabla U^{(3)}\},$ $\{\nabla U^{(4)}\}$	gradient vectors associated with quadratic, cubic and quartic contribution to the strain energy with respect to vector {X}
$\{\nabla \tilde{U}^{(4)}\}$	gradient vector associated with quadratic contribution to the strain energy with respect to vector {Z}
$\{\nabla \hat{U}^{(4)}\}$	gradient vector associated with quadratic contribution to the strain energy with respect to four transverse displacement variables
$\theta^{(k)}$	angle between principal axis (1,2) and reference axis (x,y) for kth lamina
Π_p	total potential energy
$\nabla\Pi_p$	gradient vector of total potential energy
ρ_s	mass density of faces (s=f=1,2) and core (s=c)
$\vec{\Delta}_f$	displacement vector for faces
ν	Poisson's ratio
ω	natural frequency
$\xi_1,\vec{\xi}_2,\xi_3$	absolute error value defining the terminating criterion in the minimization

LIST OF FIGURES

Figure		Page
1.	Anisotropic Sandwich Elements.	64
2.	Deformation of Sandwich Beam	65
3.	Sandwich Beam Stress Resultants.	66
4.	Stress-Strain Curve of Aluminium	67
5.	Example of Iterative-Incremental Method.	68
6.	Sandwich Beam with Overhang.	69
7.	Deflection of a Cantilever Sandwich Beam	70
8.	Variation of Deflection with Core Thickness.	71
9.	Variation of Deflection with Span Length	72
10.	Variation of Stiffness with Faceplate Thickness.	73
11.	Displacements of Sandwich Arch	74
12.	Sandwich Arch Element After Holt [9]	74
13.	Straight and Curved Sandwich Beams	75
14.	Block Shear Tests.	76
15.	Three-Point Test of Polystyrene Sandwich Beam (Typical for Beams T1, T2, T3 and T4)	77
16.	Four-point Test of Polystyrene Sandwich Beam (Beam T5) .	78
17.	Six-Point Test of Polystyrene Sandwich Team (Beam T6).	79
18.	Load-Deflection Curve of the Sandwich Beam T1.	80
19.	Load-Deflection Curve of the Sandwich Beam T2.	81
20.	Load-Deflection Curve of the Sandwich Beam T3.	82
21.	Load-Strain Curve of the Sandwich Beam T3.	83
22.	Load-Deflection Curve of the Sandwich Beam T4.	84

23. Load-Strain Curve of the Sandwich Beam T4. 85

24. Load-Deflection Curve of the Sandwich Beam T5. 86

25. Load-Deflection Curve of the Sandwich Beam T6. 87

26. Load-Strain Curve of the Sandwich Beam T6. 88

27. Wrinkling Failure - Specimen T5. 89

28. Local Failure - Specimen T6. 90

29. Three-Point Test of Polystyrene Sandwich Beam with Stiffeners (Typical for Beams T7, T8 and T9). 91

30. Typical Stiffeners Used at Loading and Support Points. . . 92

31. Load-Deflection Curve of the Sandwich Beam T7. 93

32. Load-Strain Curve of the Sandwich Beam T7. 94

33. Delaminating Failure - Specimen T7 95

34. Load-Deflection Curve of the Sandwich Beam T8. 96

35. Load-Strain Curve of the Sandwich Beam T8. 97

36. Delaminating Failure - Specimen T8 98

37. Load-Deflection Curve of the Sandwich Beam T9. 99

38. Load-Strain Curve of the Sandwich Beam T9. 100

39. Delaminating Failure - Specimen T9 101

40. Clamped Sandwich Beam with Unequal Face Thicknesses. . . . 102

41. Load-Deflection Curve of Clamped Sandwich Beam 103

42. Laminated Face 104

LIST OF TABLES

Table		Page
1.	Stiffnesses of a Sandwich Beam with Thick Laminated Faces.	106
2.	Deflections of a Sandwich Beam with Thick Laminated Faces.	107
3.	Natural Frequencies (HZ) of a Straight, Simply Supported Sandwich Beam.	108
4.	Natural Frequencies (HZ) of a Straight, Cantilever Sandwich Beam.	109
5.	Natural Frequencies (HZ) of a Curved, Clamped-Clamped Sandwich Beam.	110

CHAPTER I

INTRODUCTION

Sandwich beams are composed of two thin high-strength faces bonded to a thick low-strength and light-weight core. The faces are usually separated in order to get a high section modulus for the sandwich beams. The core must keep the faces apart to the correct distance and must not allow the faces to slide over the core; it supports the faces and transmits the shear stresses allowing them to effectively function as a unit. The faces are primarily responsible for carrying the membrane forces while the core is used for carrying nearly all the transverse shear load. The core is usually relatively weak and as such the effects of transverse shear deformation is considerable. The substantial interest in sandwich structures is mainly for its high strength to weight ratio. Other important advantages are good heat and acoustic insulation, effective vibration absorption and ease of construction installation.

Many core materials are available for sandwich constructions. Balsawood is one of the popular core materials; this core material has grains oriented perpendicular to the faces and is used mainly for its effectiveness in preventing local compression failure, particularly in the vicinity of concentrated loads and at supports point.

Expanded synthetic plastics such as polystyrene, polyurethane, phenolic and polyvinyl chloride have been used in semi-structural building panels primarily for their good insulation properties. More satisfactory cores such as the honeycomb geometry, produced from aluminium, steel, titanium, nickel-chromium and reinforced plastic, have been a popular core material especially in the aircraft industry.

For faces there are aluminium alloys, glass-reinforced plastics, steel, titanium, plywood and other suitable materials. The faces of the sandwich beams may be composed of several bonded layers. The laminated faces considered can be isotropic, anisotropic and transversely heterogeneous. Some composite materials faces have been developed from glass-reinforced plastics, boron, graphite and metal fibers. Laminated materials are designed to increase the structural efficiency. Unbalanced laminated faces such as unsymmetric cross-plied and angle-plied laminates have received considerable attention; in these type of laminations, there exist coupling action between longitudinal stretching and transverse bending in the faces which may affect the displacements and stresses of the sandwich beams considerably. With the rapidly growing importance of composite materials, analysis techniques and new materials are constantly being developed.

In the present work, the finite element technique based on the principle of minimum total potential energy is employed for the analysis of sandwich beams, including arches. The developed formulation involves geometric nonlinearities and nonlinear material

behaviour of the faces. In addition to the study of static problems, the present work also considers normal mode dynamic analysis.

1.1 Literature Review

Many investigations on the analysis of sandwich structures have been done. Hoff and Mautner (Ref. 1) presented the formulations for sandwich beams based on the principal of virtual displacements. It was assumed that the face-parallel extension stresses in the core and the shear stresses of the faces were negligible. The longitudinal and bending stresses in the faces as well as the transverse shear stresses and extension stresses perpendicular to the plane of the faces in the core were included in the formulation. The theoretical solutions were found to compare favourably with the experimental results. Formulations derived in Ref. 1, however, were restricted to sandwich beams with thin faces. Formulations for sandwich structures with no restriction with regard to the material properties and thicknesses of faces and core have been considered by a number of investigators including Yu (Ref. 2), Krajcinovic (Ref. 3 and 4); in these papers, the effects of shear deformation and normal stresses in both the faces and cores were accounted for. A more classical approach has been presented by Ogorkiewicz and Sayigh (Ref. 5, 6 and 7) for analyzing the sandwich beams with various combination of faces and core materials under various loading conditions. Equations for deflection were formulated by transforming the actual sandwich section into an equivalent section of face material; the core material was transformed into a thin web

of equivalent moment of inertia and having material properties the same as the faces. A number of investigators including Holt and Webber (Ref. 8 and 9), Abel (Ref. 10) and Reissner (Ref. 11) have reported on the theory of sandwich arches. Holt and Webber (Ref. 9) developed a formulation based on the assumed stress hybrid and equilibrium methods. Simpler formulations were developed with the assumption that faces act only as membranes and that the core is incompressible in the transverse direction. In all the above cases the sandwich structures were restricted to small deflection theory assumptions.

Some studies have been made on the geometric nonlinear analysis of sandwich structures. Reissner (Ref. 12) presented the exact analysis of sandwich plates consisting of a core and of two faces such that the face-parallel extension stresses in the core and the variation of the face stresses over the face thickness were negligible. The effect of extension stresses perpendicular to the plane of the faces in the core was included but was found to be negligibly small as compared to the core transverse shear stresses effect. In the above report (Ref. 12) both the faces and core of the sandwich plate were assumed to be isotropic. Alwan (Ref. 13) reported the finite deflection of sandwich plate with orthotropic core of honeycomb geometry. The same assumptions as in Ref. 12 were adopted except that the core transverse normal stresses effect was neglected. Kan and Huang (Ref. 14) presented the geometric nonlinear analysis of a rectangular clamped sandwich plate under uniform load using a method of successive approximations.

A geometric nonlinear formulation for a simply supported sandwich beam has been presented by Zahn (Ref. 15). The formulation include a nonlinear term in the face equilibrium equations. The core equilibrium equation was formulated in terms of four infinite sequences and integrating constants which remain the same as the linear case. The equations were then combined to give one resulting nonlinear differential equation for the displacement; the matching of the continuity of strains and displacements at the interfaces of core and faces were then solved by Fourier analysis. Finally, the numerical solutions were obtained by successive approximations. According to Zahn, the behaviour of simply supported sandwich beams, as compared to linear analysis, show negligible differences in face stresses and deflections but considerable correction to core compressive stresses. Zahn suggested that in the case of simply supported sandwich beams, the inelastic action would be of more importance.

Ditcher (Ref. 16) seemed to be aware of the importance of including the nonlinear stress-strain behaviour of faces in the formulation; he presented a theoretical analysis of a honeycomb sandwich beam with laminated faces having nonlinear material properties but without taking into account geometric nonlinearity. The formulation for the faces involves the use of the appropriate tangent moduli for each load increment and a double iteration method was employed to calculate the strains in the faces. In his paper, the study of flexural wrinkling of sandwich beam was emphasized in that this failure criterion was incorporated in the formulation to predict the failure loads.

Numerous papers have been published on the natural vibration of sandwich structures. Raville, Ueng and Lei (Ref. 17) presented the dynamic formulation to determine the natural frequencies of clamped-clamped sandwich beams based on the energy approach. The boundary conditions of the clamped beams were satisfied by utilizing the Lagrangian multiplier method. The faces were assumed to be isotropic thin skins and the core was considered to be orthotropic. It was assumed that the face-parallel extension stresses as well as the transverse normal stresses in the core were negligible. The experimental results were found to be in good agreement as compared to the theoretical solutions. A series of papers by Ahmed (Ref. 18, 19 and 20) dealt with the natural vibration of sandwich structures with various boundary conditions. Ahmed (Ref. 18) formulated the equilibrium equations of sandwich beams including arches which result in fourth-order differential equations; the analysis was based on the Kirchhoff-Love hypothesis. The faces of the sandwich beam were assumed to be stiff in bending about their own middle axis, consequently, the strain energy of the faces is appreciable when compared to the total energy of the sandwich beam and thereby included in the energy formulation. A further analysis (Ref. 19) was based on a Wang-type model in which the effect of transverse shear deformation is included in the finite element formulation. In this case, the equilibrium equations are a set of second-order differential equations. Unlike the previous analysis (Ref. 18) which employed four degrees of freedom per node, the formulation reported in Ref. 19 had six degrees of freedom per node.

The natural frequencies of cantilever sandwich beams was presented by Rubayi and Charoenree (Ref. 21) using the method of minimizing the total energy of the sandwich system. Other investigators such as Rutenberg (Ref. 22) presented a simple and yet accurate approximation formula for the natural frequencies of sandwich beams and arches under various boundary conditions.

1.2 Purpose and Scope

The finite element capability for predicting displacements, strains and natural frequencies of sandwich beams, including arches, is developed in the following chapters. The faces of the sandwich beams may be laminated. The core is considered to be relatively thick as compared to the faces and relatively weak such that the effects of transverse shear deformation is predominant. Using nonlinear strain-displacement relations, a finite displacement formulation is developed for geometric nonlinear analysis. The material nonlinearity is also included in that the nonlinear stress-strain behaviour of the faces is represented by a piecewise linear curve. Appropriate tangent moduli are used in the face stress-strain relations and a combined iterative-incremental scheme is employed to predict strains in the faces. In addition, the effect of including the nonlinear strain-displacement relation within the material nonlinear analysis has also been studied. A curvilinear coordinate system is introduced to describe the geometry in the case of sandwich arches.

Chapter II presents the general formulation of the potential and kinetic energy for the sandwich systems. The potential energy is

formulated in terms of the displacements, geometry, the stiffness constants of the faces (membrane, bending and coupling) and core (transverse shear). The kinetic energy formulation includes the translatory, rotary and coupling effects associated with the faces and core. The potential of the applied loads can be represented by a work equivalent loading system. The formulation presented neglects the shear stresses of the faces, the transverse normal stresses of the faces and core as well as the longitudinal extension stresses of the core.

Chapter III contains the discretized formulation for the potential and kinetic energy for the sandwich systems. The gradient vectors for the element strain and kinetic energy are also presented. Oscullatory interpolation formulas are selected as the displacement functions to describe the behaviour of the sandwich beam. The dynamic formulation is limited to normal mode analysis and only strain energy based on linearized strain-displacement relation is included. The discretized formulation involves twelve generalized displacements in each element.

Chapter IV presents the energy search method employed to arrive at the solutions for the sandwich beams. The Fletcher-Powell method is used as the optimization technique to minimize the total potential energy. The combined iterative-incremental procedure necessary for material nonlinear analysis is also explained. Hamilton's principle is introduced as the concept used for the dynamic solutions.

Chapter V focuses on the implementation and numerical evaluation

of the finite element method. Several numerical examples, static and dynamic, are solved and compared with other theoretical solutions and experimental results in order to demonstrate the capability and efficacy of the present analysis. Experimental studies on sandwich beams have been carried out and the results are compared with the theoretical solutions. All of the solutions are solved by direct minimization of the total potential energy using a variable metric method. The FORTRAN IV compiler and IBM 3031 digital computer are used to obtain the solutions.

Chapter VI summarizes the work and conclusions are drawn on the potential of the present analysis. Some observations and recommendations are made with respect to the experimental investigation for future research work.

CHAPTER II

GENERAL FORMULATION

2.1 General

In this chapter the general formulations necessary for the analysis of the sandwich beams are presented. Expressions for the strain energy, the kinetic energy and the potential energy of the applied loads are obtained and employed for the implementation of the function minimization technique.

A typical portion of the sandwich element is shown in Fig. 1. The general subscript, s(1,2,c), is used to identify the bottom face, top face and core. Meanwhile, the subscript, f(1,2), is used when special attention is focused on the bottom and top faces. The thickness and principal radii of curvature are denoted by t_s and R_s respectively. The reference axis of the faces (x_1,x_2) and core (x_c) are the centroidal axes shown in Fig. 1.

2.2 Face Considerations

The assumptions made for the faces are as follows:

1. the transverse deflection w is constant throughout the face thickness:

$$\tilde{w}_f(x,z_f) = w(x) \tag{2.1}$$

2. the face behaves as a beam so that the displacement of a point at distance z_f from the face reference axis varies

linearly across the face thickness:

$$\tilde{u}_f(x, z_f) = u_f(x) + z_f \phi_f(x) \tag{2.2a}$$

where

$$\phi_f(x) = \frac{-\partial w}{\partial x} + \frac{u_f}{R_f} \quad \text{for arch} \tag{2.2b}$$

$$\phi_f(x) = \frac{-\partial w}{\partial x} \quad \text{for beam} \tag{2.2c}$$

z_f represents the distance measured perpendicular to the reference axis of the face while u_f and $\frac{\partial w}{\partial x}$ represent the longitudinal displacement and slope of the face reference axis. The typical deformation of the sandwich beam element is shown in Fig. 2.

3. the thickness of the face is small compared to the radii of curvature.

Using the above assumptions, the strain-displacement relation is expressed as:

$$\epsilon_f = u_{xf} + \frac{w}{R_f} + \frac{1}{2}(w_x)^2 + z_f\left(\frac{u_{xf}}{R_f} - w_{xx}\right) \tag{2.3}$$

where

$$u_{xf} = \frac{\partial u_f}{\partial x}, \; w_x = \frac{\partial w}{\partial x} \text{ and } w_{xx} = \frac{\partial^2 w}{\partial x^2}$$

From Appendix A, the constitutive equation for the faces is defined as

$$\sigma_f = S_x(z_f)\epsilon_f \tag{2.4}$$

where σ_f, ϵ_f and $S_x(z_f)$ represent the faces longitudinal stress, strain and elastic modulus. $S_x(z_f)$ is given in Appendix A (Eqs. A.7).

The force and moment-deformation relations are expressed as (Appendix A):

$$N_f = A_f[u_{xf} + \frac{w}{R_f} + \frac{1}{2}(w_x)^2] + B_f[\frac{u_{xf}}{R_f} - w_{xx}] \tag{2.5a}$$

$$M_f = B_f[u_{xf} + \frac{w}{R_f} + \frac{1}{2}(w_x)^2] + D_f[\frac{u_{xf}}{R_f} - w_{xx}] \tag{2.5b}$$

where A_f, B_f and D_f represent the membrane, coupling and bending stiffnesses of the faces respectively and are given in Appendix A (Eqs. A.10).

2.2.1 Strain Energy

The strain energy of a face is expressible as

$$U_f = \frac{b}{2}\iint_{S_f} \epsilon_f \sigma_f \, dx \, dz_f \tag{2.6}$$

where b and S_f are the width and cross-sectional area of the faces respectively. Substituting the strain-displacement relation (Eq. 2.3) and constitutive equation (Eq. 2.4) into Eq. 2.6, the resulting expression for the strain energy after integrating over the total thickness of the faces in terms of the longitudinal displacements u_f, the transverse displacement w, the principal radii of curvatures R_f and the stiffnesses A_f, B_f and D_f can be written as:

$$U_f = \frac{1}{2} \int_{x_f} \{[A_f u_{xf}^2 + D_f w_{xx}^2 - 2B_f u_{xf} w_{xx} + \frac{1}{R_f}(\frac{A_f}{R_f} w^2 + 2\langle A_f + \frac{B_f}{R_f}\rangle w\, u_{xf}$$

$$+ \langle \frac{D_f}{R_f} + 2B_f \rangle u_{xf}^2 - 2B_f w\, w_{xx} - 2 D_f u_{xf} w_{xx})] + [A_f u_{xf} w_x^2 - B_f w_{xx} w_x^2$$

$$+ \frac{1}{R_f}(A_f w\, w_x^2 + B_f u_{xf} w_x^2)] + [\frac{1}{4} A_f w_x^4]\} \, dx \qquad (2.7)$$

where x_f represents the reference axis of the faces. By setting $\frac{1}{R_f} = 0$, the face strain energy for a sandwich beam can be obtained from Eq. 2.7.

2.2.2 Kinetic Energy

The kinetic energy of a face is written as

$$T_f = \frac{b}{2} \iint_{S_f} \rho_f(z_f) \dot{\vec{\Delta}}_f \cdot \dot{\vec{\Delta}}_f \, dx \, dz_f \qquad (2.8)$$

where b, S_f and $\rho_f(z_f)$ are the width, cross-sectional area and mass density of the faces respectively. The displacement vector for the faces is

$$\vec{\Delta}_f = [u_f + z_f (\frac{u_f}{R_f} - w_x)] \vec{e}_x + w \vec{e}_n \qquad (2.9)$$

where $\vec{e}_x$ is a unit vector in the longitudinal direction and $\vec{e}_n$ is a unit vector in the direction normal to the longitudinal axis. After differentiating Eq. 2.9 with respect to time ($\frac{d\vec{\Delta}_f}{dt} = \dot{\vec{\Delta}}_f$) and substituting into Eq. 2.8, the resulting expression for the kinetic energy is

$$\overline{T_f} = \frac{1}{2} \int_{x_f} [Q_f(\dot{u}_f^2 + \dot{w}^2) - \overline{2J_f}\ (\dot{u}_f\langle\dot{w}_x - \frac{\dot{u}_f}{R_f}\rangle)$$

$$+ I_f(\dot{w}_x - \frac{\dot{u}_f}{R_f})^2]\ dx \qquad (2.10)$$

where Q_f, J_f and I_f represent the translatory, rotary and coupling inertia constants of the faces and are given in Appendix A (Eqs. A.11). Also, the kinetic energy of the face for a sandwich beam can be extracted from Eq. 2.10 by simply putting $\frac{1}{R_f} = 0$.

2.3 Core Considerations

The core of the sandwich construction which separates the faces are bonded together so as to effectively function as a unit; it is considered to be relatively thick when compared to the thickness of the faces. The following assumptions are made for the core (see Fig. 2).

1. the core is incompressible so that the transverse deflection w remains constant throughout the core thickness:

$$\bar{w}_c(x,z_c) = \overline{w(x)} \qquad (2.11)$$

2. the displacement of a point at a distance z_c from the core reference axis varies linearly across the core thickness:

$$\bar{u}_c(x,z_c) = u_c(x) + z_c\phi_c(x) \qquad (2.12a)$$

where

$$u_c(x) = \frac{1}{2}[u_1+u_2 - (h_1-h_2)w_x] \qquad (2.12b)$$

$$\phi_c(x) = -\frac{1}{t_c}[u_1 - u_2 - (h_1+h_2)w_x] \tag{2.12c}$$

$$h_1 = \frac{t_1}{2}\frac{R_c}{R_1} \text{ and } h_2 = \frac{t_2 R_c}{2R_2} \text{ for arch} \tag{2.12d}$$

$$h_1 = \frac{t_1}{2} \text{ and } h_2 = \frac{t_2}{2} \text{ for beam} \tag{2.12e}$$

Z_c represents the distance measured perpendicular to the reference axis of the core while u_c represents the longitudinal displacement of the core.

3. the longitudinal extension stresses are negligibly small as compared to the transverse shear stresses.

Employing the above assumptions, the strain-displacement relation is written as

$$\gamma_c = \frac{1}{t_c}[e_2 u_2 - e_1 u_1 + e_3 w_x] \tag{2.13a}$$

where

$$e_1 = 1 + \frac{t_c}{2R_c} \tag{2.13b}$$

$$e_2 = 1 - \frac{t_c}{2R_c} \tag{2.13c}$$

$$e_3 = \frac{t_1}{2}\left(\frac{R_c}{R_1} + \frac{t_c}{2R_1}\right) + \frac{t_2}{2}\left(\frac{R_c}{R_2} - \frac{t_c}{2R_2}\right) + t_c \tag{2.13d}$$

The constitutive relation for the core is expressed as

$$\tau_c = G_c \gamma_c \tag{2.14}$$

where τ_c, γ_c and G_c represent core transverse shear stress, strain

and moduli respectively.

The transverse shear force resultant is written as

$$V_c = b \int_{-\frac{t_c}{2}}^{\frac{t_c}{2}} \tau_c \, dz_c \tag{2.15a}$$

or

$$V_c = (bG_c t_c)\gamma_c = B_c \gamma_c \tag{2.15b}$$

where B_c is defined as the core transverse shear stiffness.

2.3.1 Strain Energy

The strain energy of the core is

$$U_c = \frac{b}{2} \iint_{S_c} \tau_c \gamma_c \, dx \, dz_c \tag{2.16}$$

where b and S_c are the width and cross-sectional area of the core respectively. Substituting Eqs. 2.13 and 2.14 into Eq. 2.16 and integrating over the total thickness of the core, the resulting core strain energy in terms of the displacements u_f and w, the core transverse shear stiffness B_c and the geometry t_s and R_s can be expressed as

$$U_c = \frac{1}{2} \int_{x_c} \left[\frac{B_c}{t_c^2} (e_2 u_2 - e_1 u_1 + e_3 w_x)\right] dx \tag{2.17}$$

where x_c represents the reference axis of the core. e_1, e_2 and e_3 are given in Eqs. 2.13.

2.3.2 Kinetic Energy

Employing a similar approach to that of the faces, the resulting expression for core kinetic energy is

$$T_c = \frac{1}{2} \int_{x_c} [Q_c(\dot{u}_c^2+\dot{w}^2) + 2J_c(\dot{u}_c\dot{\phi}_c) + I_c(\dot{\phi}_c^2)]dx \qquad (2.18)$$

where Q_c, J_c and I_c represent the translatory, rotary and coupling inertia constants of the core and are given in Appendix A (Eqs. A.11). Substituting Eqs. 2.12 into Eq. 2.18 results in the expression for the core kinetic energy in terms of the displacements u_f and w, the geometry t_s and R_s and the inertia constants Q_c, J_c and I_c

$$T_c = \frac{1}{2} \int_{x_c} \{\frac{Q_c}{4} \langle[\dot{u}_1+\dot{u}_2-(h_1-h_2)\dot{w}_x]^2 + 4\,\dot{w}^2\rangle$$

$$- \frac{J_c}{t_c}\langle[\dot{u}_1+\dot{u}_2-(h_1-h_2)\dot{w}_x]\,[\dot{u}_1-\dot{u}_2-(h_1+h_2)\dot{w}_x]\rangle$$

$$+ \frac{I_c}{t_c^2}\langle[\dot{u}_1-\dot{u}_2-(h_1+h_2)\dot{w}_x]^2\rangle\}dx \qquad (2.19)$$

2.4 Potential Energy of the Applied Loads

The potential energy of the applied loads is represented by

$$W_f = \overline{N}_{fp}u_{fp} + \overline{N}_{fq}u_{fq} + \overline{V}_{fp}w_p + \overline{V}_{fq}w_q + \overline{M}_{fp}w_{xp} + \overline{M}_{fq}w_{xq}$$

$$+ \int_x \overline{P}_{fz}(x)w(x)dx \qquad (2.20)$$

where $\overline{N}_f$, $\overline{V}_f$ and $\overline{M}_f$ represent the applied forces and moments acting at the nodes of the faces. $\overline{P}_{fz}(x)$ represents the load distribution

in the direction z. Subscripts p and q are used to denote the end nodes of the sandwich element. The positive sign convention for the force and moment resultants is shown in Fig. 3.

CHAPTER III

DISCRETIZED FORMULATION

3.1 General

In recent years, numerical analysis of various structures by the finite element method has become relatively routine; this method is a computer orientated technique which has the advantage that a minimum of data preparation is required. In the finite element analysis, the structure is subdivided into a finite number of elements by fictitious cuts; displacement patterns are employed independently to each element. By invoking the compatibility conditions, it is possible to link these elements together to form the assembled structure which, in fact, is physically compatible with the actual structure. It is noteworthy, however, that the displacement functions selected will directly effect the accuracy of the finite element method in its ability to simulate the actual structural behaviour. One of the important features of the implemented compatibility conditions is the continuity requirement in the displacement functions; in the case of sandwich beams, the membrane displacement u_f, the transverse deflection w and, if face bending is considered, the slope w_x must be continuous within the element and at the nodal points between elements. The displacement functions employed in the present analysis for describing the longitudinal

displacement u_f and the transverse displacement w are represented by two types of interpolation formulas. They are,

1. Lagrange (zeroth order Hermite) interpolation formulas:

$$u_f(x) = (1 - \frac{x}{a})u_{fp} + (\frac{x}{a})u_{fq} \tag{3.1}$$

$$w(x) = (1 - \frac{x}{a})w_p + (\frac{x}{a})w_q \tag{3.2}$$

2. Oscullatory (first order Hermite) interpolation formulas:

$$u_f(x) = [\frac{1}{a^3}(2x^3-3ax^2+a^3)]u_{fp} + [\frac{1}{a^3}(-2x^3+3ax^2)]u_{fq} + [\frac{1}{a^2}(x^3-2ax^2+a^2x)]u_{xfp} + [\frac{1}{a^2}(x^3-ax^2)]u_{xfq} \tag{3.3}$$

$$w(x) = [\frac{1}{a^3}(2x^3-3ax^2+a^3)]w_p + [\frac{1}{a^3}(-2x^3+3ax^2)]w_q + [\frac{1}{a^2}(x^3-2ax^2+a^2x)]w_{xp} + [\frac{1}{a^2}(x^3-ax^2)]w_{xq} \tag{3.4}$$

Inspection of the Lagrange interpolation formulas (Eqs. 3.1 and 3.2) reveals the fact that interelements continuity is maintained only for longitudinal and transverse displacements but not for longitudinal strain and normal slope; the displacement behaviour, therefore, is not well represented by Lagrange functions since the longitudinal strain and normal slope are assumed to be uniform along the individual

discretized element. The Oscullatory interpolation formulas (Eqs. 3.3 and 3.4) permit satisfaction of the compatibility conditions for the longitudinal and transverse displacements together with their derivatives; the strains of the faces therefore are best predicted based on Oscullatory function. A third type of formulation where longitudinal displacement is represented by a Lagrange function while Oscullatory function is used for the transverse displacement has also been attempted. From numerical experimentation, the results based on the second type of formulation was found to be most accurate for both displacement and strain; it was decided, therefore, to use the second type of formulation for this work.

In the following, the discretized formulation using the Oscullatory displacement functions for the element strain energy and kinetic energy together with their gradient vectors are presented with detailed formulation.

3.2 Discretized Strain Energy

The strain energy of the faces given in Eq. 2.7 can be re-written as

$$U_f = U_f^{(2)} + U_f^{(3)} + U_f^{(4)} \tag{3.5}$$

where $U_f^{(2)}$, $U_f^{(3)}$ and $U_f^{(4)}$ are the face strain energy which involve quadratic, cubic and quartic terms in the displacement variables, respectively. $U_f^{(2)}$, $U_f^{(3)}$ and $U_f^{(4)}$ are expressed as

$$U_f^{(2)} = \frac{1}{2}\int_{x_f} \{A_f u_{xf}^2 + D_f w_{xx}^2 - 2B_f u_{xf} w_{xx} + \frac{1}{R_f}\left[\frac{A_f}{R_f} w^2 + 2\left(A_f + \frac{B_f}{R_f}\right) w u_{xf}\right.$$

$$\left. + \left(\frac{D_f}{R_f} + 2B_f\right) u_{xf}^2 - 2B_f w w_{xx} - 2D_f u_{xf} w_{xx}\right]\} \, dx \qquad (3.6)$$

$$U_f^{(3)} = \frac{1}{2}\int_{x_f} \{A_f u_{xf} w_x^2 - B_f w_{xx} w_x^2 + \frac{1}{R_f}(A_f w w_x^2 + B_f u_{xf} w_x^2)\} \, dx \qquad (3.7)$$

$$U_f^{(4)} = \frac{1}{2}\int_{x_f} \{\frac{1}{4} A_f w_x^4\} \, dx \qquad (3.8)$$

The total strain energy is obtained by summing the contribution of the faces (Eqs. 3.6, 3.7 and 3.8) and core (Eq. 2.17). The resulting expression for strain energy is

$$U = U_c^{(2)} + U_f^{(2)} + U_f^{(3)} + U_f^{(4)} \qquad (3.9a)$$

or

$$U = U^{(2)} + U^{(3)} + U^{(4)} \qquad (3.9b)$$

Substituting the displacement patterns (Eqs. 3.3 and 3.4) into Eqs. 3.9 and integrating as indicated, the resulting strain energy can be given in matrix form as

$$U^{(2)} = \frac{1}{2}\{X\}^T[K_c^{(2)} + K_f^{(2)}]\{X\} = \frac{1}{2}\{X\}^T[K^{(2)}]\{X\} \qquad (3.10)$$

$$U^{(3)} = \frac{1}{2}\{X\}^T[K^{(3)}]\{Z\} \qquad (3.11)$$

$$U^{(4)} = \frac{1}{2}\{Z\}^T[K^{(4)}]\{Z\} \qquad (3.12)$$

The vector $\{X\}$ contains the 12 nodal degrees of freedom of the generalized displacements for the discretized element and can be expressed as

$$\{X\}^T = \{x_1, x_2, x_3, x_4, x_5, x_6, x_7, x_8, x_9, x_{10}, x_{11}, x_{12}\}$$

$$= \{u_{1p}, u_{1q}, u_{x1p}, u_{x1q}, u_{2p}, u_{2q}, u_{x2p}, u_{x2q}, w_p, w_q, w_{xp}, w_{xq}\} \quad (3.13)$$

The vector {Z}contains the 10 possible multiples of the four degrees of freedom associated with the transverse deflection and slope.

$$\{Z\}^T = \{z_1, z_2, z_3, z_4, z_5, z_6, z_7, z_8, z_9, z_{10}\}$$

$$= \{w_p^2, w_p w_q, w_p w_{xp}, w_p w_{xq}, w_q^2, w_q w_{xp}, w_q w_{xq}, w_{xp}^2, w_{xp} w_{xq}, w_{xq}^2\} \quad (3.14)$$

The matrix $[K^{(2)}]$ showing the quadratic displacement variables can be outlined as

$[K^{(2)}]$ (12x12) =

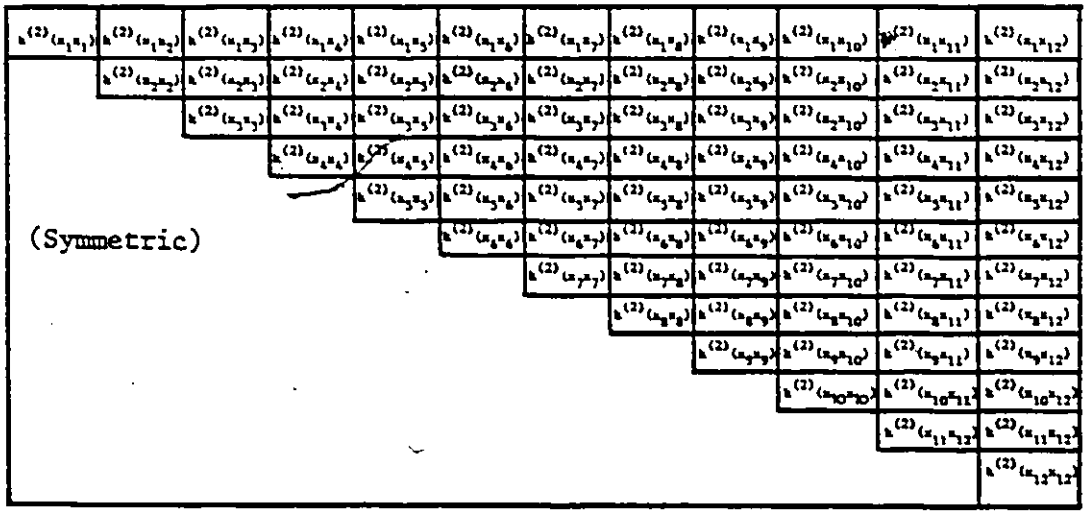

(3.15)

The elements of $[K^{(2)}]=k_{ij}^{(2)}$ (i,j=1,12) are given in Appendix B (Eq. B.1).

The matrix $[K^{(3)}]$ can be expressed as

$[K^{(3)}]_{(12x10)}=$

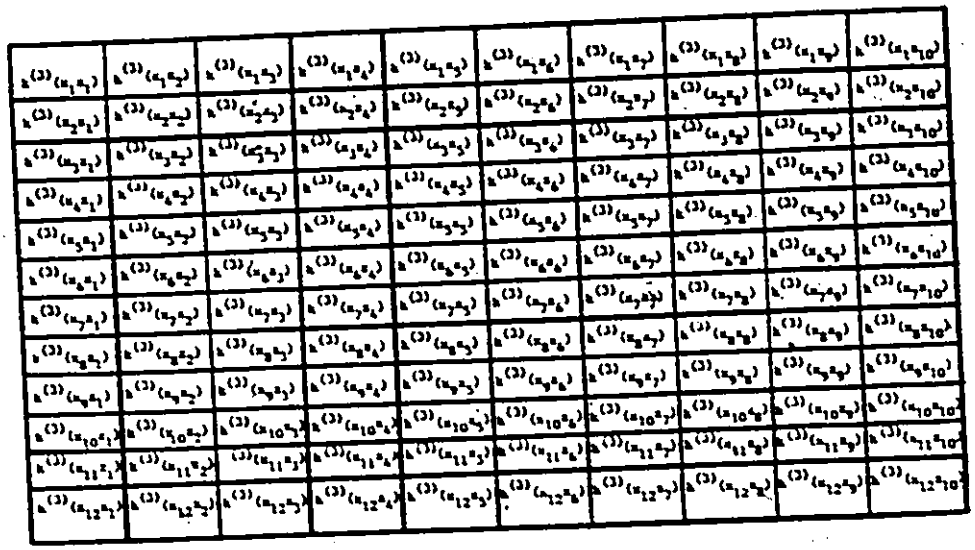

(3.16)

The elements of $[K^{(3)}]=k_{ij}^{(3)}$ (i=1,10; j=1,12) are given in Appendix B (Eq. B.2).

Similarly, the matrix $[K^{(4)}]$ is expressible as

$[K^{(4)}]_{(10x10)}=$

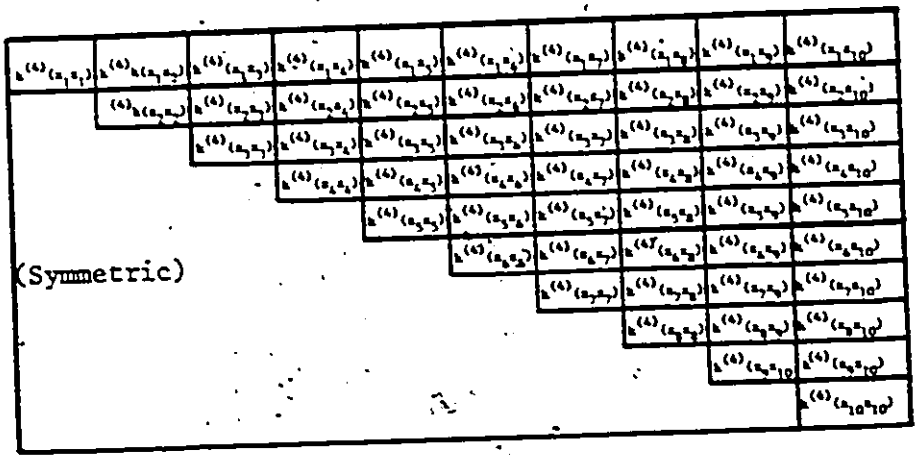

(3.17)

The elements of $[K^{(4)}]=k^{(4)}_{ij}$ (i,j=1,10) are given in Appendix B (Eq. B.3).

3.3 Discretized Kinetic Energy

The resulting expression for the total kinetic energy obtained after adding the contribution of the faces (Eq. 2.10) and core (Eq. 2.19) is

$$T^{(2)} = T_c^{(2)} + T_f^{(2)} \tag{3.18}$$

Substitution of the displacement functions (Eqs. 3.3 and 3.4) into Eq. 3.18 and then performing the integrations, the total discretized kinetic energy can be represented as

$$T^{(2)} = \frac{1}{2}\{\dot{X}\}^T[M_c^{(2)} + M_f^{(2)}]\{\dot{X}\} = \frac{1}{2}\{\dot{X}\}^T[M^{(2)}]\{\dot{X}\} \tag{3.19}$$

The vector $\{\dot{X}\}$ contains the first derivative with respect to time of the generalized displacement $\{X\}$. By assuming $\{X(t)\} = \{X\} \sin \omega t$, Eq. 3.19 is rewritten as

$$T^{(2)} = \frac{1}{2}\omega^2\{X\}^T[M^{(2)}]\{X\} \tag{3.20}$$

where ω represents the natural frequency of the sandwich systems. The mass matrix $[M^{(2)}]$ is expressed as

$$[M^{(2)}]_{(12\times12)} = \begin{bmatrix} m^{(2)}_{(x_1x_1)} & m^{(2)}_{(x_1x_2)} & m^{(2)}_{(x_1x_3)} & m^{(2)}_{(x_1x_4)} & m^{(2)}_{(x_1x_5)} & m^{(2)}_{(x_1x_6)} & m^{(2)}_{(x_1x_7)} & m^{(2)}_{(x_1x_8)} & m^{(2)}_{(x_1x_9)} & m^{(2)}_{(x_1x_{10})} & m^{(2)}_{(x_1x_{11})} & m^{(2)}_{(x_1x_{12})} \\ & m^{(2)}_{(x_2x_2)} & m^{(2)}_{(x_2x_3)} & m^{(2)}_{(x_2x_4)} & m^{(2)}_{(x_2x_5)} & m^{(2)}_{(x_2x_6)} & m^{(2)}_{(x_2x_7)} & m^{(2)}_{(x_2x_8)} & m^{(2)}_{(x_2x_9)} & m^{(2)}_{(x_2x_{10})} & m^{(2)}_{(x_2x_{11})} & m^{(2)}_{(x_2x_{12})} \\ & & m^{(2)}_{(x_3x_3)} & m^{(2)}_{(x_3x_4)} & m^{(2)}_{(x_3x_5)} & m^{(2)}_{(x_3x_6)} & m^{(2)}_{(x_3x_7)} & m^{(2)}_{(x_3x_8)} & m^{(2)}_{(x_3x_9)} & m^{(2)}_{(x_3x_{10})} & m^{(2)}_{(x_3x_{11})} & m^{(2)}_{(x_3x_{12})} \\ & & & m^{(2)}_{(x_4x_4)} & m^{(2)}_{(x_4x_5)} & m^{(2)}_{(x_4x_6)} & m^{(2)}_{(x_4x_7)} & m^{(2)}_{(x_4x_8)} & m^{(2)}_{(x_4x_9)} & m^{(2)}_{(x_4x_{10})} & m^{(2)}_{(x_4x_{11})} & m^{(2)}_{(x_4x_{12})} \\ & & & & m^{(2)}_{(x_5x_5)} & m^{(2)}_{(x_5x_6)} & m^{(2)}_{(x_5x_7)} & m^{(2)}_{(x_5x_8)} & m^{(2)}_{(x_5x_9)} & m^{(2)}_{(x_5x_{10})} & m^{(2)}_{(x_5x_{11})} & m^{(2)}_{(x_5x_{12})} \\ & & & & & m^{(2)}_{(x_6x_6)} & m^{(2)}_{(x_6x_7)} & m^{(2)}_{(x_6x_8)} & m^{(2)}_{(x_6x_9)} & m^{(2)}_{(x_6x_{10})} & m^{(2)}_{(x_6x_{11})} & m^{(2)}_{(x_6x_{12})} \\ & & & & & & m^{(2)}_{(x_7x_7)} & m^{(2)}_{(x_7x_8)} & m^{(2)}_{(x_7x_9)} & m^{(2)}_{(x_7x_{10})} & m^{(2)}_{(x_7x_{11})} & m^{(2)}_{(x_7x_{12})} \\ & & & & & & & m^{(2)}_{(x_8x_8)} & m^{(2)}_{(x_8x_9)} & m^{(2)}_{(x_8x_{10})} & m^{(2)}_{(x_8x_{11})} & m^{(2)}_{(x_8x_{12})} \\ & & & & & & & & m^{(2)}_{(x_9x_9)} & m^{(2)}_{(x_9x_{10})} & m^{(2)}_{(x_9x_{11})} & m^{(2)}_{(x_9x_{12})} \\ & & & & & & & & & m^{(2)}_{(x_{10}x_{10})} & m^{(2)}_{(x_{10}x_{11})} & m^{(2)}_{(x_{10}x_{12})} \\ & & & & & & & & & & m^{(2)}_{(x_{11}x_{11})} & m^{(2)}_{(x_{11}x_{12})} \\ & & & & & & & & & & & m^{(2)}_{(x_{12}x_{12})} \end{bmatrix} \tag{3.21}$$

(Symmetric)

The elements of $[M^{(2)}]=m^{(2)}_{ij}$ (i,j=1,12) are given in Appendix B (Eq. B.4).

3.4 Gradient Vector for the Discretized Element

The quadratic strain energy $U^{(2)}$ is given in Eq. 3.10. The vector $\{\nabla U^{(2)}\}$ represents the analytic gradient of the quadratic strain energy with respect to the displacement {X} and is expressed as

$$\{\nabla U^{(2)}\}^T = \{\frac{\partial U^{(2)}}{\partial x_1},\frac{\partial U^{(2)}}{\partial x_2},\frac{\partial U^{(2)}}{\partial x_3},\frac{\partial U^{(2)}}{\partial x_4},\frac{\partial U^{(2)}}{\partial x_5},\frac{\partial U^{(2)}}{\partial x_6},\frac{\partial U^{(2)}}{\partial x_7},\frac{\partial U^{(2)}}{\partial x_8}$$

$$\frac{\partial U^{(2)}}{\partial x_9},\frac{\partial U^{(2)}}{\partial x_{10}},\frac{\partial U^{(2)}}{\partial x_{11}},\frac{\partial U^{(2)}}{\partial x_{12}}\} \qquad (3.22a)$$

or

$$\{\nabla U^{(2)}\}^T = [K^{(2)}]\{X\} \qquad (3.22b)$$

The cubic terms of strain energy $U^{(3)}$ is given in Eq. 3.11. The vector $\{\nabla U^{(3)}\}$ defines the analytic gradient of the cubic strain energy with respect to the displacement {X} and is represented by

$$\{\nabla U^{(3)}\}^T = \{\frac{\partial U^{(3)}}{\partial x_1},\frac{\partial U^{(3)}}{\partial x_2},\frac{\partial U^{(3)}}{\partial x_3},\frac{\partial U^{(3)}}{\partial x_4},\frac{\partial U^{(3)}}{\partial x_5},\frac{\partial U^{(3)}}{\partial x_6},\frac{\partial U^{(3)}}{\partial x_7},$$

$$\frac{\partial U^{(3)}}{\partial x_8},\frac{\partial U^{(3)}}{\partial x_9},\frac{\partial U^{(3)}}{\partial x_{10}},\frac{\partial U^{(3)}}{\partial x_{11}},\frac{\partial U^{(3)}}{\partial x_{12}}\} \qquad (3.23a)$$

or

$$\{\nabla U^{(3)}\} = \frac{1}{2}[K^{(3)}]\{Z\} + \frac{1}{2}\{\frac{\partial Z}{\partial X}\}^T[K^{(3)}]\{X\} \qquad (3.23b)$$

The vector $\{\frac{\partial Z}{\partial X}\}$ is given as

$$\left\{\frac{\partial Z}{\partial X}\right\} = \begin{bmatrix} \frac{\partial z_1}{\partial x_1} & \frac{\partial z_1}{\partial x_2} & \frac{\partial z_1}{\partial x_3} & \cdots & \frac{\partial z_1}{\partial x_{12}} \\ \frac{\partial z_2}{\partial x_1} & \frac{\partial z_2}{\partial x_2} & & \cdots & \frac{\partial z_2}{\partial x_{12}} \\ \frac{\partial z_3}{\partial x_1} & & & \cdots & \frac{\partial z_3}{\partial x_{12}} \\ \vdots & & & & \vdots \\ \frac{\partial z_{10}}{\partial x_1} & \frac{\partial z_{10}}{\partial x_2} & \frac{\partial z_{10}}{\partial x_3} & \cdots & \frac{\partial z_{10}}{\partial x_{12}} \end{bmatrix} \qquad (3.24a)$$

or

$$\left\{\frac{\partial Z}{\partial X}\right\} = \begin{bmatrix} 0 & 0 & 0 & 0 & 0 & 0 & 0 & 0 & 2x_9 & 0 & 0 & 0 \\ 0 & 0 & 0 & 0 & 0 & 0 & 0 & 0 & x_{10} & x_9 & 0 & 0 \\ 0 & 0 & 0 & 0 & 0 & 0 & 0 & 0 & x_{11} & 0 & x_9 & 0 \\ 0 & 0 & 0 & 0 & 0 & 0 & 0 & 0 & x_{12} & 0 & 0 & x_9 \\ 0 & 0 & 0 & 0 & 0 & 0 & 0 & 0 & 0 & 2x_{10} & 0 & 0 \\ 0 & 0 & 0 & 0 & 0 & 0 & 0 & 0 & 0 & x_{11} & x_{10} & 0 \\ 0 & 0 & 0 & 0 & 0 & 0 & 0 & 0 & 0 & x_{12} & 0 & x_{10} \\ 0 & 0 & 0 & 0 & 0 & 0 & 0 & 0 & 0 & 0 & 2x_{11} & 0 \\ 0 & 0 & 0 & 0 & 0 & 0 & 0 & 0 & 0 & 0 & x_{12} & x_{11} \\ 0 & 0 & 0 & 0 & 0 & 0 & 0 & 0 & 0 & 0 & 0 & 2x_{12} \end{bmatrix} \qquad (3.24b)$$

The quartic strain energy $U^{(4)}$ is given in Eq. 3.12 and the corresponding gradient vector $\{\nabla\tilde{U}^{(4)}\}$ with respect to the displacements $\{Z\}$ is expressible as

$$\{\nabla\tilde{U}^{(4)}\}^T = \{\frac{\partial U^{(4)}}{\partial z_1}, \frac{\partial U^{(4)}}{\partial z_2}, \frac{\partial U^{(4)}}{\partial z_3}, \frac{\partial U^{(4)}}{\partial z_4}, \frac{\partial U^{(4)}}{\partial z_5}, \frac{\partial U^{(4)}}{\partial z_6}, \frac{\partial U^{(4)}}{\partial z_7}, \frac{\partial U^{(4)}}{\partial z_8}, \frac{\partial U^{(4)}}{\partial z_9}, \frac{\partial U^{(4)}}{\partial z_{10}}\} \tag{3.25a}$$

or

$$\{\nabla\tilde{U}^{(4)}\} = [K^{(4)}]\{Z\} \tag{3.25b}$$

However, the gradient vector $\{\nabla\hat{U}^{(4)}\}$ with respect to the four transverse displacement variables x_9, x_{10}, x_{11} and x_{12} can be obtained by using the following relation

$$\{\nabla\hat{U}^{(4)}\} = [A]\{\nabla\tilde{U}^{(4)}\} \tag{3.26}$$

where the gradient vector $\{\nabla\hat{U}^{(4)}\}$ is defined as

$$\{\nabla\hat{U}^{(4)}\}^T = \{\frac{\partial U^{(4)}}{\partial x_9}, \frac{\partial U^{(4)}}{\partial x_{10}}, \frac{\partial U^{(4)}}{\partial x_{11}}, \frac{\partial U^{(4)}}{\partial x_{12}}\} \tag{3.27}$$

The matrix [A] is expressed as

$$[A] = \begin{bmatrix} \frac{\partial z_1}{\partial x_9} & \frac{\partial z_2}{\partial x_9} & \frac{\partial z_3}{\partial x_9} & \cdots & \frac{\partial z_{10}}{\partial x_9} \\ \frac{\partial z_1}{\partial x_{10}} & \frac{\partial z_2}{\partial x_{10}} & \cdots & & \frac{\partial z_{10}}{\partial x_{10}} \\ \frac{\partial z_1}{\partial x_{11}} & \cdots & & \frac{\partial z_9}{\partial x_{11}} & \frac{\partial z_{10}}{\partial x_{11}} \\ \frac{\partial x_1}{\partial x_{12}} & \cdots & \frac{\partial z_8}{\partial x_{12}} & \frac{\partial z_9}{\partial x_{12}} & \frac{\partial z_{10}}{\partial x_{12}} \end{bmatrix} \tag{3.28a}$$

or

$$[A] = \begin{bmatrix} 2x_9 & x_{10} & x_{11} & x_{12} & 0 & 0 & 0 & 0 & 0 & 0 \\ 0 & x_9 & 0 & 0 & 2x_{10} & x_{11} & x_{12} & 0 & 0 & 0 \\ 0 & 0 & x_9 & 0 & 0 & x_{10} & 0 & 2x_{11} & x_{12} & 0 \\ 0 & 0 & 0 & x_9 & 0 & 0 & x_{10} & 0 & x_{11} & 2x_{12} \end{bmatrix} \tag{3.28b}$$

The gradient vector $\{\nabla U^{(4)}\}$ with respect to the displacement $\{X\}$ is expressed as

$$\{\nabla U^{(4)}\} = \{\frac{\partial U^{(4)}}{\partial x_1}, \frac{\partial U^{(4)}}{\partial x_2}, \frac{\partial U^{(4)}}{\partial x_3}, \frac{\partial U^{(4)}}{\partial x_4}, \frac{\partial U^{(4)}}{\partial x_5}, \frac{\partial U^{(4)}}{\partial x_6}, \frac{\partial U^{(4)}}{\partial x_7}, \frac{\partial U^{(4)}}{\partial x_8},$$

$$\frac{\partial U^{(4)}}{\partial x_9}, \frac{\partial U^{(4)}}{\partial x_{10}}, \frac{\partial U^{(4)}}{\partial x_{11}}, \frac{\partial U^{(4)}}{\partial x_{12}}\} \tag{3.29}$$

Since the quartic strain energy, $U^{(4)}$, is a function of only the transverse displacement variables x_9, x_{10}, x_{11} and x_{12}, Eq. 3.29 can be reduced to

$$\{\nabla U^{(4)}\}^T = \{0, 0, 0, 0, 0, 0, 0, 0,$$

$$\frac{\partial U^{(4)}}{\partial x_9}, \frac{\partial U^{(4)}}{\partial x_{10}}, \frac{\partial U^{(4)}}{\partial x_{11}}, \frac{\partial U^{(4)}}{\partial x_{12}}\} \tag{3.30}$$

Note that the last four terms in Eq. 3.30 is the gradient vector $\{\hat{\nabla U}^{(4)}\}$.

The kinetic energy $T^{(2)}$ is defined in Eq. 3.20 and the corresponding gradient vector $\{VT^{(2)}\}$ with respect to the displacements $\{X\}$ is given as

$$\{VT^{(2)}\}^T = \{\frac{\partial T^{(2)}}{\partial x_1}, \frac{\partial T^{(2)}}{\partial x_2}, \frac{\partial T^{(2)}}{\partial x_3}, \frac{\partial T^{(2)}}{\partial x_4}, \frac{\partial T^{(2)}}{\partial x_5}, \frac{\partial T^{(2)}}{\partial x_6}, \frac{\partial T^{(2)}}{\partial x_7},$$

$$\frac{\partial T^{(2)}}{\partial x_8}, \frac{\partial T^{(2)}}{\partial x_9}, \frac{\partial T^{(2)}}{\partial x_{10}}, \frac{\partial T^{(2)}}{\partial x_{11}}, \frac{\partial T^{(2)}}{\partial x_{12}}\} \tag{3.31a}$$

or $$\{VT^{(2)}\}^T = \omega^2[M^{(2)}]\{X\} \tag{3.31b}$$

CHAPTER IV

METHOD OF ANALYSIS

4.1 General

In the following, the methods of analysis which are employed to arrive at the solutions for the static and dynamic problems are presented. The principle of minimum total potential energy is introduced and the optimization technique based on the Fletcher-Powell method is selected as the algorithmic tool used to minimize the total potential energy; this method is classified as a gradient method which is based on the idea of conjugate directions. The combined iterative-incremental procedure is explained as the selected scheme for the analysis of material nonlinear problems. Hamilton's principle, employed for the dynamic analysis of the sandwich system, is presented. The present dynamic study is limited to normal mode analysis.

4.2 Principle of Minimum Total Potential Energy

The principle of minimum total potential energy (Ref. 23) states that,

> "Of all possible displacement configurations a body can assume which satisfy compatibility and the constraints or kinematic boundary conditions, the configuration satisfying equilibrium makes the potential energy assume a minimum value."

The total potential energy for an assemblage of n elements is expressed as

$$\Pi_p = \sum_{i=1}^{n} U_i - \sum_{i=1}^{n} W_i \tag{4.1}$$

where the total strain energy U_i is given in Eq. 3.9 and the total potential of applied load W_i obtained from Eq. 2.20 is defined as $[P]^T\{X\}$ (the vector [P] contains the 12 work equivalent loads corresponding to each of the 12 generalized displacements residing in the vector {X}).

From the principle of minimum potential energy,

$$\frac{\partial \Pi_p}{\partial \{\bar{X}\}_j} = 0; \; j = 1,2,\ldots,d \tag{4.2}$$

where $\{\bar{X}\}_j$ represents d independent nodal degrees of freedom for the assembled structure. The gradient vector of the total potential energy for the assembled structure is defined as

$$\frac{\partial \Pi_p}{\partial \{\bar{X}\}_j} = \sum_{i=1}^{n} [\{\nabla U^{(2)}\}_i + \{\nabla U^{(3)}\}_i + \{\nabla U^{(4)}\}_i - [P]_i]; \; j = 1,2,\ldots,d \tag{4.3}$$

where the element strain energy gradient vectors $\{\nabla U^{(2)}\}_i$, $\{\nabla U^{(3)}\}_i$ and $\{\nabla U^{(4)}\}_i$ are given in Eq. 3.22, 3.23 and 3.30 respectively. By employing a variable correlation scheme, the vectorial summation defined in Eq. 4.3 can be obtained.

4.3 Fletcher-Powell Method

The method of Fletcher-Powell (Ref. 24) is probably one of the most powerful procedures for finding a local minimum of a general function; it is a second order gradient method in which conjugate directions are used as the directions of descent to locate the minimum of the function. The iteration of the conjugate directions can be generated as follows:

$$\vec{s}_i = -K_i \nabla \Pi_p(\{\vec{X}_i\}) \tag{4.4}$$

where

$\vec{s}_i$ is the conjugate direction defined in the ith iteration. $\nabla \Pi_p(\{\vec{X}_i\})$ is the gradient vector of the total potential energy for the assembled structure in the ith iteration with respect to each of the d independent degrees of freedom (Eq. 4.3). K_i is a symmetric positive definite matrix in the ith iteration.

The Fletcher-Powell method starts with an initial approximations, $\{\vec{X}_0\}$ and K_0, to the minimum of $\Pi_p(\{\vec{X}\})$. The initial matrix K_0 can be any positive definite matrix, but usually is taken as the identity matrix. The step length, $l_i > 0$, is chosen such that $\Pi_p(\{\vec{X}_i\} + l_i\vec{s}_i)$ is a minimum at l_i along the direction of motion $\vec{s}_i$ (i.e., $\nabla \Pi_p(\{\vec{X}_i\} + l_i\vec{s}_i).\vec{s}_i = 0$). The new approximation $\{\vec{X}_{i+1}\} = \{\vec{X}_i\} + l_i\vec{s}_i$, is achieved and correspondingly, the new function $\Pi_p(\{\vec{X}_{i+1}\})$ with gradient $\nabla \Pi_p(\{\vec{X}_{i+1}\})$ is evaluated. The updated matrix K is generated from the relations

$$K_{i+1} = K_i + A_i + B_i \tag{4.5}$$

where

$$A_i = \frac{(l_i \vec{s}_i)(l_i \vec{s}_i)^T}{(l_i \vec{s}_i)^T \vec{y}_i} \tag{4.6}$$

$$B_i = \frac{-(K_i \vec{y}_i)(K_i \vec{y}_i)^T}{\vec{y}_i^T K_i \vec{y}_i} \tag{4.7}$$

$$y_i = \nabla \Pi_p(\{\vec{X}_{i+1}\}) - \nabla \Pi_p(\{\vec{X}_i\}) \tag{4.8}$$

With the new approximation of $\{\vec{X}_{i+1}\}$ and K_{i+1}, the iteration is repeated and continued until $\nabla \Pi_p(\{\vec{X}\}) = 0$. Theoretically, this condition is assured in d iterations for quadratic function with d degrees of freedom; in practice however, this is unlikely to be achieved because of the round-off errors. Additional iterations, therefore, are needed in order to compensate for the round-off errors. Many useful criteria can be employed for terminating the iteration, such as

$$(\vec{s}_i^T \cdot \vec{s}_i)^{1/2} = |\vec{s}_i| < \xi_1 \tag{4.9a}$$

$$\vec{s}_i < \vec{\xi}_2 \tag{4.9b}$$

$$|\Pi_p(\{\vec{X}_{i+1}\}) - \Pi_p(\{\vec{X}_i\})| < \xi_3 \tag{4.9c}$$

From the computer application using Fletcher-Powell method adopted herein, the termination criterion used is

$$|\nabla \Pi_p(\{\vec{X}\})| < \text{Eps} \tag{4.10}$$

where Eps represents the prescribed absolute error. In this work, a value of 10^{-6} was specified. Subroutine DFMFP for Fletcher-Powell method is available from the IBM 3031 subroutine package.

4.4 Hamilton's Principle

Hamilton's principle (Ref. 23) states that

> "Among all possible time histories of displacement configurations which satisfy compatibility and the constraints or kinematic boundary conditions and which also satisfy conditions at times t_1 and t_2, the history which is the actual solution makes the Lagrangian functional a minimum."

The total Lagrangian function for an assemblage of n elements is defined as

$$L = \sum_{i=1}^{n} (T_i^{(2)} - U_i^{(2)}) \tag{4.11}$$

where the total kinetic energy $T_i^{(2)}$ is given in Eq. 3.20. $U_i^{(2)}$ represents the total quadratic strain energy defined in Eq. 3.10.

The above principle takes the form

$$\frac{\partial L}{\partial \{\bar{X}\}_j} = 0; \; j=1,2. \; . \; ., \; d \tag{4.12}$$

with respect to each of the d independent nodal degrees of freedom. The gradient vector of the total Lagrangian function is given as

$$\frac{\partial L}{\partial \{\bar{X}\}_j} = \sum_{i=1}^{n} [\{\nabla T^{(2)}\}_i - \{\nabla U^{(2)}\}_i]; \; j = 1,2,\ldots,d \tag{4.13}$$

where $\{\nabla T^{(2)}\}_i$ and $\{\nabla U^{(2)}\}_i$ are given in Eqs. 3.31 and 3.22. A variable correlation scheme is used for the vectorial summation defined in Eq. 4.13. The resulting eigenvalue problem is

$$[[\bar{K}^{(2)}] - \omega^2[\bar{M}^{(2)}]]\{\bar{X}\} = \{0\} \tag{4.14}$$

where $[\bar{K}^{(2)}]$ and $[\bar{M}^{(2)}]$ are the master stiffness and mass matrices for the supported structure. Eq. 4.14 is solved using subroutines NROOT, EIGEN and ARRAY from the IBM 3031 subroutine package to obtain the normal modes of vibration.

4.5 Combined Iterative-Incremental Method

In this method, a piecewise linear load deflection curve and a combined iterative-incremental procedure is presented. Usually the stress-strain relation of a material having a nonlinear behaviour can be represented by piecewise straight lines and curves. That portion of a function with large curvature can be approximated by a polynomial function. The horizontal portions of the stress-strain relation (perfectly plastic regions) is represented by a straight line with a small positive slope. A typical stress-strain relation for aluminium with a coarse piecewise linear approximation is shown in Fig. 4.

To obtain the complete load deflection curve, small load increments are applied and in each increment, two iterations are required (see Fig. 5). Consider the initial point o in Fig. 5a. The incremental load ΔP_1 based on the initial tangent moduli $E_1^{(i)}$ yields the

incremental deflections $\Delta\delta_1^{(i)}$. The corresponding face strains $\Delta\varepsilon_1^{(i)}$ are calculated and then substituted into the tangent modulus equation to obtain a new tangent modulus slope $E_1^{(f)}$. The iteration is repeated starting from initial point o. Using the load ΔP_1 and the updated tangent moduli $E_1^{(f)}$, the final incremental deflections $\Delta\delta_1^{(f)}$ (point a) together with the final incremental strains $\Delta\varepsilon_1^{(f)}$ (point a') are obtained. Similarly, starting from point a the process is repeated to obtain point b. The second load ΔP_2 using $E_1^{(f)}$ yields $\Delta\delta_2^{(i)}$ and $\Delta\varepsilon_2^{(i)}$. The accumulated face strains ($\Delta\varepsilon_1^{(f)} + \Delta\varepsilon_2^{(i)}$) are used to determine new tangent moduli $E_2^{(i)}$. The iteration is repeated to yield $\Delta\delta_2^{(f)}$ (point b) and $\Delta\varepsilon_2^{(f)}$(point b'); in this way, the entire nonlinear stress-strain behaviour can be represented by a piecewise stress-strain line which is linear.

CHAPTER V

IMPLEMENTATION AND NUMERICAL EVALUATION

5.1 General

This chapter focuses on the implementation and numerical evaluation of the finite element formulations for static and dynamic analysis of sandwich beams, including arches. The formulations have been applied to various sandwich beams and arches, for isotropic as well as anisotropic faces, with different boundary conditions. Results are obtained and compared with other theoretical results and experimental solutions in order to demonstrate the present analysis. Among the references from published literature, selected for comparison, were Monforton (Ref. 25), Abel (Ref. 10), Yu (Ref. 2), Hoff (Ref. 1), Holt (Ref. 9), Reissner (Ref. 11), Ahmed (Ref. 18 and 19), Rutenberg (Ref. 22) and Mead (Ref. 26). The experimental tests of the sandwich beam was carried out in order to provide a more complete comparison.

The developed formulations have been implemented within a FORTRAN IV program and an IBM 3031 digital computer capability.

5.2 Theoretical Comparisons

5.2.1 Examples of Static Analysis

A. Simply Supported Sandwich Beam with Thick Laminated Faces Under Concentrated Load.

Consider a simply supported sandwich beam with overhang subjected to a concentrated load of a thousand pounds at its midspan as shown in Fig. 6. The dimensions are selected as follows:

$t_1 = 0.5$ in.; $t_2 = 1.0$ in.; $t_c = 2.0$ in.

$b = 2.0$ in.; $L = 12$ in.

The elastic constant values for graphite epoxy faces and glass fabric honeycomb core are taken as

Faces:	Longitudinal modulus	$E_{11} = 30 \times 10^6$ psi
	Transverse modulus	$E_{22} = 75 \times 10^4$ psi
	Shear modulus	$G_{12} = 75 \times 10^4$ psi
	Poisson's ratio	$\nu_{12} = 0.25$
Core:	Shear modulus	$G_c = 15 \times 10^3$ psi

Each face consists of two laminas of equal thickness. The principal axis (1,2) for laminas 2 and 3 are along the length of the beam while laminas 1 and 4 make an angle θ with respect to the longitudinal beam axis.

By taking advantage of symmetry, one-half of the beam was modeled using 4, 8 and 12 elements (26, 50 and 68 degrees of freedom respectively). The section and boundary conditions are shown in Fig. 6; the stiffnesses are given in Table 1 and the

results for midspan deflections are given in Table 2 for values of $\theta = 0°$, $30°$, $60°$ and $90°$, w refers to the deflection under the load. Note that in Table 1, when $\theta = 0°$, the coupling stiffnesses of faces vanish (i.e., $B_1=B_2=0$) and the faces are equivalent to isotropic faces. For anisotropic faces (i.e., $\theta \neq 0$) the presence of coupling stiffnesses causes the beam to become less stiff as can be seen from Table 2; for these types of beam, there occurs coupling action between longitudinal stretching and transverse bending which is the main reason for the more flexible behaviour.

Inspection of Table 2 reveals that the finite element solutions are in excellent agreement with those reported in Ref. 25 for a beam modeled using 12 elements but somewhat stiffer for a beam modeled using fewer elements. The results for a beam modeled using 4 elements differ from exact solutions for $\theta = 0°$, $30°$, $60°$ and $90°$ by 0.2%, 2.3%, 1.4% and 1.5% respectively, while for a beam modeled using 12 elements, the results improve considerably.

The matrix formulation for the present analysis was generated using the assumed displacement functions; therefore, the accuracy of the solutions not only depend upon the satisfaction of the geometry admissibility conditions for the assumed displacement functions but also depend on the number of elements used to model the sandwich beam. On the other hand, the stiffness matrix in Ref. 25 was formulated using the so-called exact displacement function; therefore, the number of elements used for modeling the beam has no effect on the results.

B. End-Loaded Cantilever Sandwich Beam

Consider a ten inch long cantilever sandwich beam of unit width with identical isotropic faces ($t_1=t_2=0.04$ in.; $E = 10.0\times10^6$ psi; $G = 4.0\times10^6$ psi) and a 0.5 in. thick core ($G_c = 1.0\times10^4$ psi). The membrane and bending stiffnesses of the faces are (f=1,2)

$$A_f = 4.0 \times 10^5 \text{ lb.}; \quad D_f = 53.3 \text{ lb. in}^2.$$

The transverse shear stiffnesses of the core is

$$B_c = 0.5 \times 10^4 \text{ lb.}$$

The boundaries of the sandwich beam are fully clamped at A and free at B (see Fig. 7). The following clamped boundary conditions were imposed at A:

$$u_1 = u_2 = w = w_x = 0$$

Evenly spaced meshes of 10 elements result in 62 degrees of freedom. The system is subjected to a unit load at the free end. The displacement solution is plotted in Fig. 7. Also, the results are compared with theoretical solutions reported by Abel (Ref. 10) and Yu (Ref. 2). Comparison of the results shows good agreement. The slight discrepancy between the present analysis and those of Ref. 10 and 2 can be attributed to the basic assumptions used for the stiffness matrix formulation. The formulations developed by Abel are based on polynomial displacement models and are capable of determining the distribution of the shearing stress of the

face; the formulation is particularly suitable for sandwich structures wherein shearing deformations in the faces are significant. Yu's formulation considers both the shearing and warping of the faces. The present formulation, however, includes face bending effect but neglects shear deformation of the faces.

C. Simply Supported Sandwich Beam Under Bending

In this example, results are presented and compared with theoretical and experimental solutions given in Ref. 1 for various core thicknesses, core materials and span lengths in order to indicate the potential of the present analysis.

Consider a simply supported sandwich beam loaded by a unit concentrated load at the midspan as shown in Figs. 8 and 9. Each face consists of identical isotropic 24ST Alclad with

$$t_1 = t_2 = 0.04 \text{ in.}; \; b = 1 \text{ in.}$$
$$E = 10.0 \times 10^6 \text{ psi}; \; G = 3.76 \times 10^6 \text{ psi}$$

Figure 8 shows the results obtained for various core thicknesses (0.25 in., 0.5 in., 1.0 in.) and core materials (balsawood, cellular cellulose acetate) with a constant span length of 10 in. The figure also contains the experimental results presented by Hoff (Ref. 1), obtained from the testing of six specimens having a balsawood core with a shear modulus of 24,000 psi and seven specimens having a cellular cellulose acetate core with shear modulus of 2,500 psi. Similar tests were carried out by Hoff (Ref. 1) for five specimens having a half inch thick balsawood core and the results together

with the theoretical solutions are plotted between midspan deflection and various span length (8 in., 10 in., 13 in., 18 in., 23 in.) (Fig. 9).

Due to symmetry, only one-half of the beam was modeled using 8 elements resulting in 50 degrees of freedom. All of the results were obtained by using a linear formulation and an overhang of 1 inch at both ends was included in the modeling. The results are then compared with the theoretical and experimental solutions reported in Ref. 1 and seem to show good agreement. The slight discrepancy, especially those exhibited for CCA core, can be attributed mainly to the assumptions made in the formulation and partly due to the usual discretization and experimental errors. The formulations developed in Hoff's paper are based on the principle of virtual displacement; the strain energy from the membrane and the bending action of the faces as well as the transverse shear and the extension perpendicular to the faces in the core are included in the formulation. However, the strain energy of the transverse shear in the faces and the longitudinal extension in the core have been neglected. It is important to realize that the present analysis differs from Hoff's formulation, in that the contribution from extension perpendicular to the faces in the core has been disregarded; this extension action may have considerable effect on the behaviour of the sandwich beam made of low shear modulus and may explain the reason for higher discrepancy in comparison with a beam made of CCA core than a beam made of balsa core. CCA core, as is known, pos-

sesses a much lower shear modulus than balsa core (about 90% lower); it is therefore more susceptible to the extension action which in turn causes the beam to be more flexible. The discrepancy, as mentioned earlier, is very small and thus it is fair to conclude that the present analysis is capable of analyzing the sandwich beam efficiently.

D. End-Loaded Cantilever Curved Sandwich Beam

Consider a cantilevered quarter circle sandwich arch subjected to a unit concentrated end radial load as shown in Fig. 10. The core is a Nomex honeycomb material with

$$t_c = 7.5 \text{ mm}; \quad R_c = 150 \text{ mm}$$

and $$G_c = 22 \text{ N/mm}; \quad b = 1 \text{ mm}$$

Each face is a single lamina of unidirectional carbon fibre reinforced plastic (CFRP) with the following material properties:

$$E_{11} = 14200 \text{ N/mm}^2; \quad E_{22} = 9800 \text{ N/mm}^2$$

$$G_{12} = 4300 \text{ N/mm}^2; \quad \nu_{12} = 0.25$$

The results are obtained for various face thickness (0.2 mm, 1.0 mm, 2.4 mm and 3.0 mm) with constant core thickness and core radius. The whole beam was modeled using 10 elements which has a total of 62 degrees of freedom. Results from the present analysis, Holt's theory (Ref. 9) and the Reissner's analysis (Ref. 11) are shown in Fig. 10 and are plotted using the stiffness under load (defined as the ratio of the applied radial load to the transverse

displacement) as ordinate and the face thickness as abscissa.

The present analysis involves twelve generalized displacements for each element with bending effects in the faces included (Fig. 11). Element 1 of Holt's theory (Ref. 9) is shown in Fig. 12a; it has fourteen generalized displacements which are used as Lagrange Multipliers to maintain interelement equilibrium. Element 2 is formulated in the same way as element 1 but without a core generalized displacement; the generalized displacements are thus reduced from fourteen to twelve. Element 3 is shown in Fig. 12b. In contrast to element 1 and 2, it does not include face bending effects and is formulated with the assumption that the faces act only as membranes. Element 4 has the same generalized displacements as element 3 but with the assumption that the core is incompressible in the transverse direction. Reissner analyzes the same way as element 3 but with the further assumption that the core thickness has to be small compared with the radius of curvature at its mid-axis.

Inspection of Fig. 10 reveals that the results for all methods of analysis are virtually the same for face thickness less than 0.4 mm as face bending effects are still not important. The results of element 1 and 2 are very close. Reissner's element 3 and element 4 results are observed to be more flexible than both of element 1 and 2, owing to the membrane face assumption. Reissner's results and the results for element 3 are in complete agreement due to the same assumption made in both formulations. Element 4 results, how-

ever, are stiffer than those of Reissner's and element 3 results due to its infinite normal core modulus assumption.

The present analysis shows very close agreement with element 3, but gradually diverge to a stiffer behaviour with increasing face thickness as face bending effects become significant. As expected, it diverges from element 3 to follow element 1 and element 2. The discrepancy of results between the present analysis and those of element 1 and 2 at higher face thickness is due to the basic assumptions made in selecting the generalized displacements and it is arguable as to which formulation yields a better solution unless an experimental study is carried out.

5.2.2 Example of Dynamic Analysis

This example aims to check the capability of the present method and formulations to calculate the natural frequencies of sandwich beams and arches. Two straight sandwich beams, one simply supported and one cantilever together with one fully clamped sandwich arch, are employed in the analysis (see Fig. 13).

a. Natural Frequencies of Straight Sandwich Beams

Ahmed (Ref. 18 and 19), Rutenberg (Ref. 22) and Mead (Ref. 26) have reported the theoretical results to determine the natural frequencies of straight cantilever sandwich beams. In addition, Ahmed and Mead have also reported the results of simply-supported sandwich beams.

The beam considered has the following dimensions:

$t_1 = t_2 = 0.018$ in.; $t_c = 0.5$ in.; $b = 1.0$ in.

The material properties of the aluminium faces are taken as

$$E = 10 \times 10^6 \text{ psi}; \nu = 0.33; \rho_f = 2.509 \times 10^{-4} \text{lb-sec}^2/\text{in.}^4$$

and for the honeycomb core

$$G_c = 12 \times 10^3 \text{ psi}; \rho_c = 3.07 \times 10^{-6} \text{lb-sec}^2/\text{in.}^4$$

The lengths of the beams are $L = 36$ in. for simply supported and $L = 28$ in. for cantilever.

The membrane, coupling and bending stiffnesses of the faces are ($f = 1,2$).

$$A_f = 1.8 \times 10^5 \text{ lb.}; B_f = 0; D_f = 4.86 \text{ lb. in.}^2$$

The transverse shear stiffness of the core is

$$B_c = 6 \times 10^3 \text{ lb.}$$

The translatory, rotary and coupling inertia constants of the faces are ($f = 1,2$).

$$Q_f = 4.5155 \times 10^{-6} \text{ lb-sec}^2/\text{in.}^2; J_f = 0; I_f = 1.2192 \times 10^{-10} \text{lb-sec}^2$$

For the core

$$Q_c = 1.5351 \times 10^{-6} \text{ lb-sec}^2/\text{in.}^2; J_c = 0; I_c = 3.1981 \times 10^{-8} \text{lb-sec}^2$$

The simply supported beam is modeled using 4, 6 and 10 elements and the cantilever beam is modeled using 8 and 10 elements. The present analysis results, as given in Tables3 and 4, compare favourably with the theoretical results reported in Ref. 18, Ref. 19, Ref. 22 and Ref. 26.

B. Natural Frequencies of Curved Sandwich Beam

In this example, the natural frequencies of vibration for a clamped-clamped sandwich arch are calculated. The arch considered has dimensions and material properties identical to those given in Section A except that the arch length is L = 28 in. and R_c = 168 in. (see Fig. 13).

The stiffnesses and inertia constants for the faces and the core are calculated to be the same as those given in section A.

The arch is modeled using 6, 8 and 10 elements (34, 46 and 58 degrees of freedom respectively). The results are compared to the theories reported in Ref. 18 and 19. The first five natural frequencies are given in Table 5. The present analysis solutions are observed to be in good agreement with results from Ref. 19 but somewhat lower than those reported in Ref. 18. The explanation for the discrepancy is that the frequencies are sensitive to the effect of transverse shear deformation which has been neglected in Ref. 18.

By comparing the results in Tables 3, 4 and 5, it is noteworthy that the first few frequencies are in better correlation and is evident that the relatively coarse modeling has only a slight effect on the accuracy of the natural frequency.

5.3 Experimental Programs

In the following, the experimental studies are carried out on nine sandwich beams. Six beams are tested for various beam dimensions and loading conditions to determine the core transverse shear modulus. The other three are tested for comparison with nonlinear

theoretical solutions. All beams consists of 0.068 in. thick identical isotropic aluminium faces and a 3 in. thick expanded polystyrene foam core. The stress-strain behaviour of aluminium faces were tested and are shown in Fig. 4.

5.3.1 Experimental Study of the Core Transverse Shear Modulus

Several methods of testing core shear rigidities have been devised over the year. The most common method is the use of the block shear tests (Fig. 14); but Kelsey et al (Ref. 27) has criticized the validity of these tests for several reasons, including: the shear stress is wrongly assumed to be uniformly distributed throughout the core and face bending effects is neglected; these assumptions have lead to a low value of core shear modulus. Alternatively, other methods are used. Bigg (Ref. 28) developed several standard bending tests to calculate the core shear modulus from the measured deflection of the beam; he summarized the criteria for a standard test and presented the chart as a guide for a suitable selection of beam dimension. It is claimed that Bigg's method produces satisfactory results for various expanded plastic, aluminium honeycomb and aerated concrete cores. A similar method was also used by Hoff (Ref. 1), in that the shearing rigidity of the core material is determined with the aid of the theoretical deflection formulas. A good investigation has been done at the University of Windsor by Fazio (Ref. 29) in which both the direct shear test and bending test for determining core shear modulus were performed. The results from the direct

shear test (single-block shear test) however were found to be surprisingly low and widely scattered. The bending test results were also found to vary somewhat depending upon the beams dimension and loading conditions. However, Fazio recommended the bending test method because it most closely represents the conditions of the later intended experimental studies.

In the present experimental studies, the direct shear test is not carried out for the same reasons mentioned earlier. Instead, the bending test for various beam dimensions and loading conditions are used. Six beams made of aluminium faces and expanded polystyrene foam core were tested. Figures 15, 16, 17 show the set up of the test for three-(beams T1, T2, T3 and T4), four-(beam T5) and six-point (beam T6) bending tests respectively. The first four beams (T1, T2, T3 and T4) were each tested six times while the last two beams (T5 and T6) were each tested once to failure. Two dial indicators at midspan were used in all beams to measure the deflection of the beam. For beams T3, T4 and T6, strain gauges were installed to measure the strain in the aluminium faces. The experimental load versus midspan deflection for each beam was plotted and shown on Figs. 18, 19, 20, 22, 24 and 25. Figures 21, 23 and 26 show load versus strain for beams T3, T4 and T6 respectively. Figures 27 and 28 show the failure patterns of beams T5 and T6 which will be discussed in a more detailed manner in the next section. The shear modulus of core for each beam was then determined from the measured deflection of the beam by means of linear theoretical deflection

formulation. The experimental results of shear modulus are relatively consistent. The shear modulus for beams T1 to T6 are calculated to be 1150 psi, 975 psi, 1100 psi, 1300 psi, 1150 psi and 1150 psi respectively. The average value is 1138 psi. Beams T1, T5 and T6 show most consistency. Beam T2 and T3, however, yield slightly low values (14.3% and 4.4% below the average value), but beam T4 shows higher shear modulus which differ by 14.3% from the average value.

The shear modulus recommended for the polystyrene core is taken to be 1150 psi as given by the rounded value of the average of six beams tested. The above tests are considered to be satisfactory, therefore, the value of G_c = 1150 psi is used as theoretical value for all experimental studies of sandwich beams in this work.

5.3.2 Experimental Study of Simply Supported Sandwich Beams

The following example serves to investigate the behaviour of simply supported sandwich beams under an increasing central vertical load and aims to check the capability of the present method and formulations to predict the behaviour of simply supported sandwich beams which later will be compared to experimental test results. Geometric nonlinear analysis together with material nonlinear analysis has each been analyzed separately. The effects of combining both geometric and material nonlinear contributions has also been studied.

Three beams (T7, T8 and T9) consisting of the polystyrene

core and aluminium faces were tested. The core shear modulus, based on the previous experimental bending test results, is taken as 1150 psi. The nonlinear stress-strain behaviour of aluminium faces was tested and the typical curve is shown in Fig. 4. It is extremely important to guarantee the correct stress-strain behaviour of the aluminium. In ensuring this, six specimens were tested in tension using the universal testing machine; the elongation in the first four specimens were monitored by an electrical extensometer while for the last two specimens, the strains reading were obtained by strain gauges. The results show good consistency and the final stress-strain equation was obtained by averaging the results from the six specimens tested.

The beams were tested in the universal testing machine (Fig. 29). All three beams were tested to failure according to the three-point loading test. In all tests, rollers were used at support points and at the point of applied load, rubber was used to reduce local compression effects. Plexiglass stiffeners were installed to all beams at loading and support point; these stiffeners are important in the sense that they delay the premature local failure which often occurs at the concentrated load caused by the compressibility of the core. In referring to section 5.3.1, this type of failure is observed to occur for beam T6. The six-point bending tests without stiffeners are seen to fail prematurely in the loading region where strains in the faces were still in the elastic range (see Fig. 28). Furthermore, beam T5, which was tested in four-point

bending, failed by face wrinkling in the region between the two applied loads. Because the face strains were still in the linear range, no nonlinearity is present in the load-deflection curve. The failure pattern is shown in Fig. 27. Consequently, the load deflection curves for beams T5 and T6 could only be plotted in the elastic region. The placing of the stiffeners allow a more complete load deflection curve, thus permitting a better and a more complete comparison with the results obtained from theoretically developed formulation. The typical stiffener along with its dimensions is shown in Fig. 30; they are glued into position with adhesive similar to that used between faces and core.

The set up of the test is shown in Fig. 29. Two dial indicators placed at midspan are used in all beams in order to measure the deflection of the beam. The strain at the midspan of the bottomface is monitored by a strain gauge.

The experimental load versus midspan deflection and strain as well as the failure patterns for each beam are shown in Figs. 31 to 39. Figures 31 and 32 show load-deflection and strain curves for beam T7; the experimental results are observed to reach beyond the elastic region. The placing of the stiffeners in this beam was effective in delaying the premature local failure, thus permitting a more complete experimental result. The beam failed mainly because of high concentration of stresses in the load region. It failed by local compression yielding at the top face, followed by local core crushing causing delamination between the faces and the

core which propagated well into the supports point. Failure was characterized by a load noise and close inspection at midspan revealed that the core had almost split in half. The delamination failure is shown in Fig. 33.

The load-deflection and strain curves, plotted in Figs. 34 and 35 for beam T8 and in Figs. 37 and 38 for beam T9, show only little nonlinearity. The deflection reading diverges gradually from a straight line, and this may be indicative of the development of local instability in the compression faces. In the case of beams T8 and T9, the basic type of failure similar to that of beam T7 is exhibited except that the delamination is more narrowly developed for beam T9. The failure patterns for beams T8 and T9 are shown in Figs. 36 and 39 respectively. A possible explanation for earlier local instabilities in beams T8 and T9 is that the plexiglass stiffeners used are smaller (0.25 in. thick) compared to the width of the beams which measured to be 4 inches for beam T8 and 6 inches for beam T9. Unlike beam T7 (3 inches wide), the other two beams have a larger unstiffened portion which implies that the effect of local concentrated load may be more severe.

All three beams show a similar trend in load-deflection and strain. Only one beam, namely T7 (Fig. 31), will be discussed thoroughly. Curve 1 in Fig. 31 shows the behaviour of the beam predicted using linear analysis; it compares favourably with experimental results for small loads but is obviously invalid for larger loads. The geometric nonlinear analysis is found to

be the same as the linear curve. Curve 2 represents the results obtained from the material nonlinear analysis. The solutions are observed to show a good trend but a rather stiff behaviour compared to experiment. In this analysis, the load deflection curve is obtained by using the iterative-incremental method; this method is very sensitive to the load increment magnitude. In this particular problem, one large load increment is used in the linear range followed by a much smaller size of load increment in the nonlinear range. The size of load increment is reduced subsequently knowing that the region near the plastic zone is very sensitive even to a very small load increment. The curve denoted by 3 utilizes the iterative-incremental method for material nonlinearity but also includes the geometry nonlinearity. The combined geometric and material nonlinear analysis fits the experimental data somewhat better than the previously mentioned curves. This curve represents the analytical solution for predicting the actual behaviour of the beam. Although the model still overestimates the rigidity to some degree, better correlation is obtained. The stiffer behaviour may be remedied by modeling the beam using more elements (see Fig. 31). The same beam modeled with 16 elements instead of 10 elements is observed to show better agreement with experiment. It may still be possible to achieve better results by modeling the beam using more element; however, increasing the number of elements requires a considerable increase in computer time and storage.

The experimental and theoretical load-strain curves for all three beams, plotted in Figs. 32, 35 and 38, show a considerable dis-

crepancy even at very low load. Although the stiffeners prevented crushing of the core, it tended to transfer the applied load to the bottom face to cause delamination. The discrepancy of the strain reading seems to be initiated by a protrusion of the stiffener at the loading point which may have disturbed the bottom face behaviour (see Figs. 33, 36 and 39). This phenomenon will inevitably cause the faces to yield earlier and consequently make the beam more flexible. As seen on the linear range in Figs. 31, 34 and 37, the stiffeners seem to make the beam slightly stiffer.

5.4 Numerical Example on Fully Clamped Beam Under Bending

Some solutions are available for fully clamped sandwich plates using large deflection theory. Yet, very little or probably nothing has been presented on clamped-clamped sandwich beams. Zahn (Ref. 15) once concerned himself with large deflection theory of sandwich beams; his study, however, was limited to beams which are simply supported. In this example, the behaviour of a clamped-clamped sandwich beam subjected to an increasing central vertical load has been investigated. The sandwich beam is made of the expanded polystyrene core and the aluminium faces with unequal face thicknesses. The shear modulus of the core was determined from experimental tests to be 1150 psi and the nonlinear stress-strain behaviour of aluminium was tested and plotted as shown in Fig. 4. The section, dimensions and boundary conditions are shown in Fig. 40.

The imposed displacement boundary conditions of the fully clamped beam are taken to be

$$u_1 = u_2 = w = w_x = 0 \quad \text{at} \quad x = A \text{ and } x = B$$

By taking advantage of symmetry, only one-half of the beam was modeled using 10 elements which results in 59 degrees of freedom.

The analytical solutions considered herein are classified into four types as follows:

1. Linear analysis
2. Material nonlinear analysis
3. Geometric nonlinear analysis
4. Combined material and geometric nonlinear analysis.

This example is employed to demonstrate clearly the differences between the four types of analyses. The load was gradually increased and the corresponding deflection was calculated and plotted for mid-span load versus center deflection for all four types of analyses (Fig. 41).

In the linear analysis (curve 1), both the linear stress-strain behaviour and the linear strain-displacement relation of the faces are used. The solution is characterized by a straight line as shown in Fig. 41. A deflection of 1.54 inches was obtained at a load of 650 pounds.

In the material nonlinear solutions, the same linear strain-displacement relation is used, but the nonlinear material behaviour of faces is included. Instead of the initial linear modulus used in the linear solution, the modification in the face formulations involves the use of appropriate tangent moduli for each increment. According to the material nonlinear (curve 2), the deflection under

a load of 650 pounds was found to be 1.80 inches.

The third curve in the same figure represents the solution based on geometric nonlinear analysis only. The beam shows stiffer behaviour as load increases. This phenomenon is due to the clamping effect at both ends of the beam; the deflection is reduced considerably to 1.07 inches under the same load of 650 pounds. The result differs from that obtained in linear analysis by 30.5%.

The final solution (curve 4) involves the combined geometric and material nonlinear analysis; it represents the actual behaviour of the beam in that both the nonlinear strain-displacement relation and the nonlinear stress-strain behaviour of the faces are employed in the formulation. Initially the curve follows curve 3 as the strain in all faces is still in the linear range but gradually it diverges from curve 3 to follow curve 2 indicating that the faces exhibit inelastic strain. The maximum deflection of 1.68 inches was found under a load of 650 pounds.

CHAPTER VI

SUMMARY, CONCLUSIONS AND RECOMMENDATIONS

6.1 Summary

A finite element capability for predicting displacements, strains and natural frequencies of sandwich beams and arches has been presented. The method is applicable to sandwich beams with isotropic, anisotropic and transversely heterogeneous faces. Using a set of nonlinear strain-displacement relations, geometric nonlinearity is incorporated in the analysis. Material nonlinearity was incorporated in the analysis for isotropic faces by using a nonlinear stress-strain relation of the faces. Dynamic analysis is limited to the study of normal mode of vibration and only a linearized strain-displacement relation is included in the formulation.

Specific element stiffness and mass matrices have been developed for static and dynamic analysis of the straight and curved sandwich beams. The static formulation was described in terms of the geometry and the various stiffnesses of the faces (membrane, coupling and bending) and core (transverse shear). Similarly, the dynamic analysis was formulated in terms of the various inertia constants (translatory, rotary and coupling) of the faces and core. The displacement behaviour of the sandwich system was described by the

longitudinal displacements of the faces, u_f(f=1,2) and the transverse displacement w. The displacement patterns, necessary for describing the displacement behaviour of the sandwich system, were approximated using Oscullatory (first order Hermite) interpolation polynomials.

The solutions for static problems were obtained by direct minimization of the total potential energy using the variable metric method. A second order gradient algorithm based on Fletcher-Powell method was employed as the directions of descent to locate the minimum of the function. In the material nonlinear analysis, appropriate tangent moduli were used in the nonlinear stress-strain relations for the faces and an iterative-incremental scheme was used to calculate the strains in the faces. For dynamic solutions, a linear eigenvalue solution technique was used in order to obtain the natural frequencies of the sandwich systems.

Several numerical results have been presented for static and dynamic analysis of sandwich beams and arches. Also, an experimental study of simply-supported sandwich beams has been carried out and the results were presented and compared with the finite element method.

6.2 Conclusions

The following conclusions may be drawn from the present investigation:

1. The method proposed is valid and capable of analyzing sandwich beams exhibiting geometric nonlinear displacements and having inelastic strains in the faces.

2. The displacement and natural frequency results are found to compare favourably with the existing published results for sandwich beams and arches under various boundary conditions.
3. Experimental deflections of simply-supported sandwich beams are good compared to the present theoretical formulation. Differences between theoretical and experimental strains, however, are significant especially in the inelastic region.
4. The energy search method employing the Fletcher-Powell minimization technique proved to be a powerful and efficient procedure for the analysis of sandwich systems.
5. Geometric nonlinearity has negligible effects on simply supported sandwich beams but has significant effect on fixed-fixed sandwich beams.
6. Relatively few elements are required to predict accurately the natural frequencies.

6.3 Recommendations

A useful extension for the present method would be to predict flexural wrinkling in the faces. Such a formulation would make it possible to predict the failure load which would be of great importance for the analysis of thin faces sandwich systems. Moreover, the inclusion of thermal effects due to the temperature difference through the thickness of the sandwich system would be worth investigating since it could be used to predict the residual stresses and strains due to

curing temperatures. It is recommended that more experimental studies be carried out using core materials which have a higher compressive strength in the transverse direction. It is felt that higher compressive strength core materials such as honeycomb and balsawood, oriented such that the grain is perpendicular to the faces, might be a proper choice of core material to prevent local compressive failure. Also, the results of the finite element analysis of clamped-clamped sandwich beam has not yet been verified. More study, theoretically or experimentally, should therefore be carried out in order to verify the solutions.

FIGURES

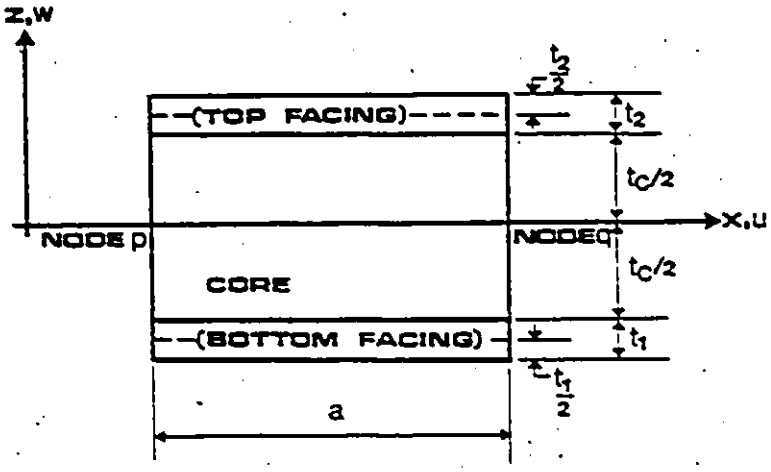

(a) SANDWICH BEAM ELEMENT

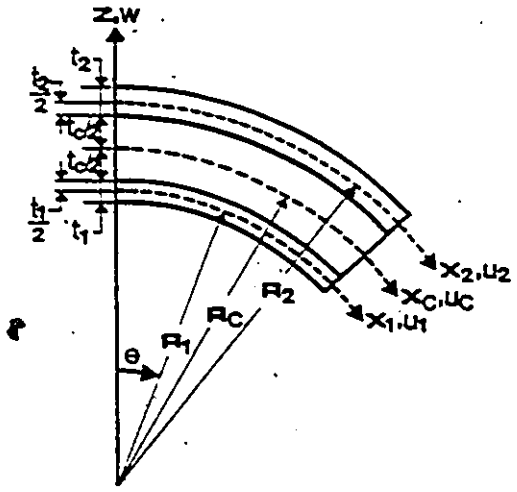

(b) SANDWICH ARCH ELEMENT

FIGURE. 1 ANISOTROPIC SANDWICH ELEMENTS

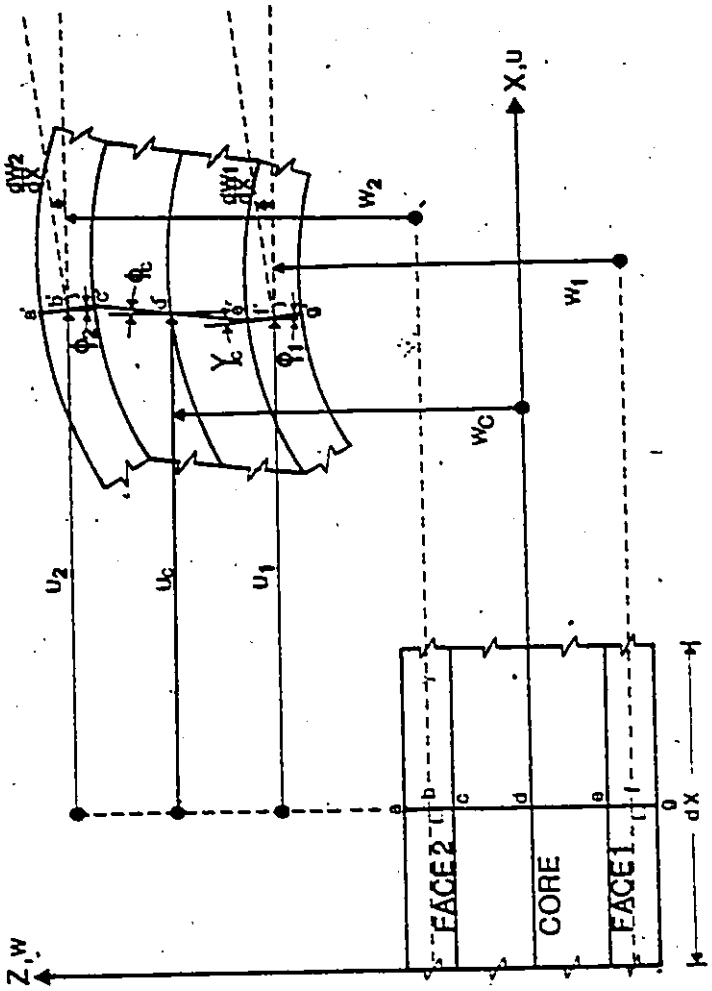

FIGURE.2 DEFORMATION OF SANDWICH BEAM

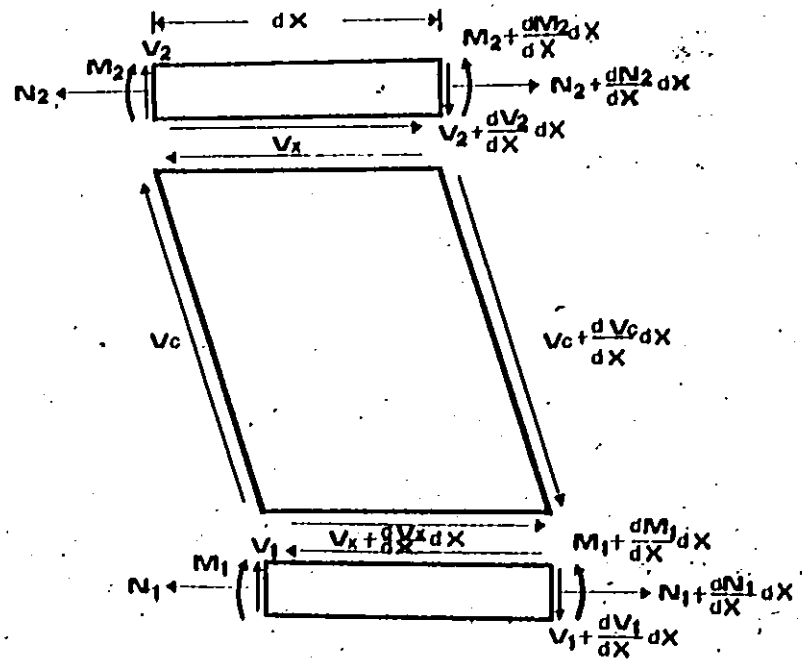

FIGURE.3 SANDWICH BEAM STRESS RESULTANTS

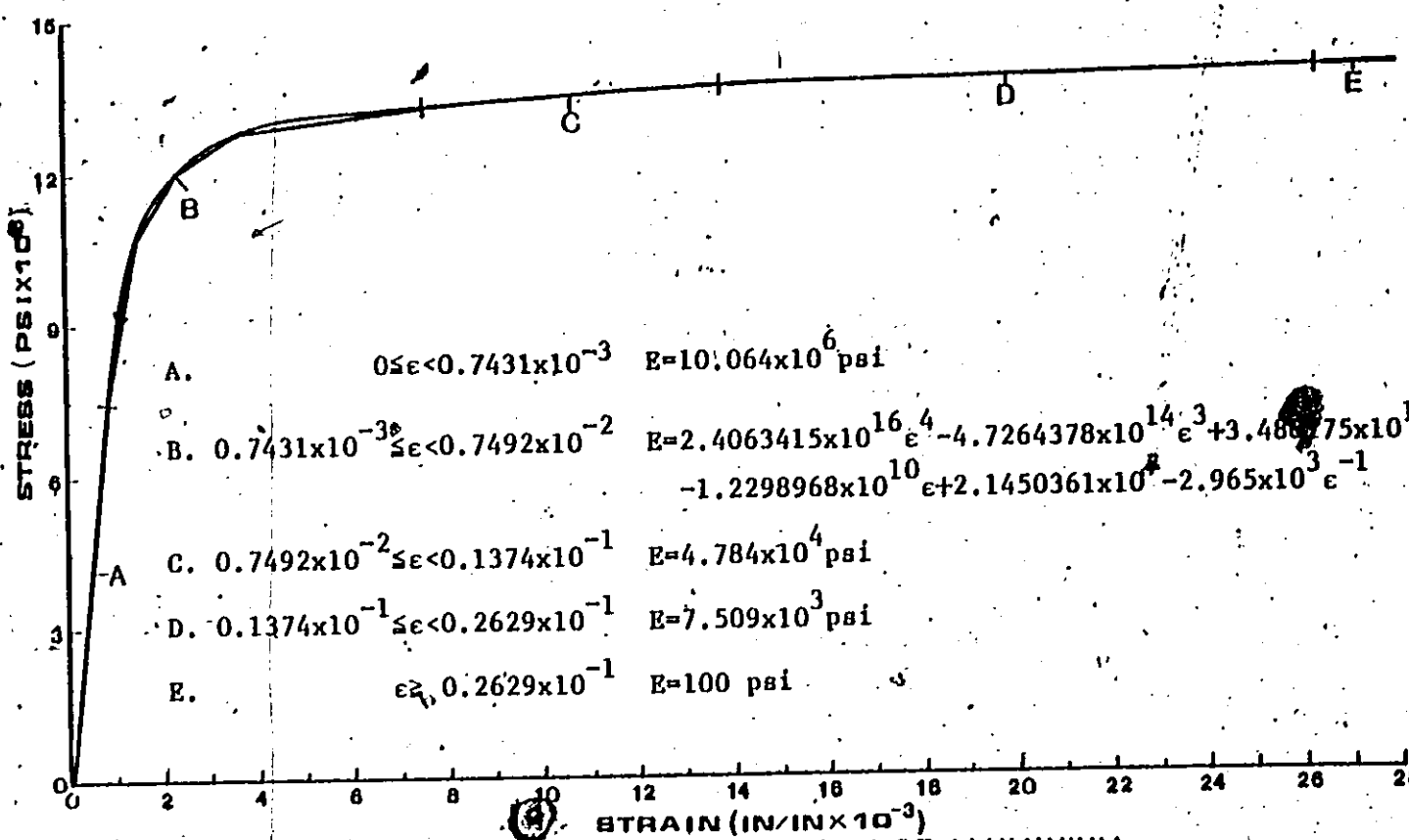

FIGURE.4 STRESS-STRAIN CURVE OF ALUMINIUM
(1 in.= 25.4 mm ; 1 psi = 6.89x10⁻³ N/mm²)

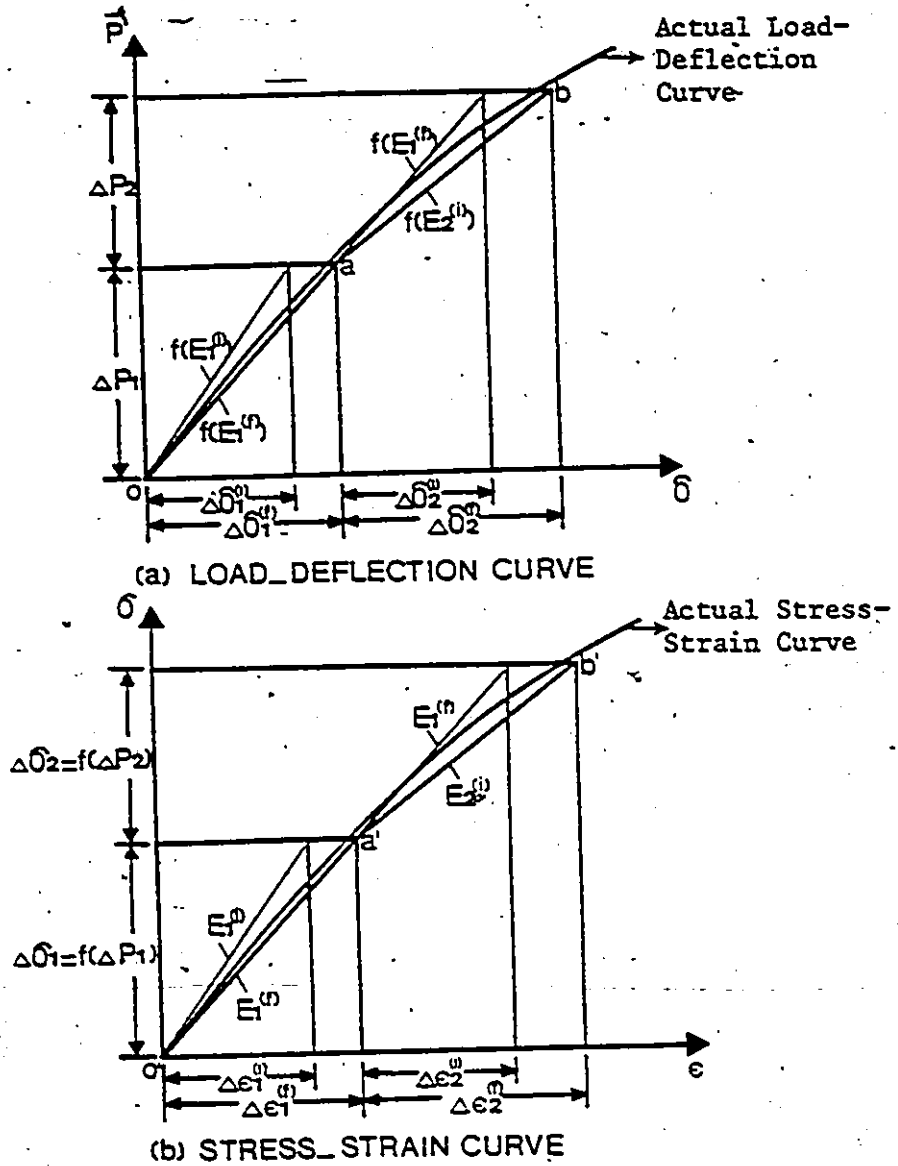

FIGURE.5 EXAMPLE OF ITERATIVE_INCREMENTAL METHOD

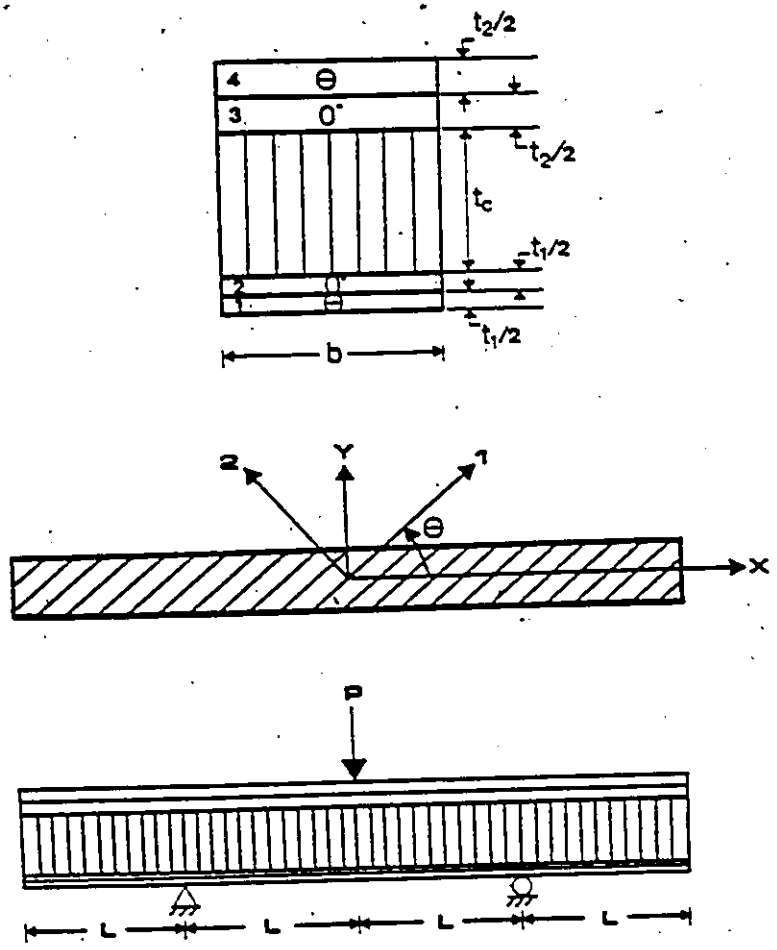

FIGURE.6 SANDWICH BEAM WITH OVERHANG

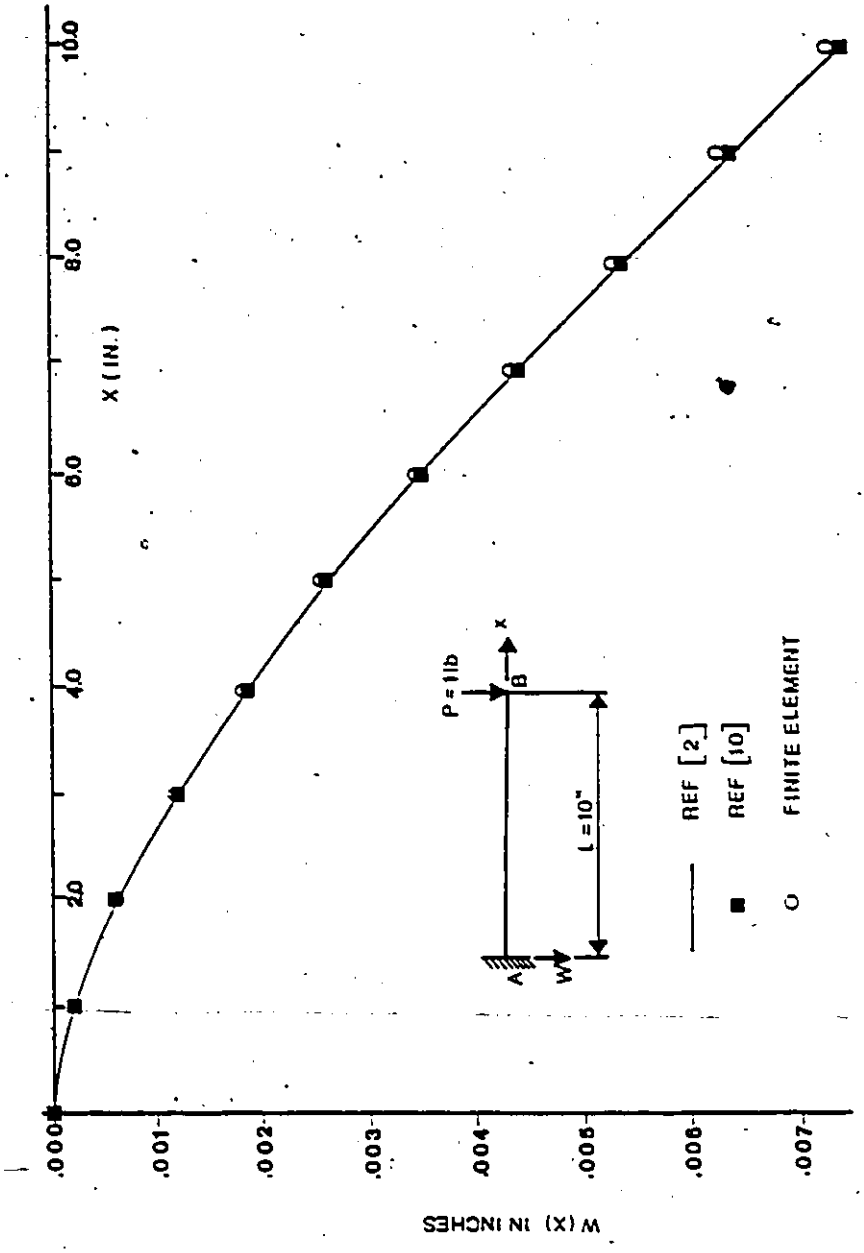

FIGURE. 7 DEFLECTION OF A CANTILEVER SANDWICH BEAM
(1 in.= 26.4 mm.; 1 lb=4.46 N.)

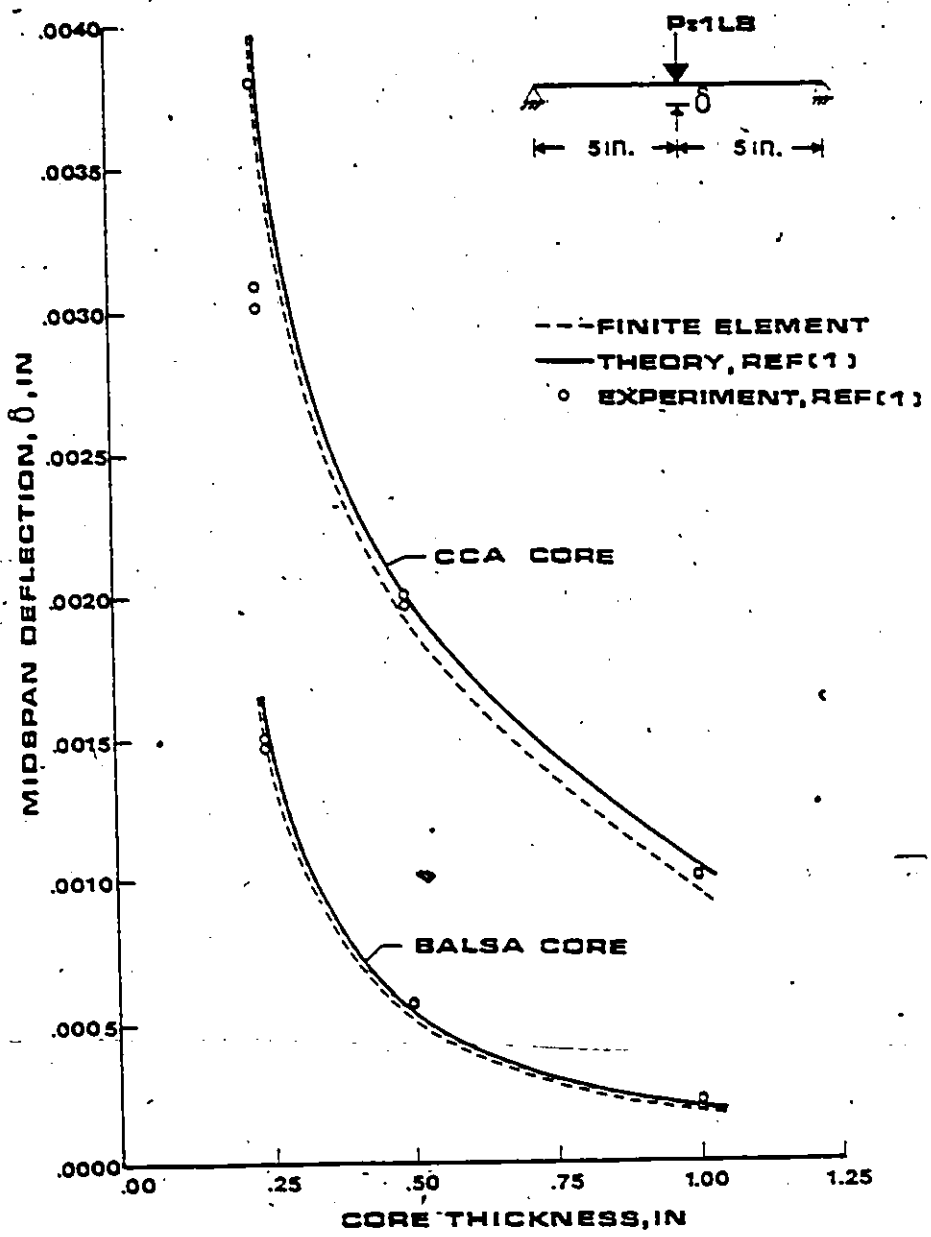

FIGURE. 8 VARIATION OF DEFLECTION WITH CORE THICKNESS
(1 in.= 25.4 mm. ; 1 lb=4.45 N.)

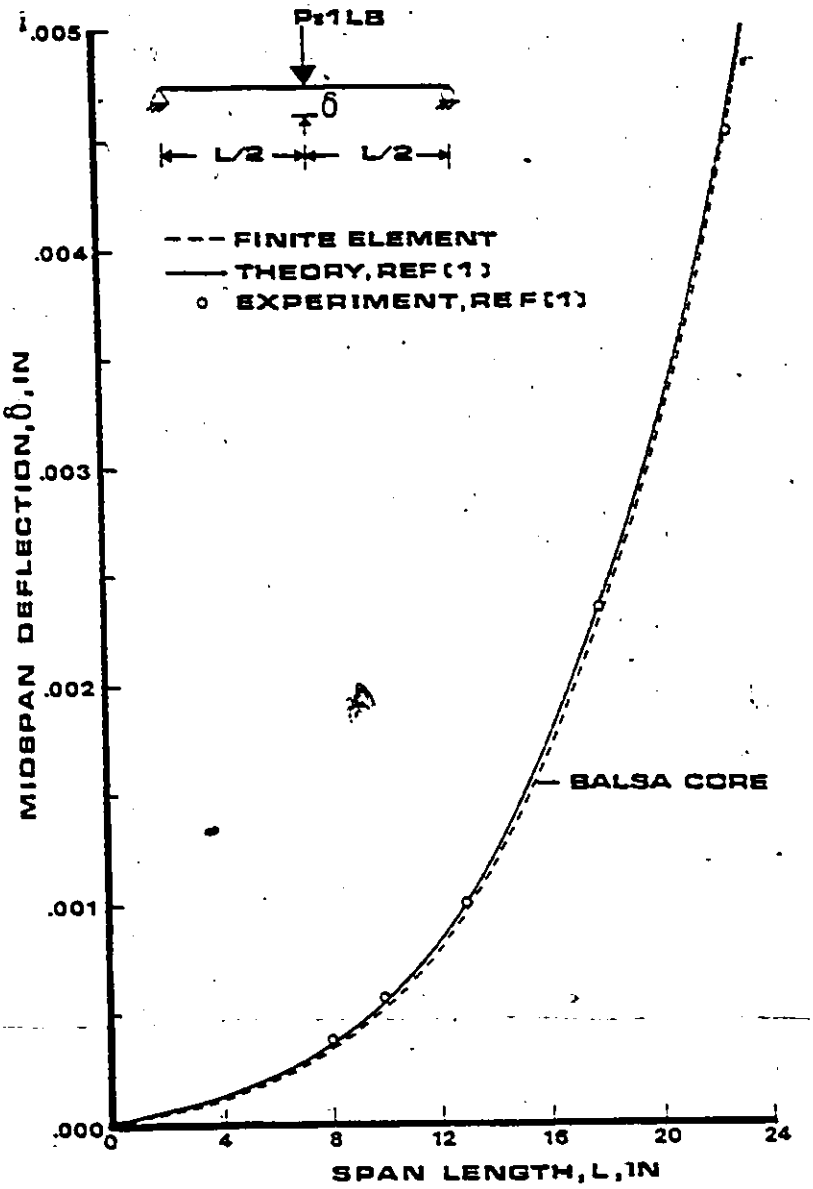

FIGURE. 9 VARIATION OF DEFLECTION WITH SPAN LENGTH

(1 in. = 25.4 mm. ; 1 lb = 4.45 N.)

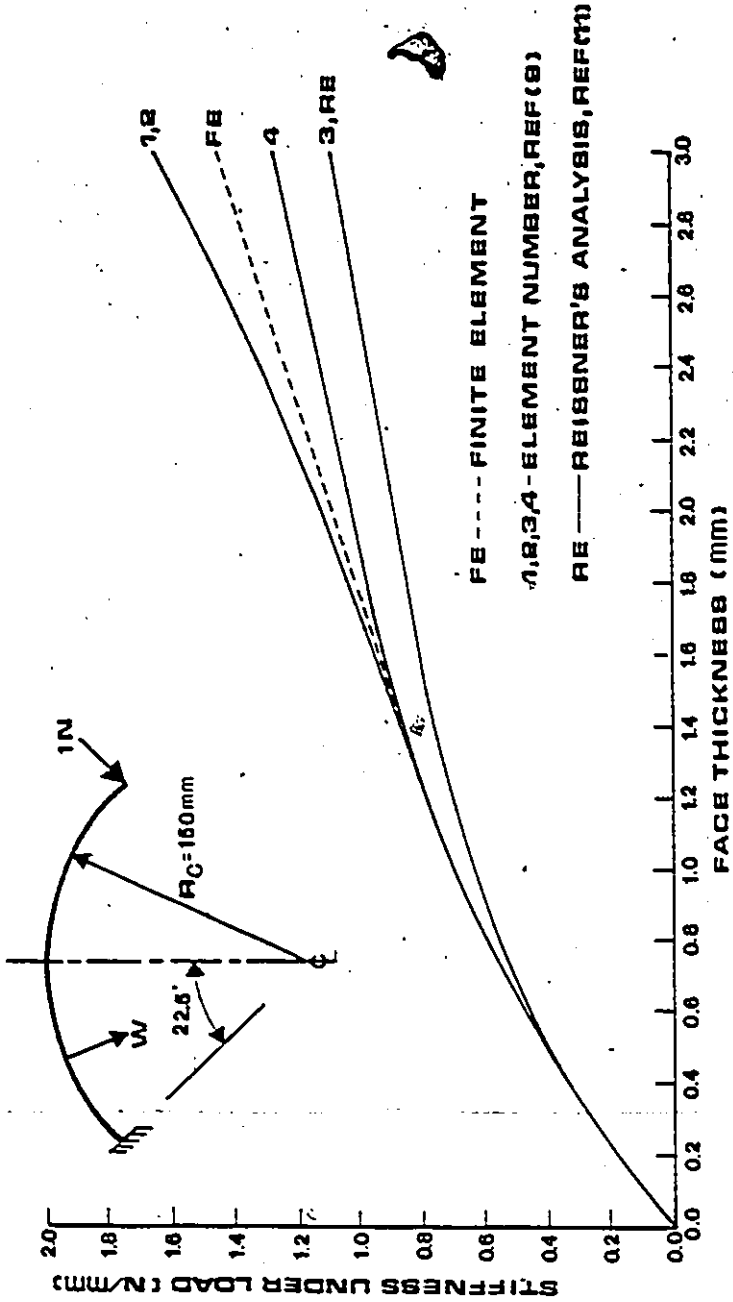

FIGURE.10 VARIATION OF STIFFNESS WITH FACEPLATE THICKNESS
(1in=26.4 mm , 1lb=4.45 N.)

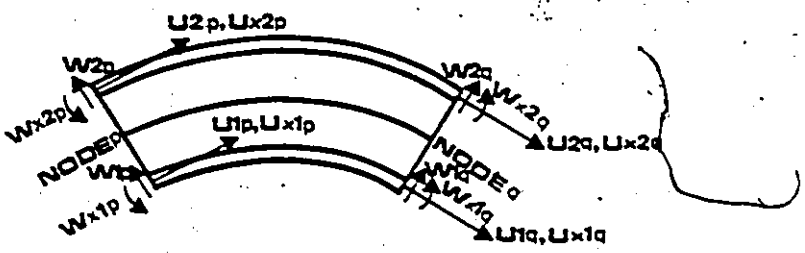

FIGURE.11 DISPLACEMENTS OF SANDWICH ARCH

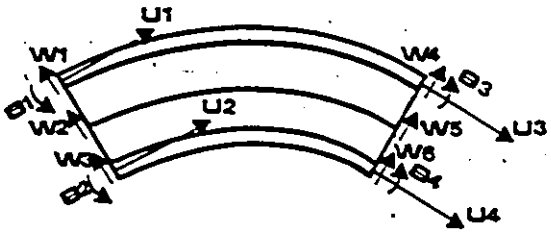

(a) ELEMENT 1

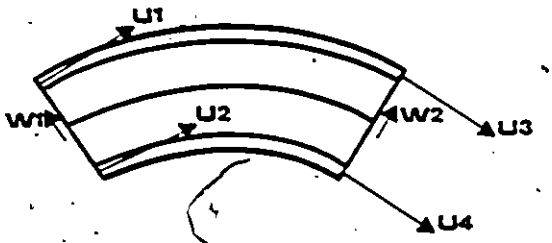

(b) ELEMENT 3

FIGURE.12 SANDWICH ARCH ELEMENT AFTER HOLT [9]

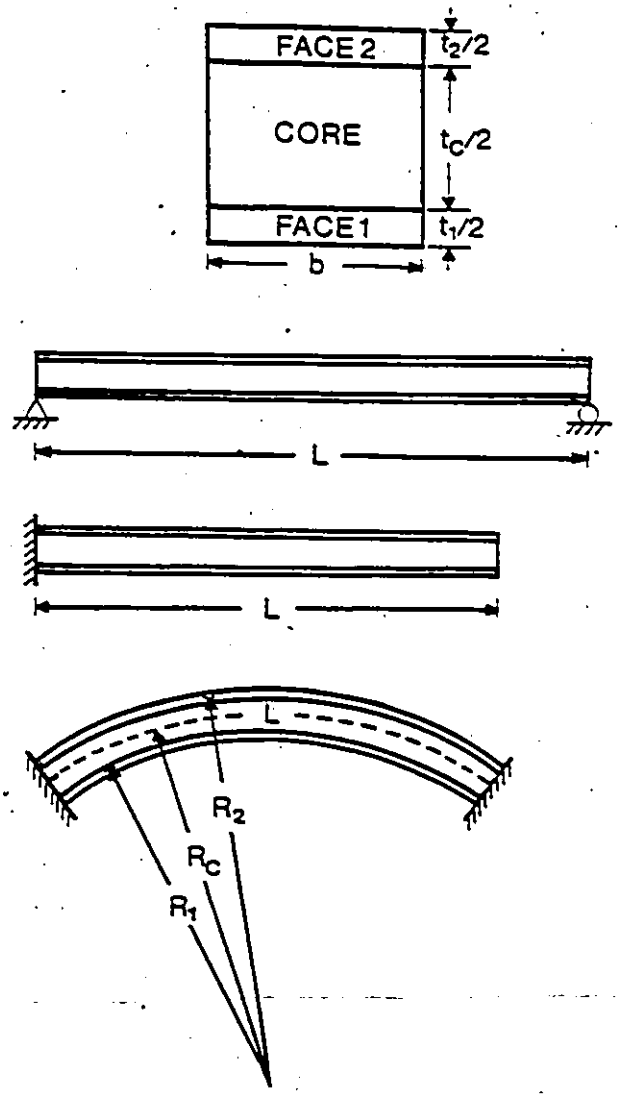

FIGURE.13 STRAIGHT AND CURVED SANDWICH BEAMS

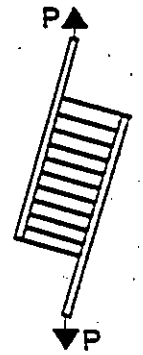

(a) SINGLE-BLOCK SHEAR TEST

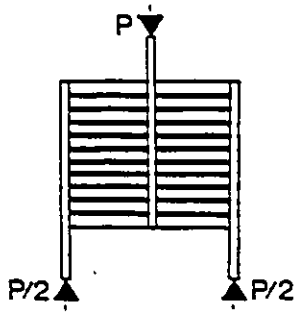

(b) DOUBLE-BLOCK SHEAR TEST

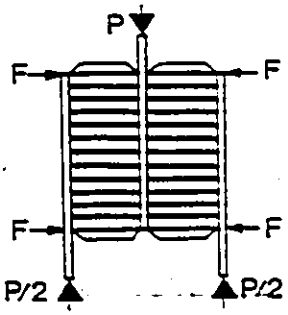

(c) DOUBLE-BLOCK SHEAR TEST WITH BRIDGE-PIECES

FIGURE 14 · BLOCK SHEAR TESTS

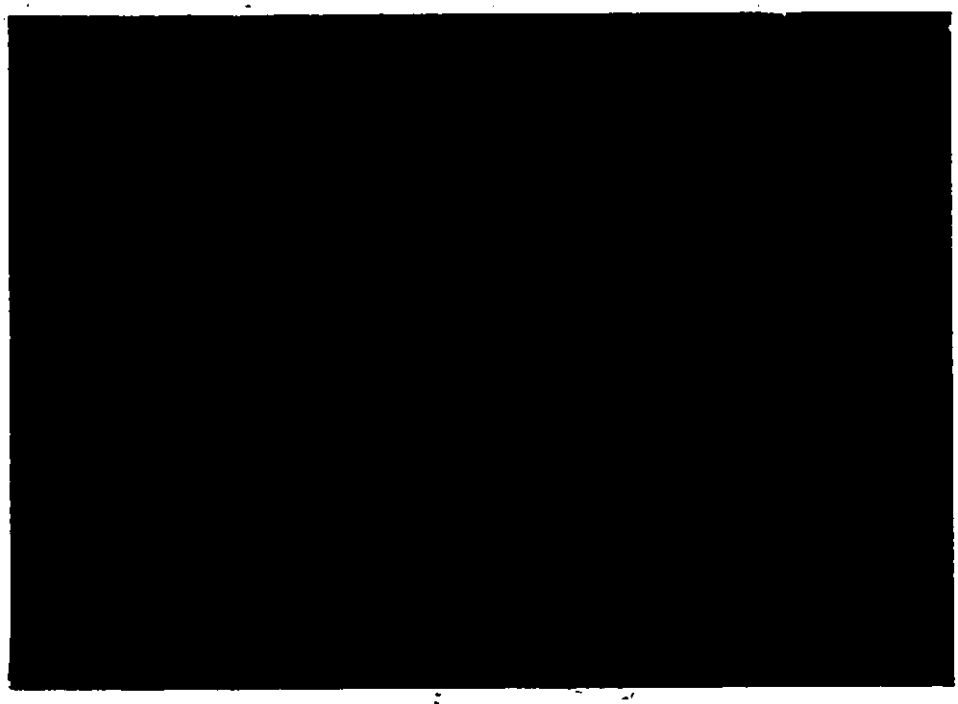

FIGURE 15. THREE-POINT TEST OF POLYSTYRENE SANDWICH BEAM (TYPICAL FOR BEAMS T1, T2, T3, AND T4).

FIGURE 16. FOUR-POINT TEST OF POLYSTYRENE SANDWICH BEAM (BEAM T5).

FIGURE 17. SIX-POINT TEST OF POLYSTYRENE SANDWICH BEAM (BEAM T6).

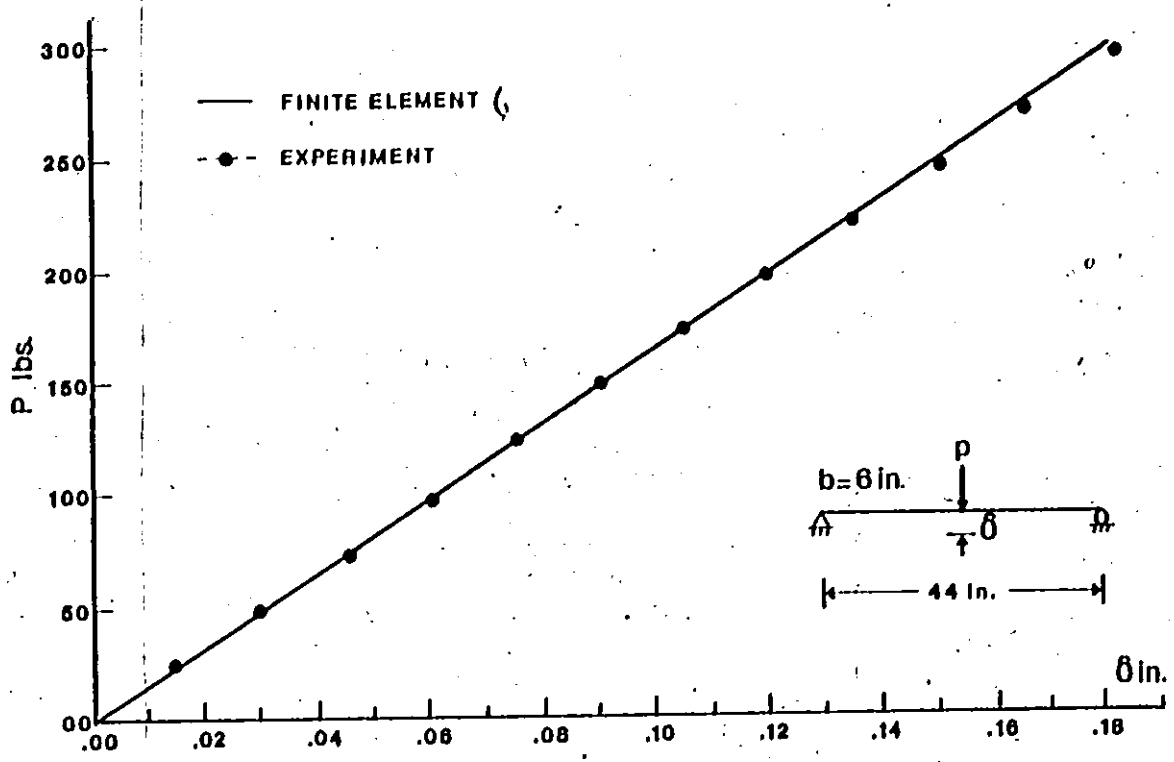

FIGURE.18 LOAD_DEFLECTION CURVE OF THE SANDWICH BEAM T1

(1 In= 25.4 mm.; 1 lb=4.45 N.)

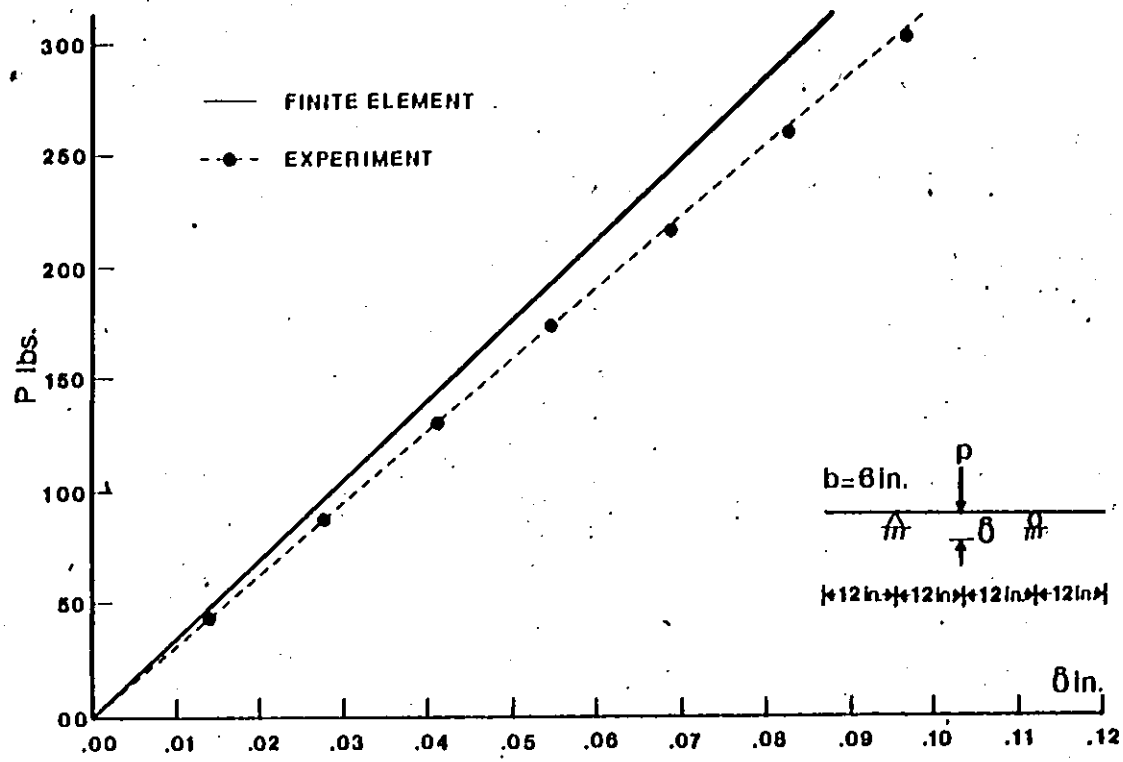

FIGURE.19 LOAD_DEFLECTION CURVE OF THE SANDWICH BEAM T2

(1 in.= 25.4 mm.; 1 lb=4.45 N.)

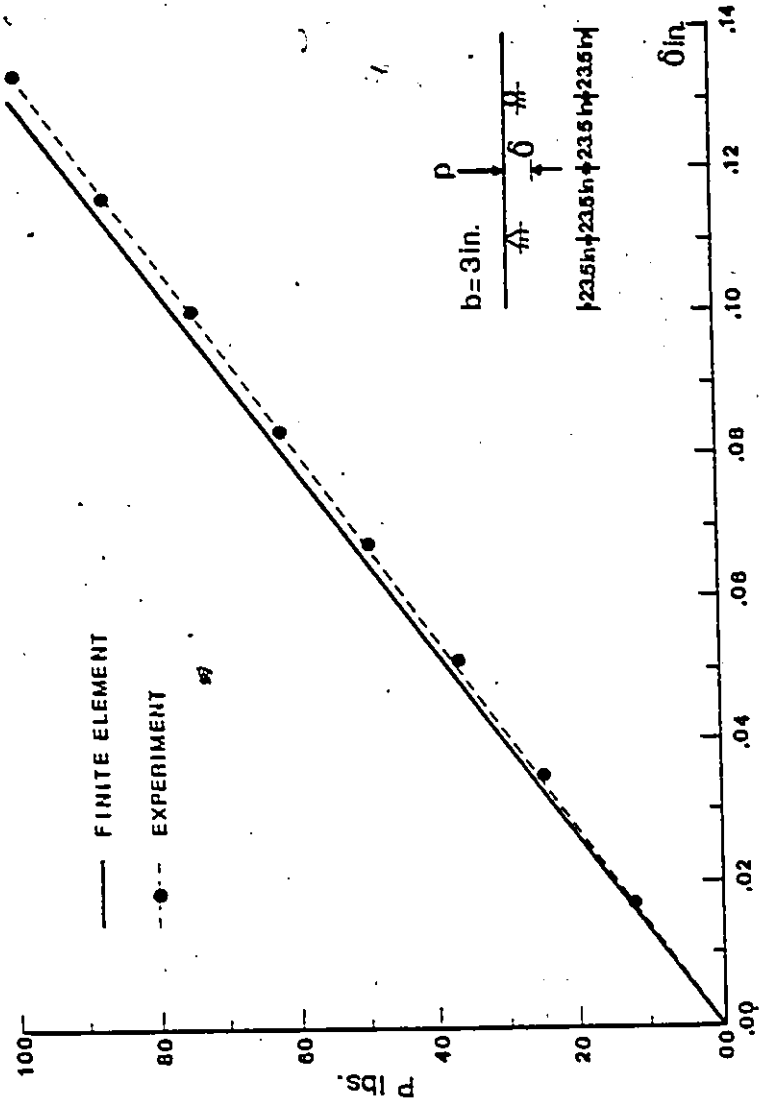

FIGURE 20 LOAD_DEFLECTION CURVE OF THE SANDWICH BEAM T3

(1 in.= 25.4 mm. ; 1 lb=4.46 N.)

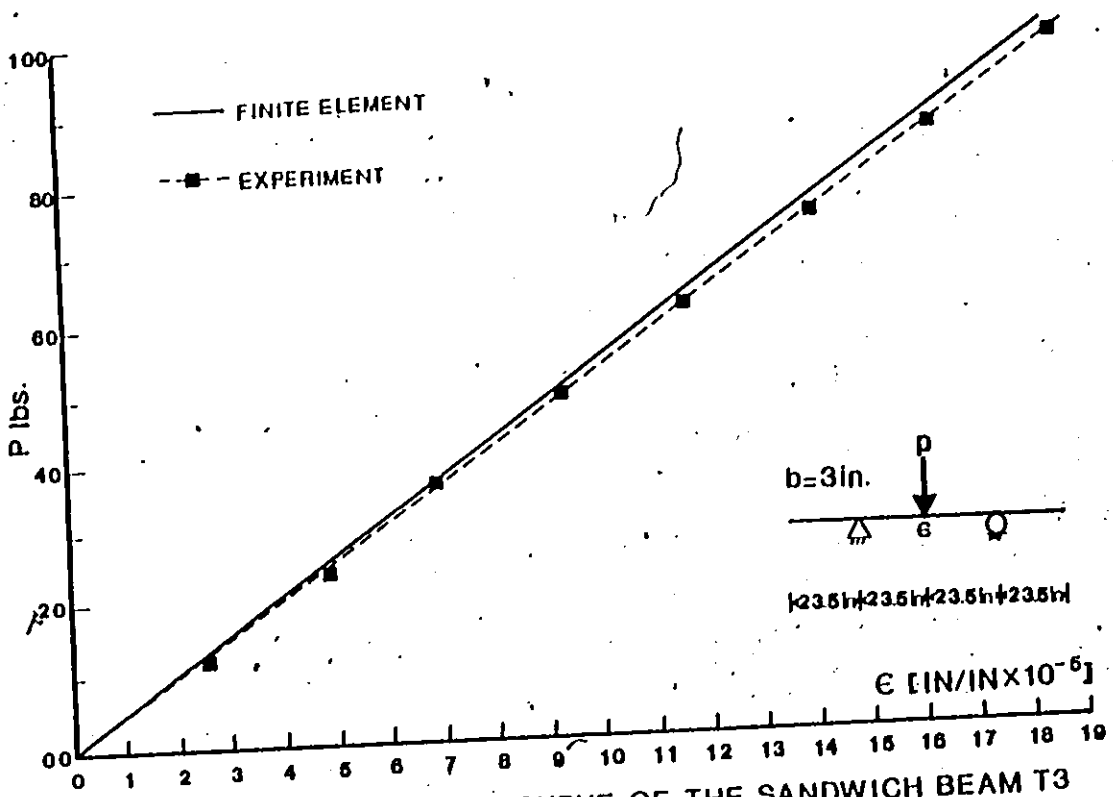

FIGURE.21 LOAD_STRAIN CURVE OF THE SANDWICH BEAM T3

(1 in.= 26.4 mm. ; 1 lb= 4.45 N.)

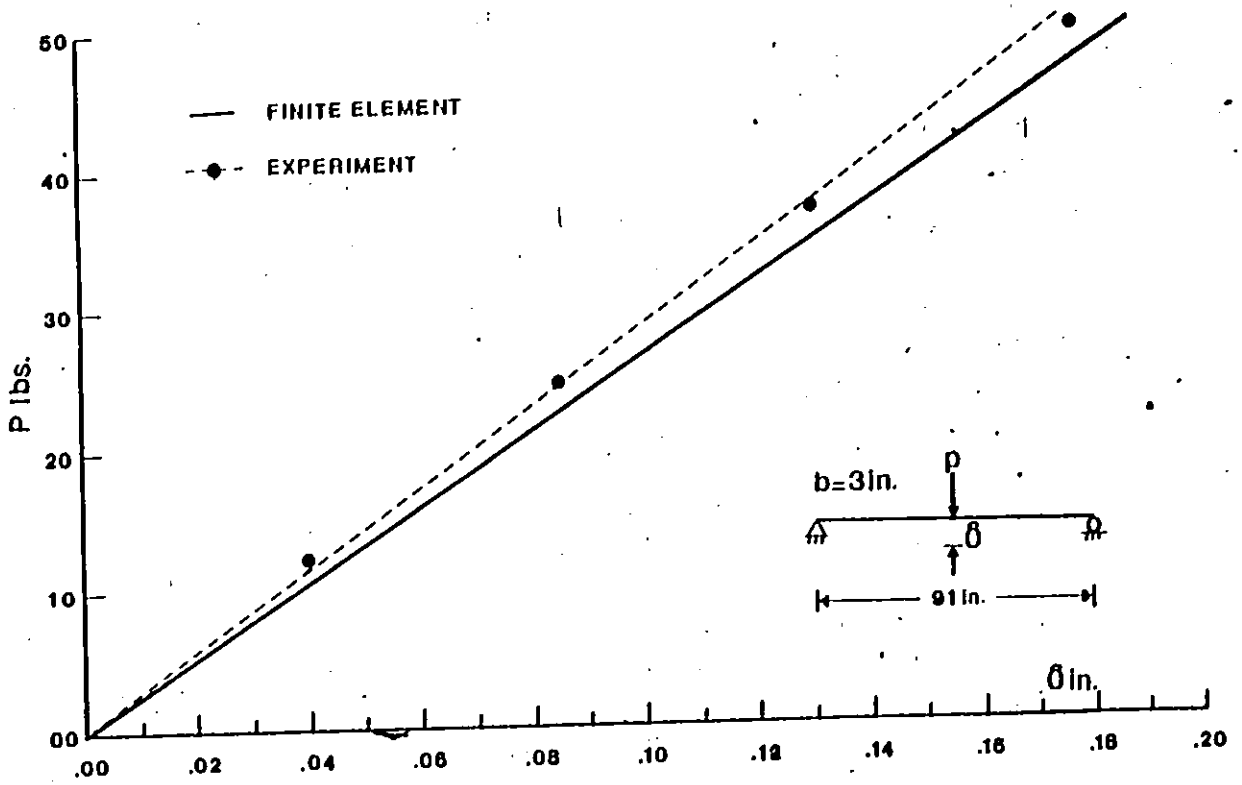

FIGURE.22LOAD_DEFLECTION CURVE OF THE SANDWICH BEAM T4
(1 in= 25.4 mm. ; 1lb=4.45 N.)

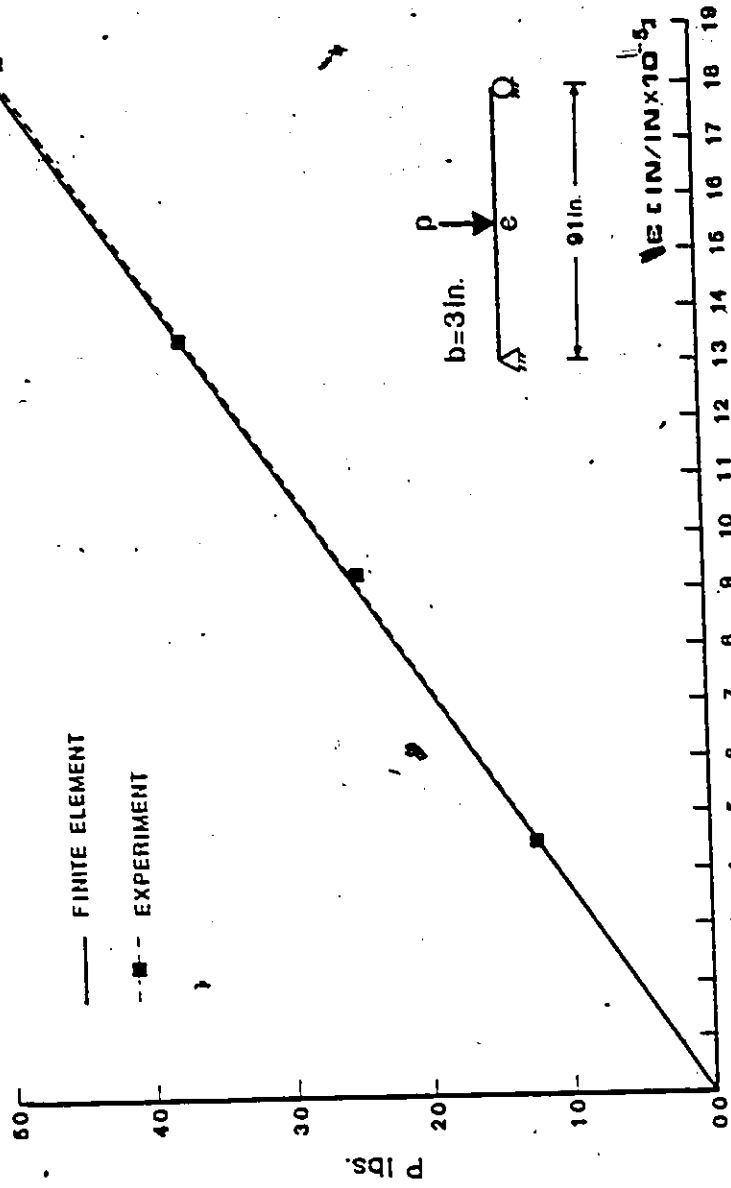

FIGURE.23 LOAD_STRAIN CURVE OF THE SANDWICH BEAM T4
(1 in.= 25.4 mm.; 1lb=4.45 N.)

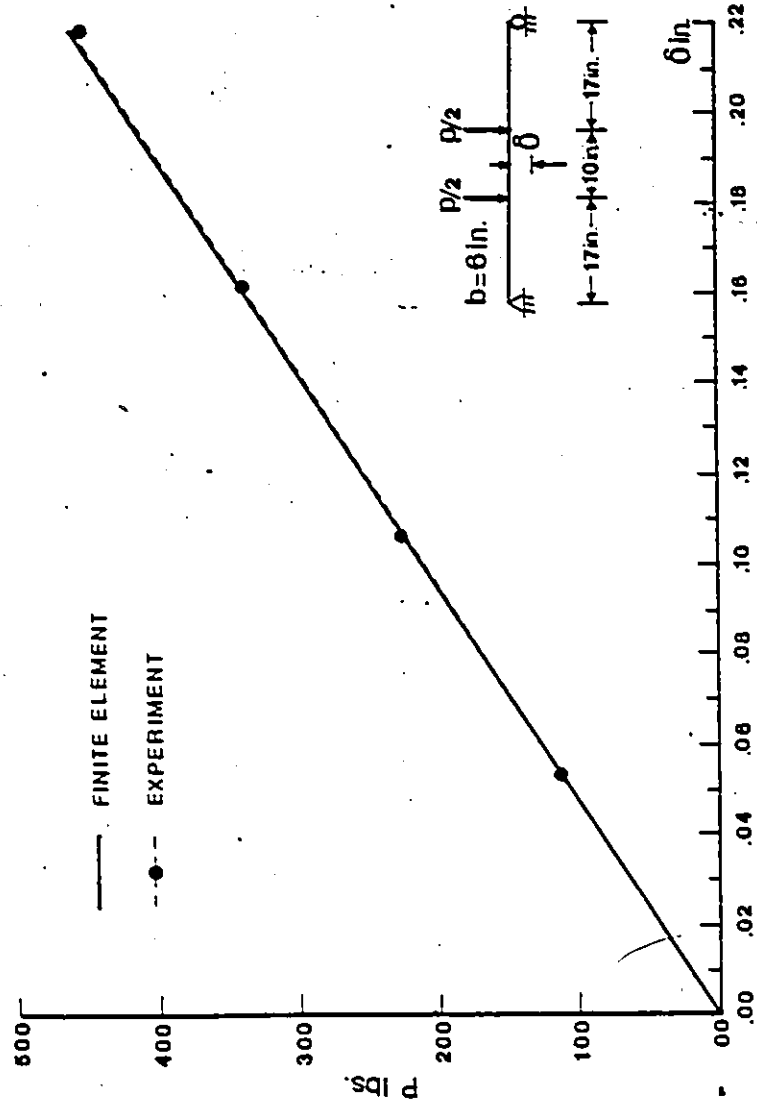

FIGURE.24 LOAD_DEFLECTION CURVE OF THE SANDWICH BEAM T6

(1 in.= 26.4 mm. ; 1 lb= 4.46 N.)

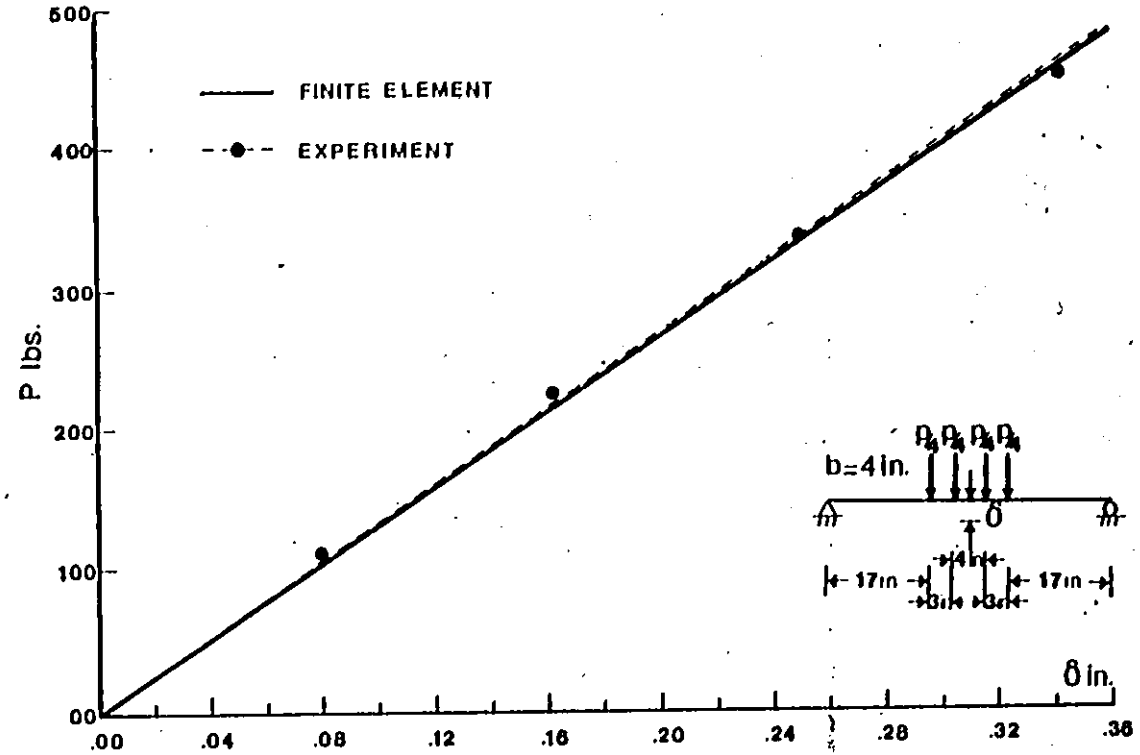

FIGURE.25 LOAD_DEFLECTION CURVE OF THE SANDWICH BEAM T6
(1 in.=25.4 mm.; 1 lb=4.45 N.)

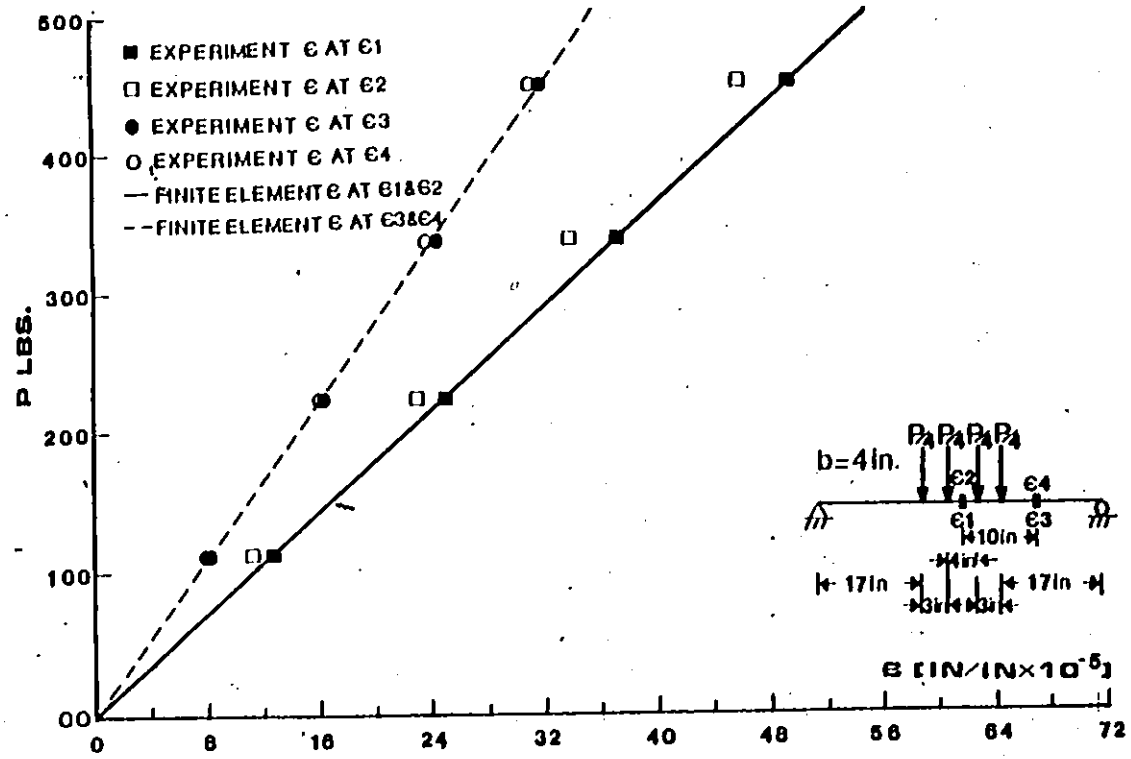

FIGURE.26 LOAD_STRAIN CURVE OF THE SANDWICH BEAM T6

(1 in.= 26.4 mm.; 1lb=4.45N.)

(a) Distant View

(b) Close-up

FIGURE 27. WRINKLING FAILURE - SPECIMEN T5

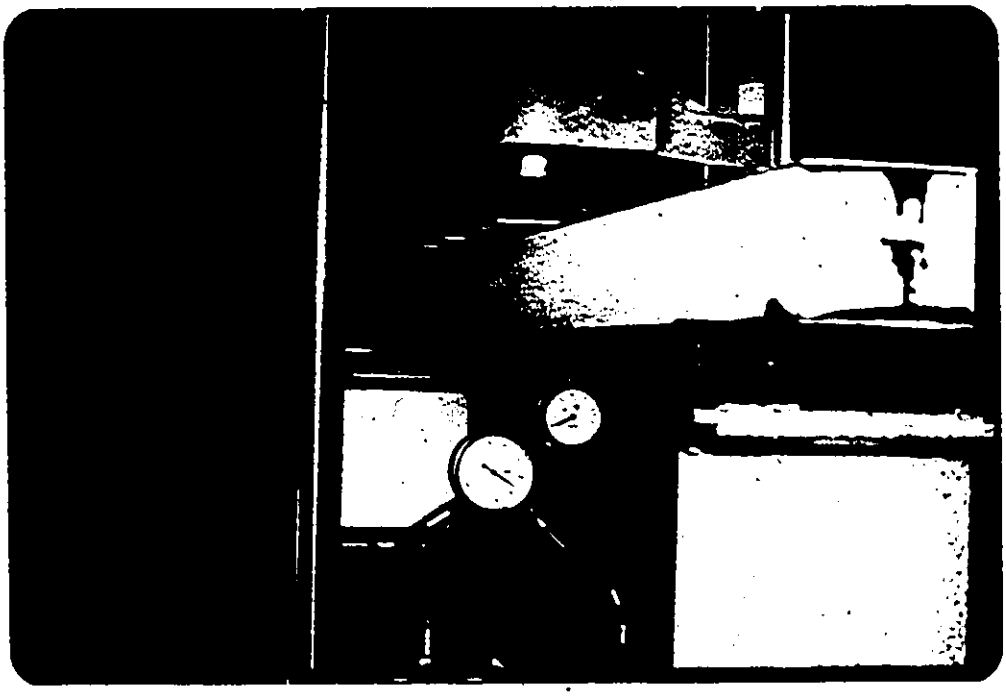

(a) Distant View

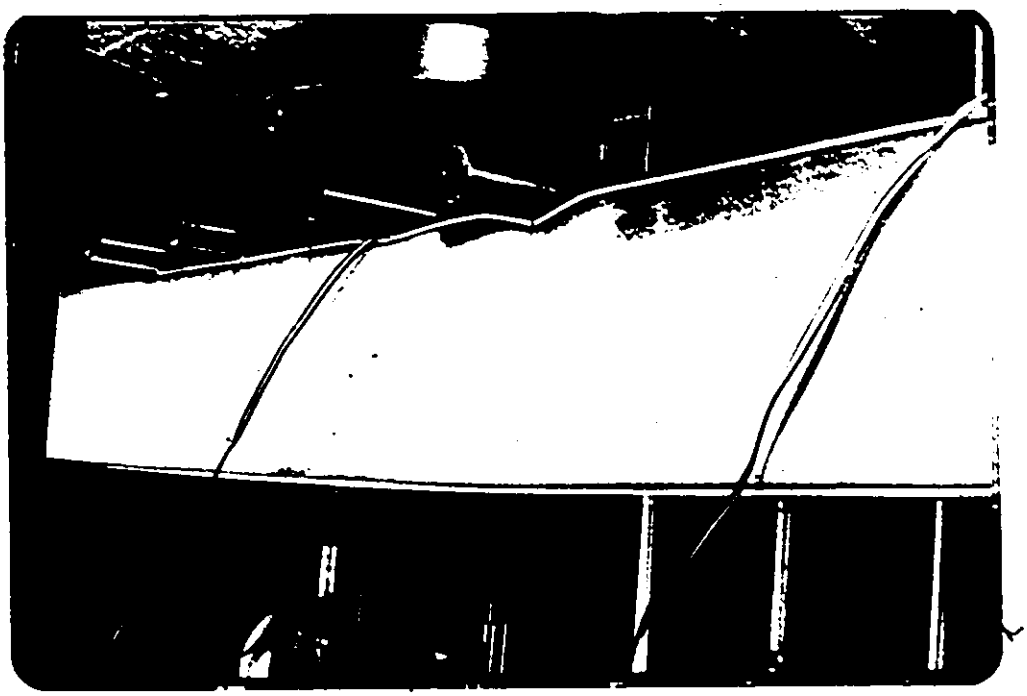

(b) Close-up

FIGURE 28. LOCAL FAILURE - SPECIMEN T6.

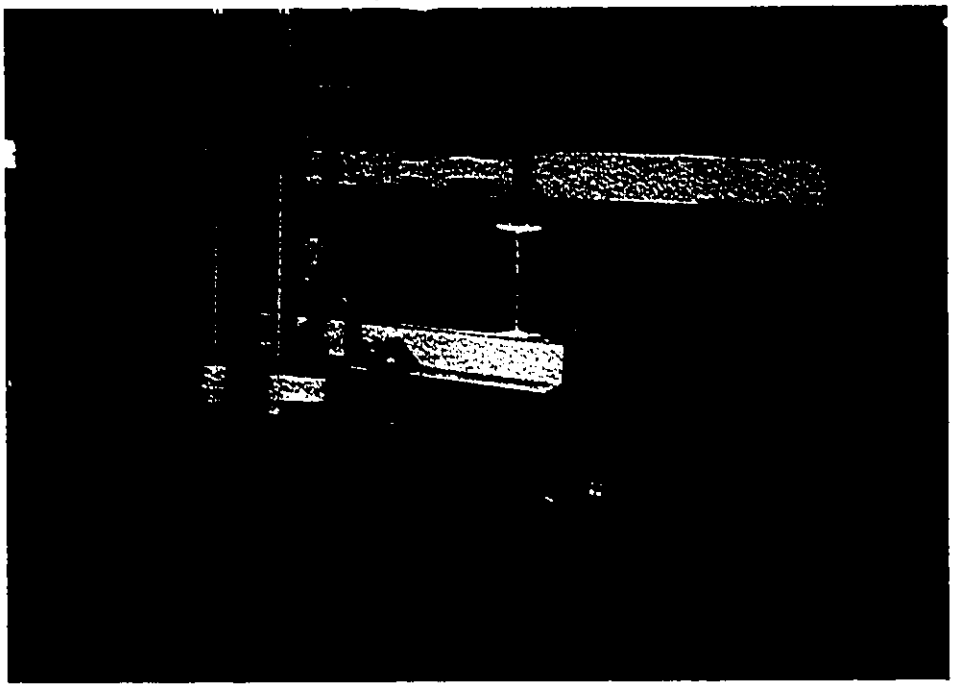

FIGURE 29. THREE-POINT TEST OF POLYSTYRENE SANDWICH BEAM WITH STIFFENERS (TYPICAL FOR BEAMS T7, T8 AND T9).

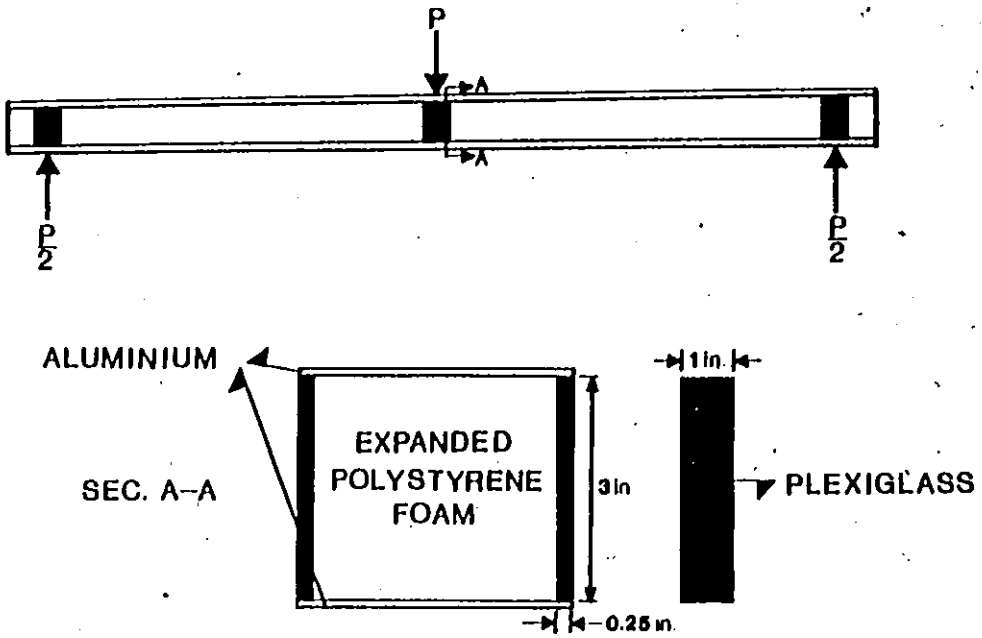

FIGURE. 30 TYPICAL STIFFENERS USED AT LOADING AND SUPPORT POINTS

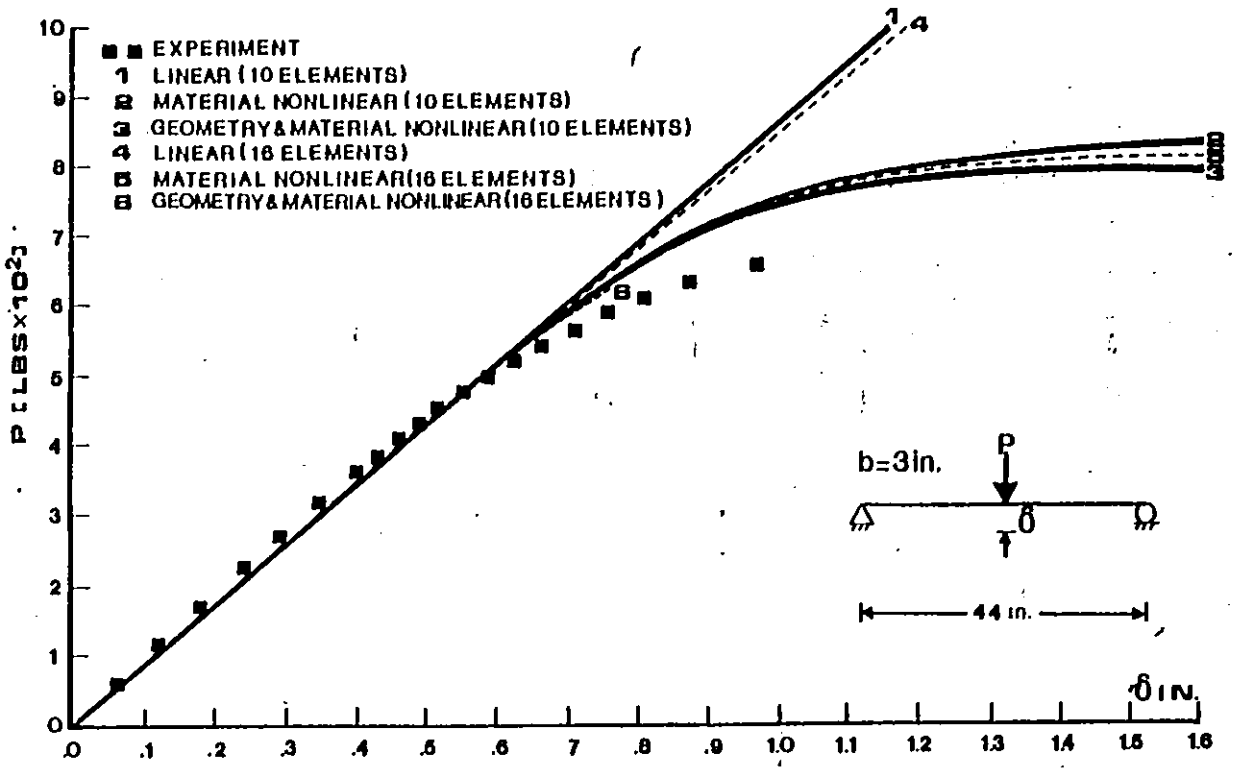

FIGURE.31 LOAD_DEFLECTION CURVE OF THE SANDWICH BEAM T7

(1 In.=25.4 mm. ; 1 lb=4.45 N.)

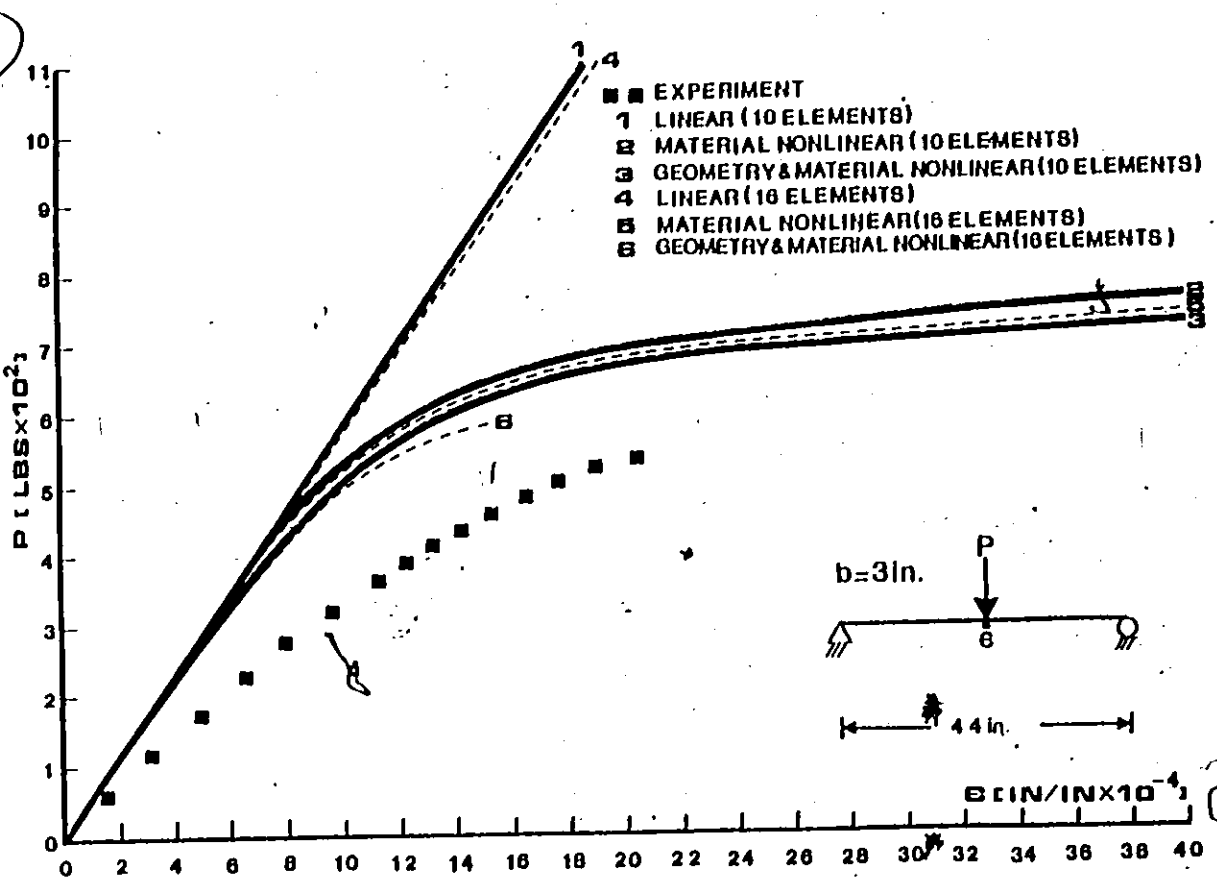

FIGURE.32 LOAD_STRAIN CURVE OF THE SANDWICH BEAM T7

(1 In.= 25.4 mm. ; 1 lb = 4.45 N.)

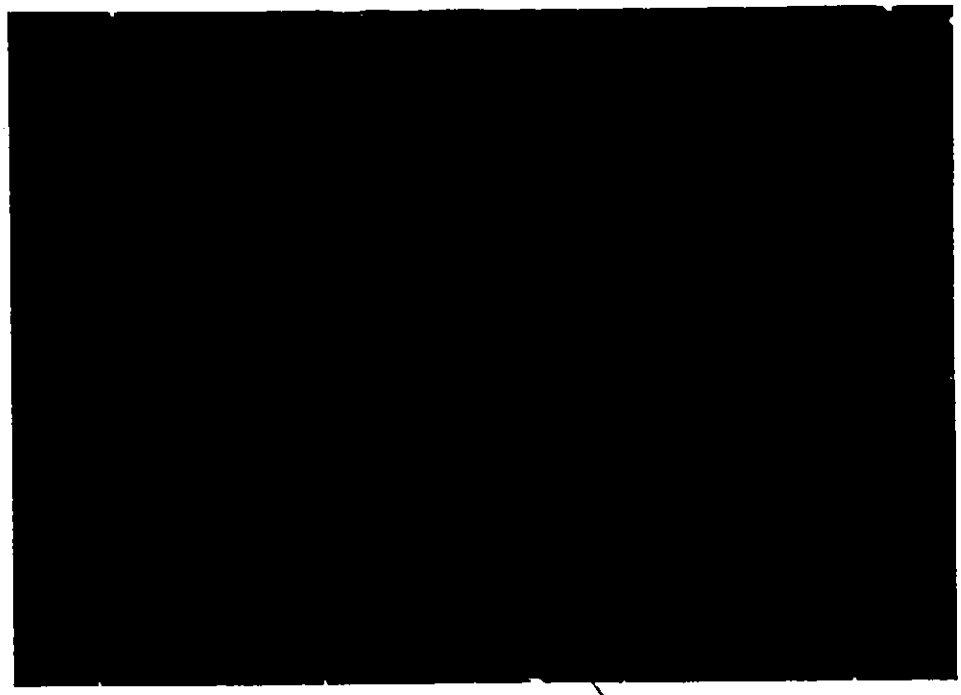

FIGURE 33. DELAMINATING FAILURE - SPECIMEN T7.

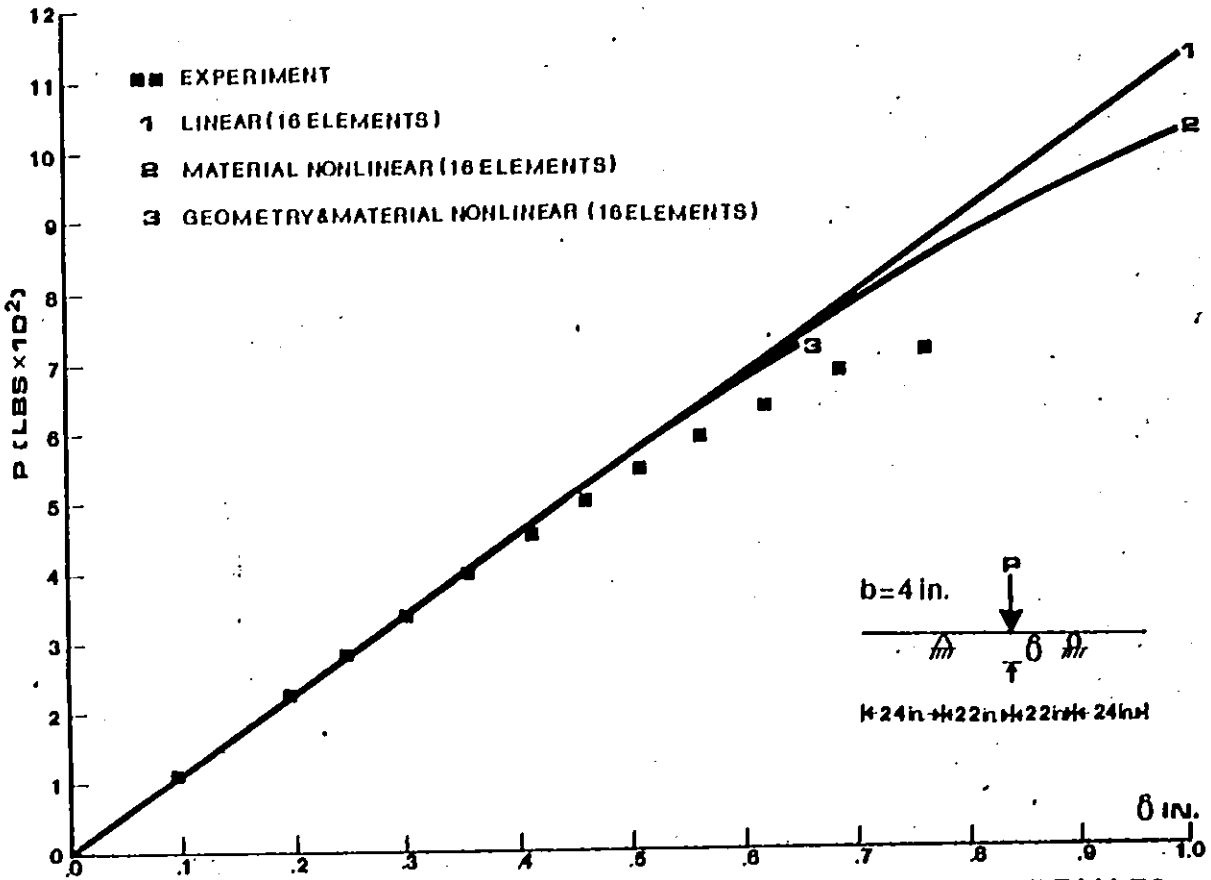

FIGURE.34 LOAD_DEFLECTION CURVE OF THE SANDWICH BEAM T8
(1 in.= 25.4 mm.; 1 lb=4.45 N.)

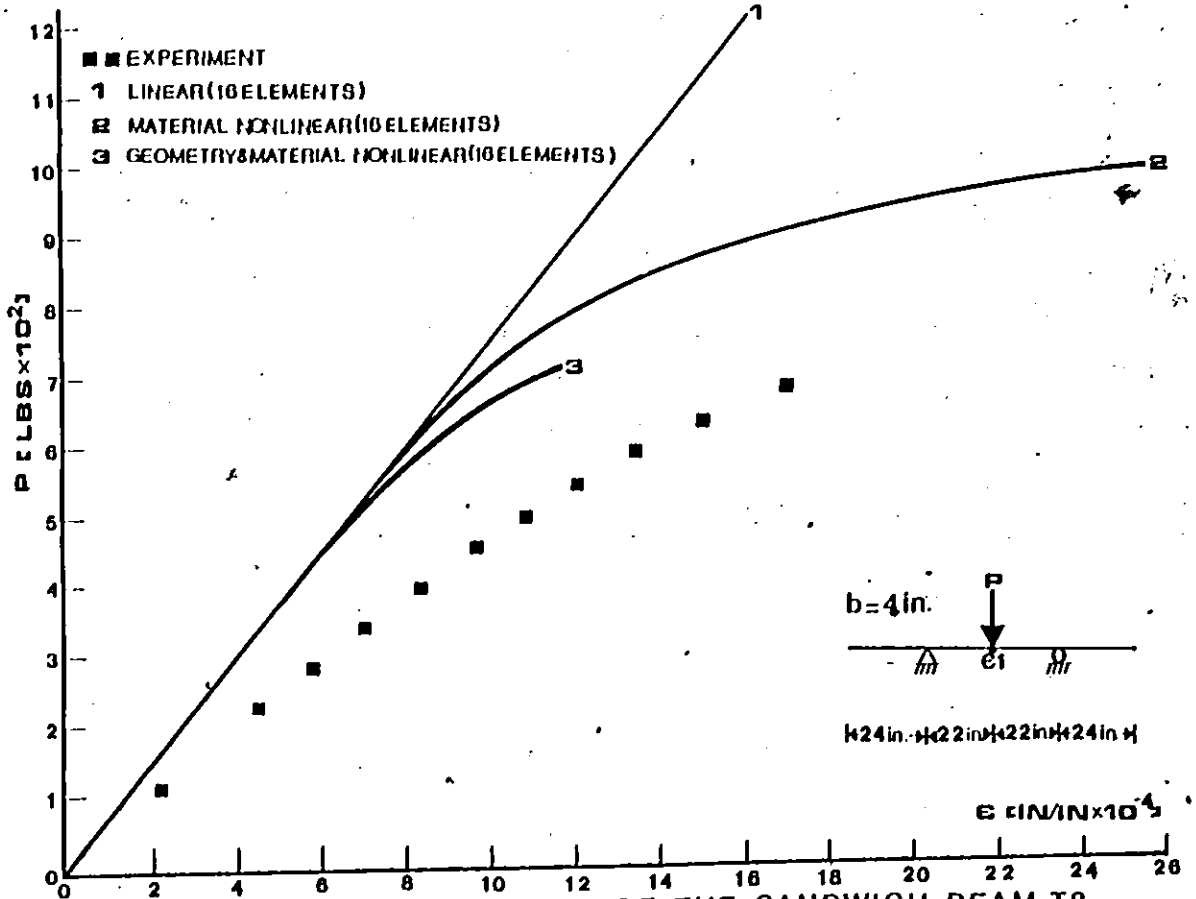

FIGURE.35 LOAD_STRAIN CURVE OF THE SANDWICH BEAM T8.
(1 in.= 25.4 mm. ; 1 lb= 4.45 N.)

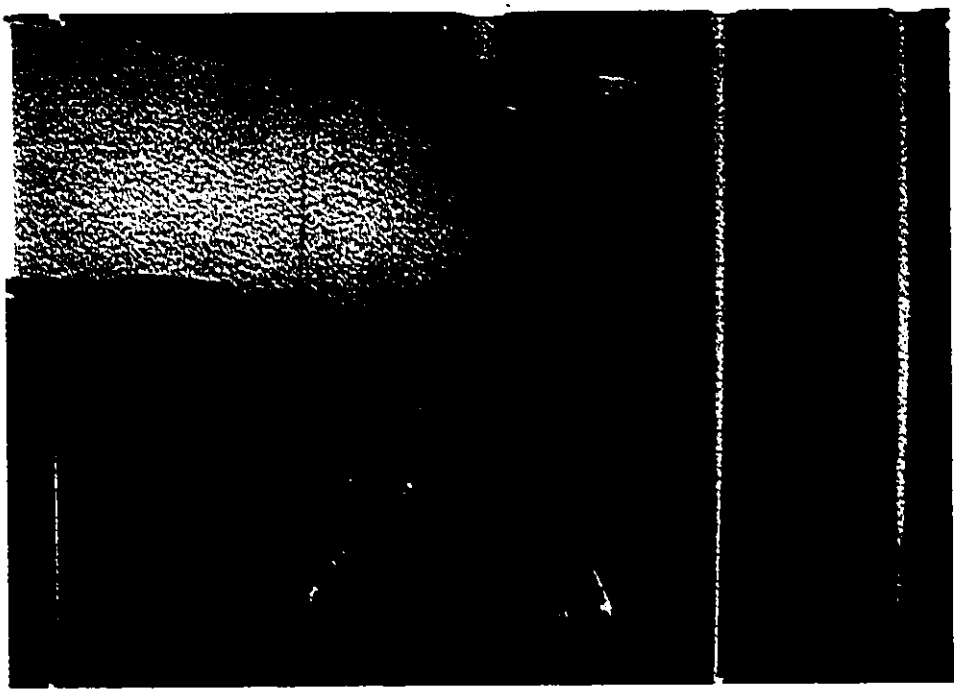

FIGURE 36. DELAMINATING FAILURE - SPECIMEN T8.

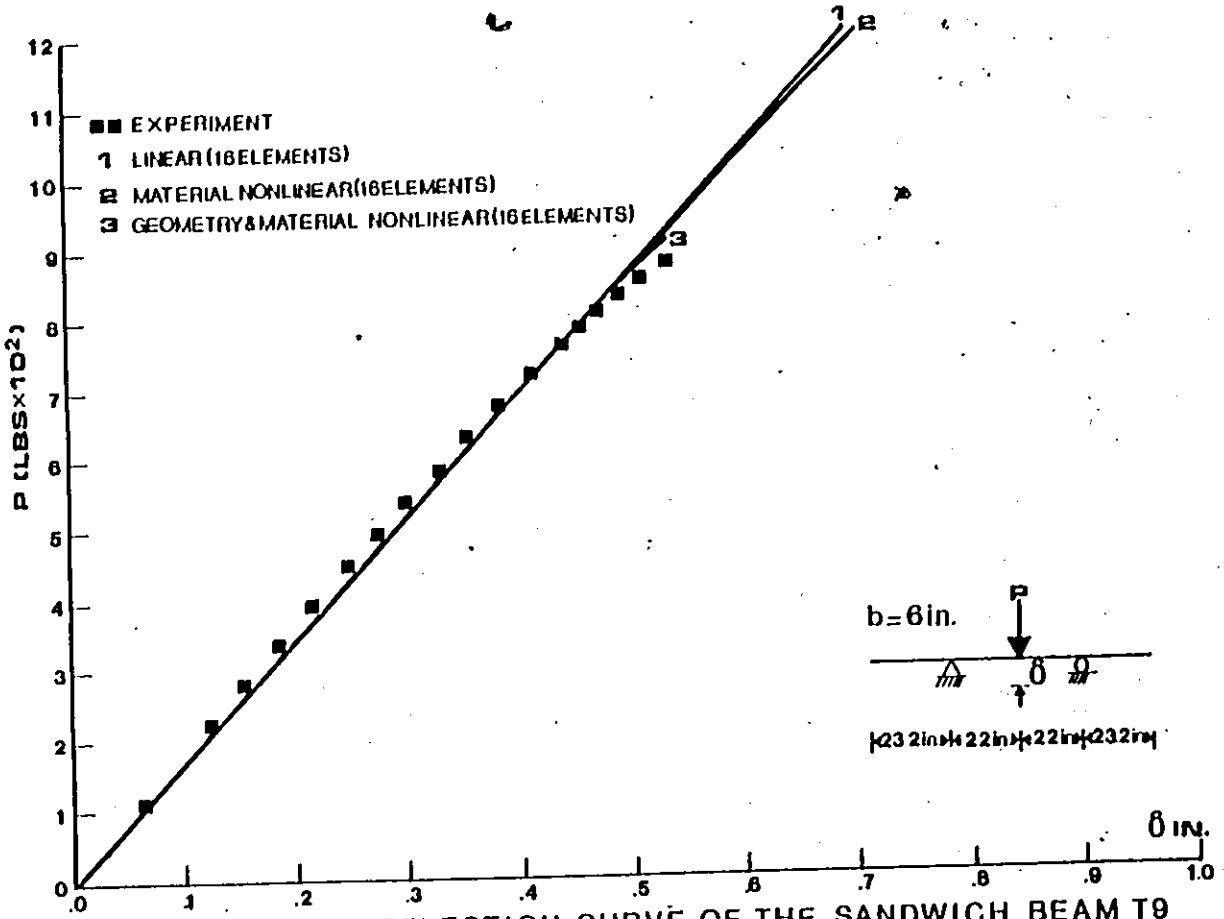

FIGURE.37 LOAD_DEFLECTION CURVE OF THE SANDWICH BEAM T9
(1in.=25.4 mm. ; 1lb=4.45 N.)

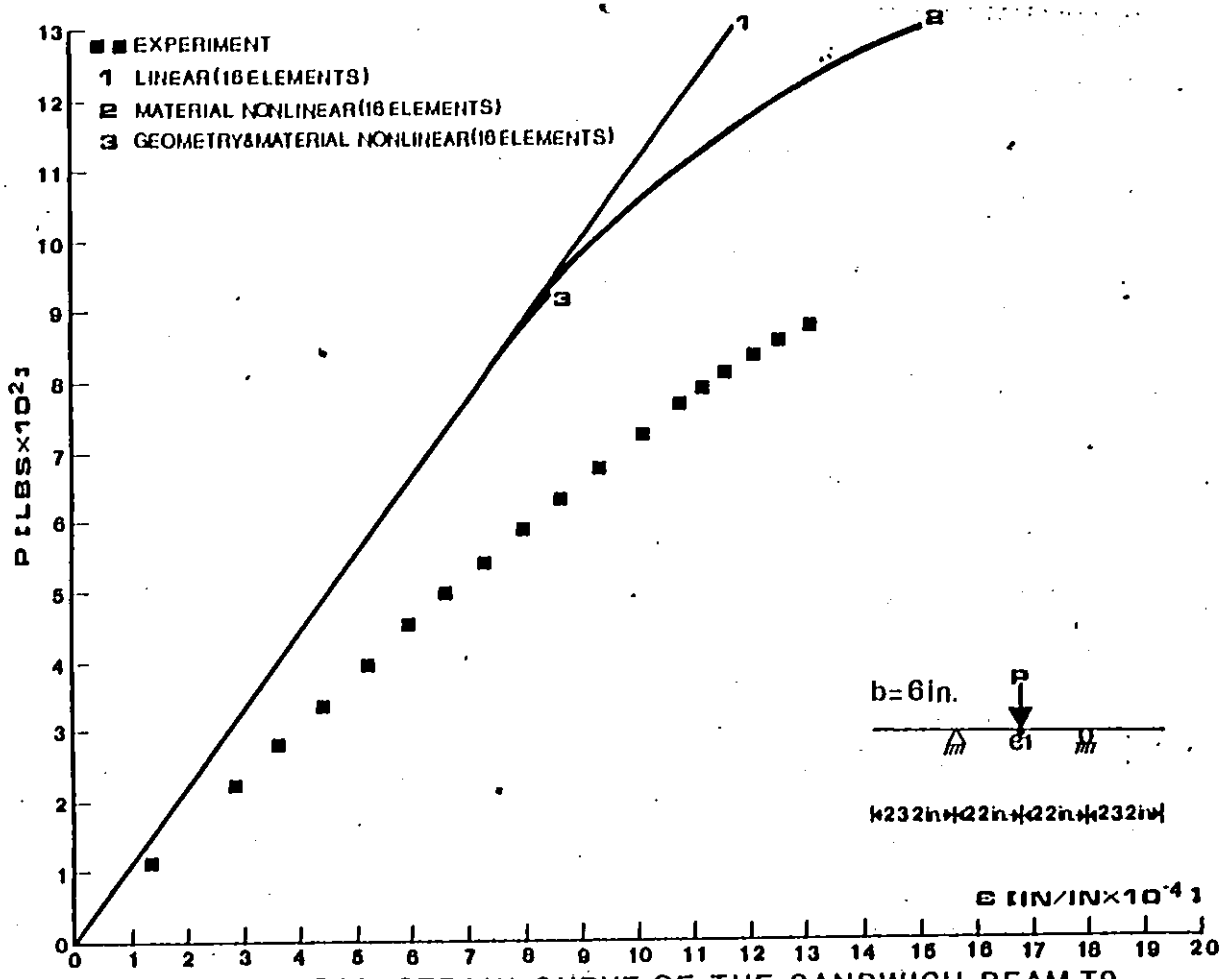

FIGURE.38 LOAD_STRAIN CURVE OF THE SANDWICH BEAM T9

(1in.= 25.4 mm. ; 1lb = 4.45 N.)

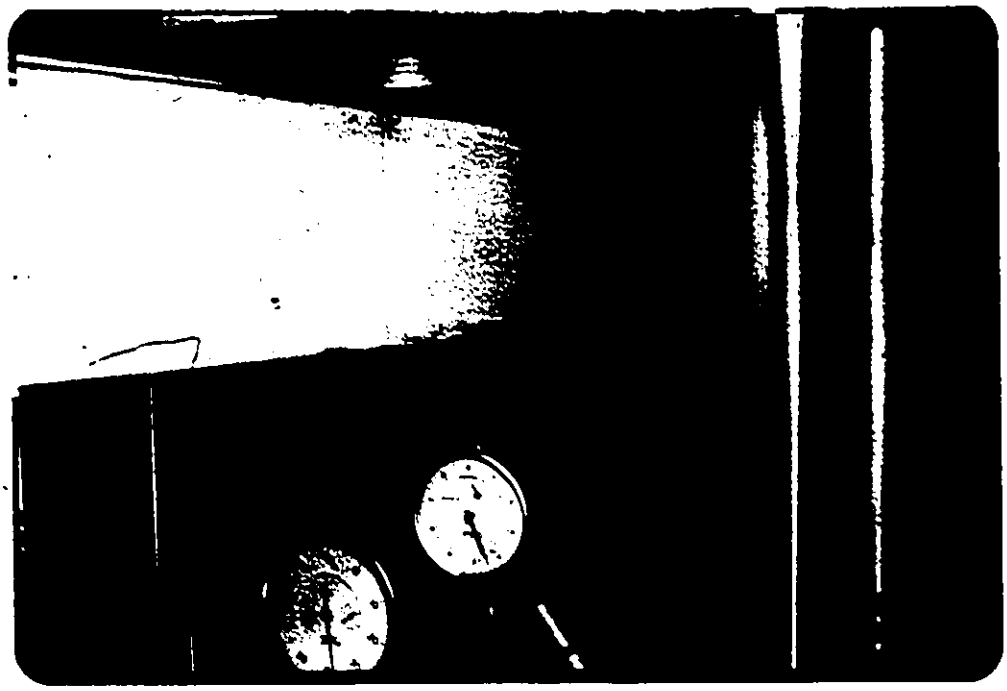

FIGURE 39. DELAMINATING FAILURE - SPECIMEN T9.

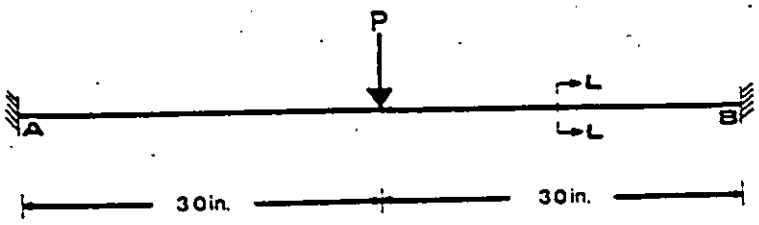

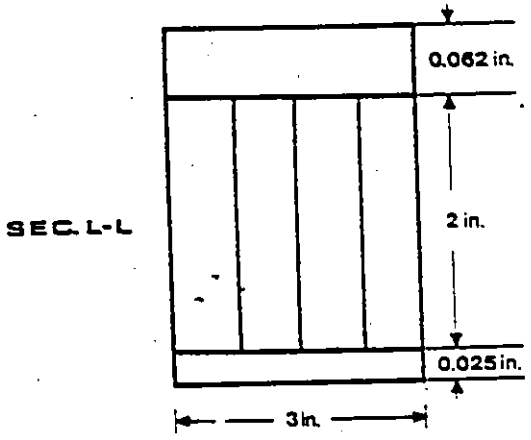

FIGURE. 40 CLAMPED SANDWICH BEAM WITH UNEQUAL FACE THICKNESSES

(1 in. = 25.4 mm.)

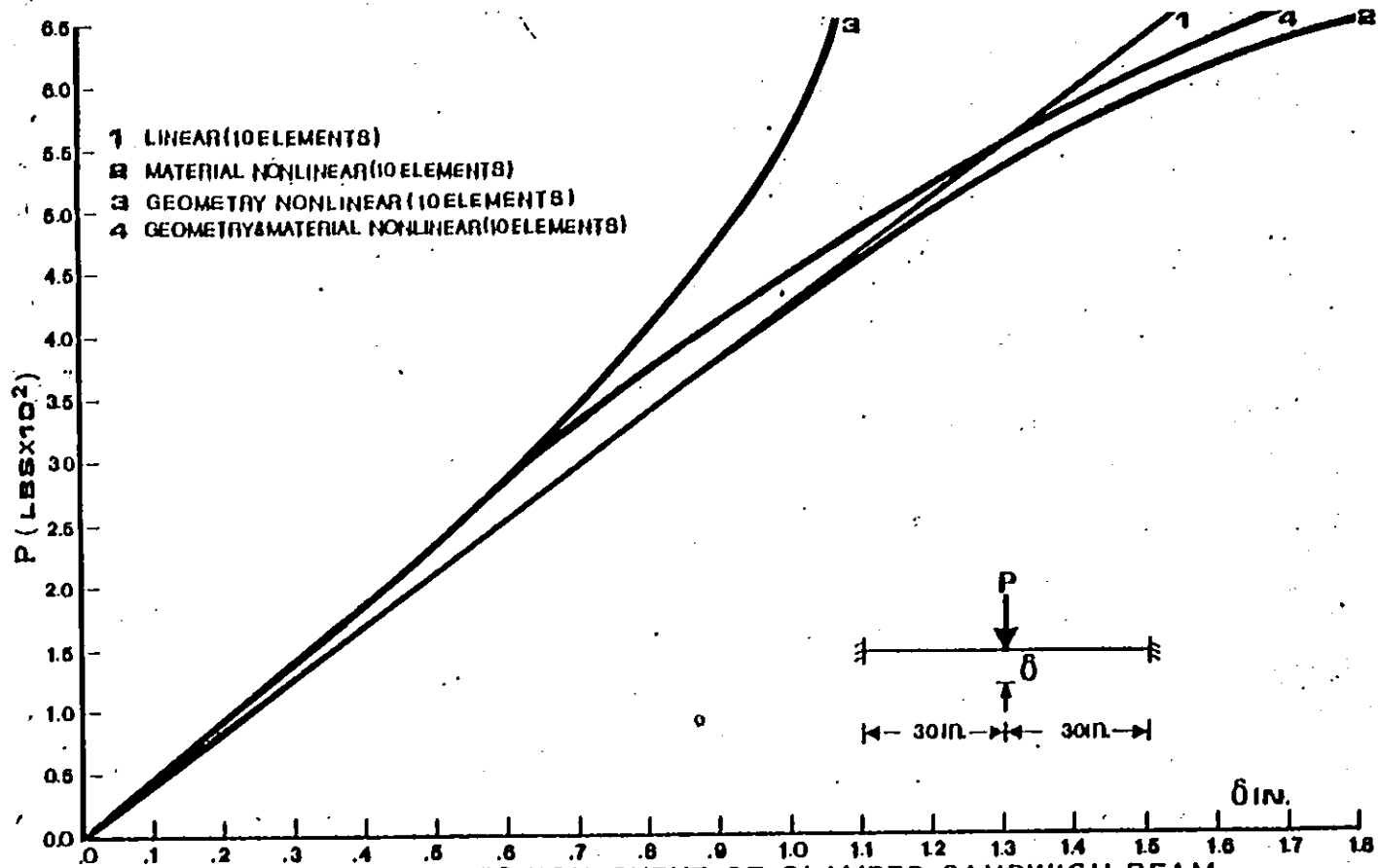

FIGURE.41 LOAD_DEFLECTION CURVE OF CLAMPED SANDWICH BEAM
(1 in. = 25.4 mm.; 1 lb = 4.45 N.)

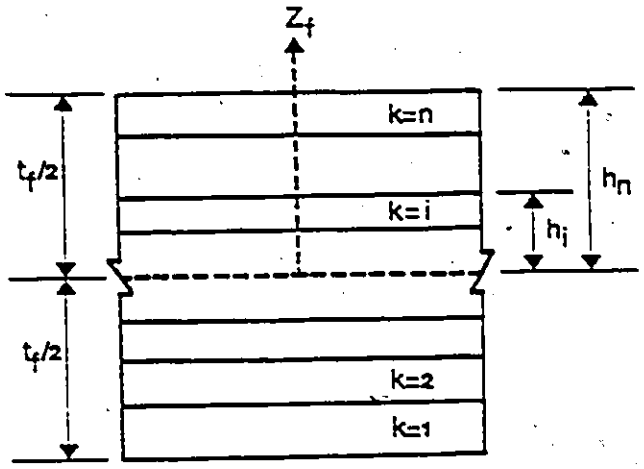

(a) CROSS-SECTION OF LAMINATED FACE

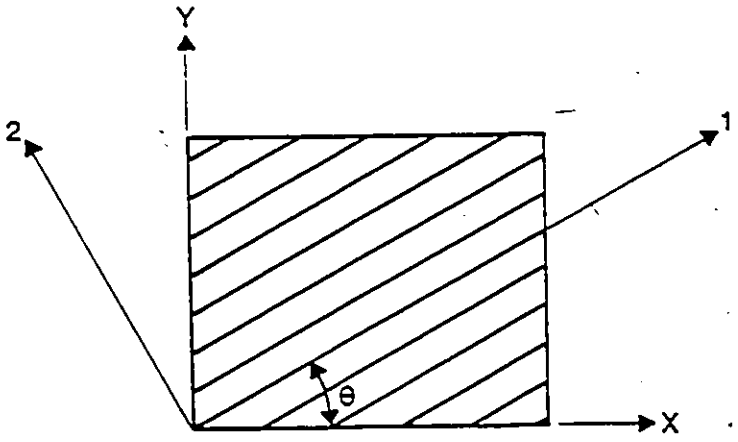

(b) ORIENTATION OF AXES

FIGURE.42 LAMINATED FACE

TABLES

TABLE 1

STIFFNESSES OF A SANDWICH BEAM WITH THICK LAMINATED FACES

θ	FACES						CORE
	Membrane Stiffnesses x 10^6 lb.		Coupling Stiffnesses x 10^6 lb. in.		Bending Stiffnesses x 10^6 lb. $in.^2$		Shear Stiffnesses x 10^6 lb.
	A_1	A_2	B_1	B_2	D_1	D_2	B_c
0°	30	60	0	0	0.625	5	0.060
30°	16.433	32.866	1.696	-6.784	0.342	2.739	0.060
60°	15.501	31.001	1.812	-7.250	0.323	2.583	0.060
90°	15.375	30.750	1.828	-7.313	0.320	2.563	0.060

TABLE 2

DEFLECTIONS OF A SANDWICH BEAM WITH THICK LAMINATED FACES

θ	w (inches)			
	Finite Element Method			Ref. 26
	4 elements	8 elements	12 elements	Exact Solution
0°	0.01822	0.01826	0.01826	0.01826
30°	0.03782	0.03811	0.03816	0.03872
60°	0.04407	0.04457	0.04468	0.04471
90°	0.04517	0.04571	0.04583	0.04587

TABLE 3

NATURAL FREQUENCIES (HZ) OF A STRAIGHT, SIMPLY SUPPORTED SANDWICH BEAM

Mode No.	Finite Element Method			Ref. 19			Ref. 18	Mead Results (Ref. 27)			
	4 elements	6 elements	10 elements	4 elements	6 elements	10 elements	15 elements	Exact Solution	Modified Stodola Frequencies		
									Cubic	Simpson	Trapezoidal
1	57.13	57.13	57.13	55.5	55.5	55.5	57.5	56.03	56.00	56.00	56.02
3	466.54	464.92	464.67	453.0	451.0	451	467	457.12	456.86	456.89	459.14
5	1142.60	1109.10	1105.10	1112.0	1077.0	1073.0	1111.0	1090.26	1089.92	1090.12	1107.70
7	2171.50	1860.70	1832.70	2242.0	1807.0	1779.0	1842.0	1809.8	1811.60	1811.60	1876.30
9	2563.50	2563.60	2563.70	2741.0	2580.0	2510.0	2594.0	2549.5	2561.30	2555.60	2723.00

TABLE 4

NATURAL FREQUENCIES (HZ) OF A STRAIGHT, CANTILEVER SANDWICH BEAM

Mode No.	Finite Element Method		Ref. 19		Ref.18	Ref. 22		Mead Results (Ref. 27)			
								Total Number of Iterations			
	8 Elements	10 Elements	8 Elements	10 Elements	10 Elements	Beam Approx.	Proposed Formula	r=20	r=15	r=10	r=5
1	33.76	33.76	32.79	32.79	33.97	34.35	33.71	34.242	34.29	34.13	34.30
2	199.34	199.23	193.6	193.5	200.5	215.3	203.4	201.85	202.38	202.05	204.76
3	514.58	513.89	499	499	517	602.8	525.6	520.85	521.68	527.37	523.46
4	914.26	912.18	888	886	918	1181	934.3	925.40	925.74	951.90	823.40
5	1364.10	1359.6	1325	1320	1368	1953	1387	1381.3	1382	1452	1974.6

TABLE 5

NATURAL FREQUENCIES (HZ) OF A CURVED, CLAMPED-CLAMPED SANDWICH BEAM

Mode No.	Finite Element Method			Ref. 19			Ref. 18
	6 elements	8 elements	10 elements	6 elements	8 elements	10 elements	10 elements
1	244.86	244.72	244.64	240	240	240	264
2	492.03	489.88	488.67	477	475	474	522
3	878.27	871.47	867.99	853	846	843	889
4	1314.50	1298.60	1291.20	1276	1261	1253	1312
5	1790.50	1760.60	1747.50	1738	1709	1697	1767

LIST OF REFERENCES

LIST OF REFERENCES

1. Hoff, N. J. and Mautner, S. E., "Bending and Buckling of Sandwich Beams," J. of Aero. Sci., Vol. 15, No. 12, December 1948, pp. 707-720.

2. Yu, Y. Y., "A New Theory of Elastic Sandwich Plate - One Dimensional Case," J. Appl. Mech. Vol. 26, 1959, pp. 415-421.

3. Krajcinovic, D., "Sandwich Beams with Arbitrary Boundary Conditions," ASME, Paper No. 74-WA/De-11, July 1974.

4. Krajcinovic, D., "Sandwich Beam Analysis," Journal of Applied Mechanics, Trans. ASME, Vol. 38, 1971, pp. 773-778.

5. Ogorkiewicz, R. M. and Sayigh, A.A.M., "Plastics Sandwich Beams Under Bending Loads of Short Duration," Journal of Mechanical Engineering Science, Vol. 9, No. 5, 1967, pp. 355-361.

6. Ogorkiewicz, R. M. and Sayigh, A.A.M., "Deflection of Carbon Fibre/Acrylic Foam Sandwich Beams," Composites, Vol. 4, No. 6, November 1973, pp. 254-257.

7. Sayigh, A.A.M., and Ogorkiewicz, R. M., "Bending of Plastics Sandwich Beam Under Uniformly Distributed Loads," Engineer, Vol. 223, 1967, pp. 303-306.

8. Holt, P. J. and Webber, J.P.H., "Exact Solutions to some Honeycomb Sandwich Beam, Plate, and Shell Problems," J. Strain Analysis, Vol. 17, No. 1, January 1982, pp. 1-8.

9. Holt, P. J. and Webber, J.P.H., "Finite Elements for Curved Sandwich Beams," Aeronautical Quarterly, XXVIII, May 1977, pp. 123-141.

10. Abel, J. F., "Static and Dynamic Analysis of Sandwich Shells with Viscoelastic Damping," presented to the Dept. of Civil Engineering, at the Univ. of California at Berkeley, in 1968 in partial fulfillment of the requirements for the degree of Doctor of Philosophy.

11. Reissner, E., "Small Bending and Stretching of Sandwich-type Shells," NACA Report 975, 1950.

12. Reissner, E., "Finite Deflections of Sandwich Plates," J. Aero. Sci., Vol. 15, No. 7, July 1948, pp. 435-440.

13. Alwan, A. M., "Large Deflection of Sandwich Plates with Orthotropic Cores," AIAA Journal, Vol. 2, No. 10, October 1964, pp. 1820-1822.

14. Huang, J. C. and Kan, H. P., "Large Deflection of Rectangular Sandwich Plates," AIAA Journal, Vol. 5, No. 9, 1967, pp. 1706-1708.

15. Zahn, J. J., "Simply-Supported Sandwich Beam. A Non-Linear Theory, "Report No. 2157, Forest Products Laboratory, Madison, Wisconsin, 1959.

16. Ditcher, A. K. and Webber, J.P.H., "Non-Linear Stress-Strain Effects in the Flexural Wrinkling of Carbon Fibre Honeycomb Sandwich Beams," Aeronautical Quarterly, Vol. 33, pt. 1, February 1982, pp. 1-24.

17. Raville, M. E., Ueng, E.S. and Lei, M. M., "Natural Frequencies of Vibration of Fixed-Fixed Sandwich Beams," J. Appl. Mech., Vol. 28, No. E3, September 1961, pp. 367-372.

18. Ahmed, K. M., "Free Vibration of Curved Sandwich Beams by the Method of Finite Elements, "J. Sound Vibration, Vol. 18, 1971, pp. 61-74.

19. Ahmed, K. M., "Dynamic Analysis of Sandwich Beams," J. Sound Vibration, Vol. 21, 1972, pp. 263-276.

20. Ahmed, K. M., "Static and Dynamic Analysis of Sandwich Structures by the Method of Finite Element," Journal of Sound and Vibration, Vol. 18, 1971, pp. 75-91.

21. Rubayi, N. A. and Charoenree, S., "Natural Frequencies of Vibration of Cantilever Sandwich Beams," Computer & Structures, Vol. 6, October 1976, pp. 345-353.

22. Rutenberg, A., "An Accurate Approximation Formula for the Natural Frequencies of Sandwich Beams," Computer & Structures, Vol. 10, 1978, pp. 875-878.

23. Desai, C. S. and Abel, J. F., Introduction to the Finite Element Method - A Numerical Method for Engineering Analysis, Van Nostrand Reinhold Company, 1972.

24. Fletcher, R. and Powell, M.J.D., "A Rapidly Convergent Descent Method for Minimization," Computer Journal, Vol. 6, 1963, pp. 163-168.

25. Monforton, G. R., "Stiffness Matrix for Sandwich Beams with Thick Anisotropic Laminated Faces," Computer & Structures, Vol. 10, July 1978, pp. 547-551.

26. Mead, D. J., and Sivakumaran, S., "The Stodola Method Applied to Sandwich Beam Vibration," Proceedings of the Symposium on

Numerical Methods for Vibration Problems, University of Southampton, 1966.

27. Kelsey, S., Gellatly, R. A. and Clark, B. W., "The Shear Modulus of Foil Honeycomb Cores," Aircraft Engineering, October 1958.

28. Biggs, W. D. and Riley, V. R., "Bending of Sandwich Beams - Elastic Shear Modulus of Sandwich Building Core Materials," Engineering Institute of Canada - Trans Paper EIC-65-BR & STR 12, December 1965, 10 p.

29. Fazio, P. P., "Folded Sandwich Plate Structures," Ph.D. Thesis, Department of Civil Engineering, University of Windsor, Windsor, Ontario, 1968.

30. Ashton, J. E., Halpin, J. C. and Petit, P.H., Primer on Composite Materials: Analysis, Technomic Publishing Co., Inc., Connecticut, 1969.

31. Allen, H. G., Analysis and Design of Structural Sandwich Panels, Pergamon Press, London, 1969.

32. Plantema, F. J., Sandwich Construction, John Wiley & Sons, Inc., New York, 1966.

33. Monforton, G. R. and Schmit, L. A., Jr., "Finite Element Analysis of Sandwich Plates and Cylindrical Shells with Laminated Faces," Proceedings of the Conference on Matrix Methods in Structural Mechanics, AFFDL-TR-68-150, Air Force Flight Dynamics Laboratory, Wright-Patterson Air Force Base, Ohio, 1968, pp. 573-616.

34. Monforton, G. R., "Discrete Element Finite Displacement Analysis of Anisotropic Sandwich Shells," Ph.D. Thesis, Division of Solid Mechanics, Structures and Mechanical Design, Case Western Reserve University, Cleveland, Ohio, 1970.

35. Schmit, L. A., Jr. and Monforton, G. R., "Finite Deflection Discrete Element Analysis of Sandwich Plates and Cylindrical Shells with Laminated Faces," AIAA Journal, Vol. 8, No. 8, August 1970, pp. 1454-1461.

36. Box, M. J., "A Comparison of Several Current Optimization Methods, and the Use of Transformations in Contrained Problems," Computer Journal, Vol. 9, 1966, pp. 67-77.

37. Fletcher, R. and Reeves, C. M., "Function Minimization by Conjugate Gradients," Computer Journal, Vol. 7, 1964, pp. 149-154.

38. Habip, L. M., "A Review of Recent Russian Work on Sandwich Structures," Int. J. Mech. Sci., Vol. 6, 1964, pp. 483-487.

39. Habip, L. M., "A Survey of Modern Developments in the Analysis of Sandwich Structures," Applied Mechanics Review, Vol. 18, No. 2, 1965, pp. 93-98.

40. Zienkiewicz, O. C., The Finite Element Method, McGraw-Hill Book Company Limited, 1977.

APPENDIX A

STIFFNESS AND INERTIA CONSTANTS OF SANDWICH BEAMS

APPENDIX A

STIFFNESS AND INERTIA CONSTANTS OF SANDWICH BEAMS

In this section, a method for determining the constitutive equation, the force and moment resultants, together with the membrane, coupling and bending stiffnesses of laminated faces, as well as the translatory, rotary and coupling inertia of faces and core are presented. A laminated face may be composed of several bonded laminas, each lamina making up the face is assumed to be homogeneous and may have different thickness, material properties and orientation of elastic axis.

A.1 Constitutive Equation

The lamina could be considered to be in a plane stress state. The stress-strain relation for an individual kth lamina with respect to its principal axis 1 and 2 (Fig. 42) is

$$\begin{Bmatrix} \sigma_1^{(k)} \\ \sigma_2^{(k)} \\ \tau_{12}^{(k)} \end{Bmatrix} = \begin{bmatrix} \dfrac{E_{11}^{(k)}}{(1-\nu_{12}^{(k)}\nu_{21}^{(k)})} & \dfrac{\nu_{21}^{(k)}E_{11}^{(k)}}{(1-\nu_{12}^{(k)}\nu_{21}^{(k)})} & 0 \\ & \dfrac{E_{22}^{(k)}}{(1-\nu_{12}^{(k)}\nu_{21}^{(k)})} & 0 \\ \text{(SYMMETRIC)} & & G_{12}^{(k)} \end{bmatrix} \begin{Bmatrix} \varepsilon_1^{(k)} \\ \varepsilon_2^{(k)} \\ \gamma_{12}^{(k)} \end{Bmatrix} \quad \text{(A.1a)}$$

or $$\{\sigma_{12}^{(k)}\} = [\bar{S}^{(k)}]\,\{\varepsilon_{12}^{(k)}\} \quad \text{(A.1b)}$$

where $\nu_{21}^{(k)} E_{11}^{(k)} = \nu_{12}^{(k)} E_{22}^{(k)}$. If the lamina principal axis (1,2) make an angle θ with the reference axis (x,y) for the laminate, the lamina stress-strain relation transformed to the laminate reference axis are

$$\begin{Bmatrix} \sigma_1^{(k)} \\ \sigma_2^{(k)} \\ \tau_{12}^{(k)} \end{Bmatrix} = \begin{bmatrix} \cos^2\theta^{(k)} & \sin^2\theta^{(k)} & \sin2\theta^{(k)} \\ \sin^2\theta^{(k)} & \cos^2\theta^{(k)} & -\sin2\theta^{(k)} \\ -\frac{1}{2}\sin2\theta^{(k)} & -\frac{1}{2}\sin2\theta^{(k)} & \cos2\theta^{(k)} \end{bmatrix} \begin{Bmatrix} \sigma_x^{(k)} \\ \sigma_y^{(k)} \\ \tau_{xy}^{(k)} \end{Bmatrix} \tag{A.2a}$$

or $$\{\sigma_{12}^{(k)}\} = [T_\sigma^{(k)}]\ \{\sigma_{xy}^{(k)}\} \tag{A.2b}$$

and

$$\begin{Bmatrix} \varepsilon_1^{(k)} \\ \varepsilon_2^{(k)} \\ \gamma_{12}^{(k)} \end{Bmatrix} = \begin{bmatrix} \cos^2\theta^{(k)} & \sin^2\theta^{(k)} & \frac{1}{2}\sin2\theta^{(k)} \\ \sin^2\theta^{(k)} & \cos^2\theta^{(k)} & -\frac{1}{2}\sin2\theta^{(k)} \\ -\sin2\theta^{(k)} & \sin2\theta^{(k)} & \cos2\theta^{(k)} \end{bmatrix} \begin{Bmatrix} \varepsilon_x^{(k)} \\ \varepsilon_y^{(k)} \\ \gamma_{xy}^{(k)} \end{Bmatrix} \tag{A.3a}$$

or $$\{\varepsilon_{12}^{(k)}\} = [T_\varepsilon^{(k)}]\ \{\varepsilon_{xy}^{(k)}\} \tag{A.3b}$$

where $$[T_\sigma^{(k)}]^{-1} = [T_\varepsilon^{(k)}]^T \tag{A.4}$$

Substituting Eqs. A.2 and A.3 into A.1 results in

$$\begin{Bmatrix} \sigma_x^{(k)} \\ \sigma_y^{(k)} \\ \tau_{xy}^{(k)} \end{Bmatrix} = \begin{bmatrix} S_{11}^{(k)} & S_{12}^{(k)} & S_{16}^{(k)} \\ & S_{22}^{(k)} & S_{26}^{(k)} \\ \text{(SYMMETRIC)} & & S_{66}^{(k)} \end{bmatrix} \begin{Bmatrix} \varepsilon_x^{(k)} \\ \varepsilon_y^{(k)} \\ \gamma_{xy}^{(k)} \end{Bmatrix} \tag{A.5a}$$

$$\text{or} \quad \{\sigma_{xy}^{(k)}\} = [S^{(k)}]\ \{\varepsilon_{xy}^{(k)}\} \tag{A.5b}$$

$$\text{where} \quad [S^{(k)}] = [T_\varepsilon^{(k)}]^T [\bar{S}^{(k)}][T_\varepsilon^{(k)}] \tag{A.5c}$$

As mentioned previously, each lamina making up the face is assumed to be homogeneous and may have different material properties, thickness as well as elastic axis orientation. The matrix $[S^{(k)}]$ for each lamina, therefore, may be different. The laminated face which is formed from several bonded laminas, however, is considered as heterogeneous in nature; its constitutive equation is expressible as

$$\begin{Bmatrix} \sigma_{fx} \\ \sigma_{fy} \\ \tau_{fxy} \end{Bmatrix} = \begin{bmatrix} S_{11}(z_f) & S_{12}(z_f) & S_{16}(z_f) \\ & S_{22}(z_f) & S_{26}(z_f) \\ \text{(SYMMETRIC)} & & S_{66}(z_f) \end{bmatrix} \begin{Bmatrix} \varepsilon_{fx} \\ \varepsilon_{fy} \\ \gamma_{fxy} \end{Bmatrix} \tag{A.6a}$$

$$\text{or} \quad \{\sigma_{fxy}\} = [S(z_f)]\{\varepsilon_{fxy}\} \tag{A.6b}$$

For beam analysis, the laminated face may be assumed to be in

a state of uniaxial stress (i.e., $\sigma_{fy} = \tau_{fxy} = 0$), Eqs. A.6 become

$$\sigma_{fx} = S_x(z_f)\, \varepsilon_{fx} \tag{A.7a}$$

$$\varepsilon_{fy} = S_y(z_f)\, \varepsilon_{fx} \tag{A.7b}$$

$$\tau_{fxy} = S_{xy}(z_f)\varepsilon_{fx} \tag{A.7c}$$

where

$$S_x(z_f) = S_{11}(z_f) + S_{12}(z_f)\, S_y(z_f) + S_{16}(z_f)S_{xy}(z_f) \tag{A.7d}$$

$$S_y(z_f) = (S_{16}(z_f)\, S_{26}(z_f) - S_{12}(z_f)S_{66}(z_f))/S(z_f) \tag{A.7e}$$

$$S_{xy}(z_f) = (S_{12}(z_f)S_{26}(z_f) - S_{16}(z_f)S_{22}(z_f))/S(z_f) \tag{A.7f}$$

$$S(z_f) = S_{22}(z_f)S_{66}(z_f) - S_{26}(z_f)S_{26}(z_f) \tag{A.7g}$$

A.2 Force-Deformation Relations

The following expressions for the force and moment resultants are used to obtain the force-deformation relations for the faces,

$$N_f = b \int_{-\frac{t_f}{2}}^{\frac{t_f}{2}} \sigma_{fx}\, dz_f \tag{A.8a}$$

$$M_f = b \int_{-\frac{t_f}{2}}^{\frac{t_f}{2}} \sigma_{fx} . z_f . dz_f \tag{A.8b}$$

where b and t_f represent the width and thickness of the faces respectively. Substituting the strain-displacement equation (Eq. 2.3) and stress-strain relation (Eq. A.7) for the faces into Eqs. A.8, the resulting force-deformation relations are defined as

$$N_f = A_f[u_{xf} + \frac{w}{R_f} + \frac{1}{2}(w_x)^2] + B_f[\frac{u_{xf}}{R_f} - w_{xx}] \qquad (A.9a)$$

$$M_f = B_f[u_{xf} + \frac{w}{R_f} + \frac{1}{2}(w_x)^2] + D_f[\frac{u_{xf}}{R_f} - w_{xx}] \qquad (A.9b)$$

The terms A_f, B_f and D_f represent the membrane, coupling,bending stiffnesses of the faces are expressed as

$$A_f = b \int_{-\frac{t_f}{2}}^{\frac{t_f}{2}} S_x(z_f).dz_f \qquad (A.10a)$$

$$B_f = b \int_{-\frac{t_f}{2}}^{\frac{t_f}{2}} S_x(z_f).z_f.dz_f \qquad (A.10b)$$

$$D_f = b \int_{-\frac{t_f}{2}}^{\frac{t_f}{2}} S_x(z_f).z_f^2.dz_f \qquad (A.10c)$$

A.3 Inertia Constants

The terms Q_s, J_s and I_s (s=1,2,c) represent the translatory, rotary and coupling inertia constants for the sandwich beams are

defined as

$$Q_s = b \int_{-\frac{t_s}{2}}^{\frac{t_s}{2}} \rho_s(z_s).dz_s \qquad \text{(A.11a)}$$

$$J_s = b \int_{-\frac{t_s}{2}}^{\frac{t_s}{2}} \rho_s(z_s).z_s.dz_s \qquad \text{(A.11b)}$$

$$I_s = b \int_{-\frac{t_s}{2}}^{\frac{t_s}{2}} \rho_s(z_s).z_s^2.dz_s \qquad \text{(A.11c)}$$

where $\rho_s(z_s)$ represents the mass density of the faces and core and is allowed to vary throughout the thickness of the faces and core. When the mass density is constant, Eq. A.11 can be rewritten as

$$Q_s = b\,\rho_s t_s \qquad \text{(A.12a)}$$

$$J_s = 0 \qquad \text{(A.12b)}$$

$$I_s = \frac{1}{12} b\rho_s t_s^3 \qquad \text{(A.12c)}$$

APPENDIX B

STIFFNESS AND MASS MATRICES

FOR CURVED SANDWICH BEAMS

APPENDIX B

STIFFNESS AND MASS MATRICES FOR CURVED SANDWICH BEAM

This appendix presents the stiffness matrices $[K^{(2)}]$, $[K^{(3)}]$ and $[K^{(4)}]$ as well as the mass matrix $[M^{(2)}]$. The matrices presented from Eq. B.1 to Eq. B.4 are valid for both straight beam ($\frac{1}{R_1} = \frac{1}{R_2} = \frac{1}{R_c} = 0$, $\frac{R_c}{R_1} = \frac{R_c}{R_2} = 1$) and curved beam.

The stiffness matrix $[K^{(2)}]$ is

$$
\begin{bmatrix}
k^{(2)}_{(1,1)} & k^{(2)}_{(1,2)} & k^{(2)}_{(1,3)} & k^{(2)}_{(1,4)} & k^{(2)}_{(1,5)} & k^{(2)}_{(1,6)} & k^{(2)}_{(1,7)} & k^{(2)}_{(1,8)} & k^{(2)}_{(1,9)} & k^{(2)}_{(1,10)} & k^{(2)}_{(1,11)} & k^{(2)}_{(1,12)} \\
 & k^{(2)}_{(2,2)} & k^{(2)}_{(2,3)} & k^{(2)}_{(2,4)} & k^{(2)}_{(2,5)} & k^{(2)}_{(2,6)} & k^{(2)}_{(2,7)} & k^{(2)}_{(2,8)} & k^{(2)}_{(2,9)} & k^{(2)}_{(2,10)} & k^{(2)}_{(2,11)} & k^{(2)}_{(2,12)} \\
 & & k^{(2)}_{(3,3)} & k^{(2)}_{(3,4)} & k^{(2)}_{(3,5)} & k^{(2)}_{(3,6)} & k^{(2)}_{(3,7)} & k^{(2)}_{(3,8)} & k^{(2)}_{(3,9)} & k^{(2)}_{(3,10)} & k^{(2)}_{(3,11)} & k^{(2)}_{(3,12)} \\
 & & & k^{(2)}_{(4,4)} & k^{(2)}_{(4,5)} & k^{(2)}_{(4,6)} & k^{(2)}_{(4,7)} & k^{(2)}_{(4,8)} & k^{(2)}_{(4,9)} & k^{(2)}_{(4,10)} & k^{(2)}_{(4,11)} & k^{(2)}_{(4,12)} \\
 & & & & k^{(2)}_{(5,5)} & k^{(2)}_{(5,6)} & k^{(2)}_{(5,7)} & k^{(2)}_{(5,8)} & k^{(2)}_{(5,9)} & k^{(2)}_{(5,10)} & k^{(2)}_{(5,11)} & k^{(2)}_{(5,12)} \\
 & & & & & k^{(2)}_{(6,6)} & k^{(2)}_{(6,7)} & k^{(2)}_{(6,8)} & k^{(2)}_{(6,9)} & k^{(2)}_{(6,10)} & k^{(2)}_{(6,11)} & k^{(2)}_{(6,12)} \\
 & & & & & & k^{(2)}_{(7,7)} & k^{(2)}_{(7,8)} & k^{(2)}_{(7,9)} & k^{(2)}_{(7,10)} & k^{(2)}_{(7,11)} & k^{(2)}_{(7,12)} \\
 & & & & & & & k^{(2)}_{(8,8)} & k^{(2)}_{(8,9)} & k^{(2)}_{(8,10)} & k^{(2)}_{(8,11)} & k^{(2)}_{(8,12)} \\
 & & & & & & & & k^{(2)}_{(9,9)} & k^{(2)}_{(9,10)} & k^{(2)}_{(9,11)} & k^{(2)}_{(9,12)} \\
 & & & & & & & & & k^{(2)}_{(10,10)} & k^{(2)}_{(10,11)} & k^{(2)}_{(10,12)} \\
 & & & & & & & & & & k^{(2)}_{(11,11)} & k^{(2)}_{(11,12)} \\
 & & & & & & & & & & & k^{(2)}_{(12,12)}
\end{bmatrix}
\quad \text{(B.1)}
$$

where

$$k^{(2)}(1,1) = \frac{6}{5a}\left(A_1 + \frac{2B_1}{R_1} + \frac{D_1}{R_1^2}\right) + \frac{39ae_1^2B_c}{105t_c^2}$$

$$k^{(2)}(1,2) = -\frac{6}{5a}\left(A_1 + \frac{2B_1}{R_1} + \frac{D_1}{R_1^2}\right) + \frac{9ae_1^2B_c}{70t_c^2}$$

$$k^{(2)}(1,3) = \frac{1}{10}\left(A_1 + \frac{2B_1}{R_1} + \frac{D_1}{R_1^2}\right) + \frac{11a^2e_1^2B_c}{210t_c^2}$$

$$k^{(2)}(1,4) = \frac{1}{10}\left(A_1 + \frac{2B_1}{R_1} + \frac{D_1}{R_1^2}\right) - \frac{13a^2e_1^2B_c}{420t_c^2}$$

$$k^{(2)}(1,5) = -\frac{39ae_1e_2B_c}{105t_c^2}$$

$$k^{(2)}(1,6) = -\frac{9ae_1e_2B_c}{70t_c^2}$$

$$k^{(2)}(1,7) = -\frac{11a^2e_1e_2B_c}{210t_c^2}$$

$$k^{(2)}(1,8) = \frac{13a^2e_1e_2B_c}{420t_c^2}$$

$$k^{(2)}(1,9) = -\frac{1}{2}\left(\frac{A_1}{R_1} + \frac{B_1}{R_1^2}\right) + \frac{e_1e_3B_c}{2t_c^2}$$

$$k^{(2)}(1,10) = -\frac{1}{2}\left(\frac{A_1}{R_1} + \frac{B_1}{R_1^2}\right) - \frac{e_1e_3B_c}{2t_c^2}$$

$$k^{(2)}(1,11) = -\frac{1}{a}\left(B_1 + \frac{D_1}{R_1}\right) - \frac{a}{10}\left(\frac{A_1}{R_1} + \frac{B_1}{R_1^2}\right) - \frac{ae_1e_3B_c}{10t_c^2}$$

$$k^{(2)}(1,12) = -k^{(2)}(1,11)$$

$$k^{(2)}(2,2) = k^{(2)}(1,1)$$

$$k^{(2)}(2,3) = -k^{(2)}(1,4)$$

$$k^{(2)}(2,4) = -k^{(2)}(1,3)$$

$$k^{(2)}(2,5) = k^{(2)}(1,6)$$

$$k^{(2)}(2,6) = k^{(2)}(1,5)$$

$$k^{(2)}(2,7) = -k^{(2)}(1,8)$$

$$k^{(2)}(2,8) = -k^{(2)}(1,7)$$

$$k^{(2)}(2,9) = -k^{(2)}(1,10)$$

$$k^{(2)}(2,10) = -k^{(2)}(1,9)$$

$$k^{(2)}(2,11) = -k^{(2)}(1,11)$$

$$k^{(2)}(2,12) = k^{(2)}(1,11)$$

$$k^{(2)}(3,3) = \frac{2a}{15}\left(A_1 + \frac{2B_1}{R_1} + \frac{D_1}{R_1^2}\right) + \frac{a^3 e_1^2 B_c}{105 t_c^2}$$

$$k^{(2)}(3,4) = -\frac{a}{30}\left(A_1 + \frac{2B_1}{R_1} + \frac{D_1}{R_1^2}\right) - \frac{a^3 e_1^2 B_c}{140 t_c^2}$$

$$k^{(2)}(3,5) = k^{(2)}(1,7)$$

$$k^{(2)}(3,6) = -k^{(2)}(1,8)$$

$$k^{(2)}(3,7) = -\frac{a^3 e_1 e_2 B_c}{105 t_c^2}$$

$$k^{(2)}(3,8) = \frac{a^3 e_1 e_2 B_c}{140 t_c^2}$$

$$k^{(2)}(3,9) = - k^{(2)}(1,11)$$

$$k^{(2)}(3,10) = k^{(2)}(1,11)$$

$$k^{(2)}(3,11) = \frac{1}{2}\left(B_1 + \frac{D_1}{R_1} \right)$$

$$k^{(2)}(3,12) = \frac{1}{2}\left(B_1 + \frac{D_1}{R_1} \right) + \frac{a^2}{60}\left(\frac{A_1}{R_1} + \frac{B_1}{R_1^2} \right) + \frac{a^2 e_1 e_3 B_c}{60 t_c^2}$$

$$k^{(2)}(4,4) = k^{(2)}(3,3)$$

$$k^{(2)}(4,5) = k^{(2)}(1,8)$$

$$k^{(2)}(4,6) = - k^{(2)}(1,7)$$

$$k^{(2)}(4,7) = k^{(2)}(3,8)$$

$$k^{(2)}(4,8) = k^{(2)}(3,7)$$

$$k^{(2)}(4,9) = k^{(2)}(1,11)$$

$$k^{(2)}(4,10) = - k^{(2)}(1,11)$$

$$k^{(2)}(4,11) = - k^{(2)}(3,12)$$

$$k^{(2)}(4,12) = - k^{(2)}(3,11)$$

$$k^{(2)}(5,5) = \frac{6}{5a}\left(A_2 + \frac{2B_2}{R_2} + \frac{D_2}{R_2^2} \right) + \frac{39 a e_2^2 B_c}{105 t_c^2}$$

$$k^{(2)}(5,6) = -\frac{6}{5a}\left(A_2 + \frac{2B_2}{R_2} + \frac{D_2}{R_2^2}\right) + \frac{9ae_2^2B_c}{70t_c^2}$$

$$k^{(2)}(5,7) = \frac{1}{10}\left(A_2 + \frac{2B_2}{R_2} + \frac{D_2}{R_2^2}\right) + \frac{11a^2e_2^2B_c}{210t_c^2}$$

$$k^{(2)}(5,8) = \frac{1}{10}\left(A_2 + \frac{2B_2}{R_2} + \frac{D_2}{R_2^2}\right) - \frac{13a^2e_2^2B_c}{420t_c^2}$$

$$k^{(2)}(5,9) = -\frac{1}{2}\left(\frac{A_2}{R_2} + \frac{B_2}{R_2^2}\right) - \frac{e_2e_3B_c}{2t_c^2}$$

$$k^{(2)}(5,10) = -\frac{1}{2}\left(\frac{A_2}{R_2} + \frac{B_2}{R_2^2}\right) + \frac{e_2e_3B_c}{2tc^2}$$

$$k^{(2)}(5,11) = -\frac{1}{a}\left(B_2 + \frac{D_2}{R_2}\right) - \frac{a}{10}\left(\frac{A_2}{R_2} + \frac{B_2}{R_2^2}\right) + \frac{ae_2e_3B_c}{10t_c^2}$$

$$k^{(2)}(5,12) = -k^{(2)}(5,11)$$

$$k^{(2)}(6,6) = k^{(2)}(5,5)$$

$$k^{(2)}(6,7) = -k^{(2)}(5,8)$$

$$k^{(2)}(6,8) = -k^{(2)}(5,7)$$

$$k^{(2)}(6,9) = -k^{(2)}(5,10)$$

$$k^{(2)}(6,10) = -k^{(2)}(5,9)$$

$$k^{(2)}(6,11) = -k^{(2)}(5,11)$$

$$k^{(2)}(6,12) = k^{(2)}(5,11)$$

$$k^{(2)}(7,7) = \frac{2a}{15}\left(A_2 + \frac{2B_2}{R_2} + \frac{D_2}{R_2^2}\right) + \frac{a^3 e_2^2 B_c}{105 t_c^2}$$

$$k^{(2)}(7,8) = -\frac{a}{30}\left(A_2 + \frac{2B_2}{R_2} + \frac{D_2}{R_2^2}\right) - \frac{a^3 e_2^2 B_c}{140 t_c^2}$$

$$k^{(2)}(7,9) = -k^{(2)}(5,11)$$

$$k^{(2)}(7,10) = k^{(2)}(5,11)$$

$$k^{(2)}(7,11) = \frac{1}{2}\left(B_2 + \frac{D_2}{R_2}\right)$$

$$k^{(2)}(7,12) = \frac{1}{2}\left(B_2 + \frac{D_2}{R_2}\right) + \frac{a^2}{60}\left(\frac{A_2}{R_2} + \frac{B_2}{R_2^2}\right) - \frac{a^2 e_2 e_3 B_c}{60 t_c^2}$$

$$k^{(2)}(8,8) = k^{(2)}(7,7)$$

$$k^{(2)}(8,9) = k^{(2)}(5,11)$$

$$k^{(2)}(8,10) = -k^{(2)}(5,11)$$

$$k^{(2)}(8,11) = -k^{(2)}(7,12)$$

$$k^{(2)}(8,12) = -k^{(2)}(7,11)$$

$$k^{(2)}(9,9) = \frac{12D}{a^3} + \frac{13a}{35}\left(\frac{A_1}{R_1^2} + \frac{A_2}{R_2^2}\right) + \frac{12}{5a}\left(\frac{B_1}{R_1} + \frac{B_2}{R_2}\right) + \frac{6e_3^2 B_c}{5at_c^2}$$

$$k^{(2)}(9,10) = -\frac{12D}{a^3} + \frac{9a}{70}\left(\frac{A_1}{R_1^2} + \frac{A_2}{R_2^2}\right) - \frac{12}{5a}\left(\frac{B_1}{R_1} + \frac{B_2}{R_2}\right) - \frac{6e_3^2 B_c}{5at_c^2}$$

$$k^{(2)}(9,11) = \frac{6D}{a^2} + \frac{11a^2}{210}\left(\frac{A_1}{R_1^2} + \frac{A_2}{R_2^2}\right) + \frac{6}{5}\left(\frac{B_1}{R_1} + \frac{B_2}{R_2}\right) + \frac{e_3^2 B_c}{10t_c^2}$$

$$k^{(2)}(9,12) = \frac{6D}{a^2} - \frac{13a^2}{420}\left(\frac{A_1}{R_1^2} + \frac{A_2}{R_2^2}\right) + \frac{1}{5}\left(\frac{B_1}{R_1} + \frac{B_2}{R_2}\right) + \frac{e_3^2 B_c}{10t_c^2}$$

$$k^{(2)}(10,10) = k^{(2)}(9,9)$$

$$k^{(2)}(10,11) = -k^{(2)}(9,12)$$

$$k^{(2)}(10,12) = -k^{(2)}(9,11)$$

$$k^{(2)}(11,11) = \frac{4D}{a} + \frac{a^3}{105}\left(\frac{A_1}{R_1^2} + \frac{A_2}{R_2^2}\right) + \frac{4a}{15}\left(\frac{B_1}{R_1} + \frac{B_2}{R_2}\right) + \frac{2ae_3^2 B_c}{15t_c^2}$$

$$k^{(2)}(11,12) = \frac{2D}{a} - \frac{a^3}{140}\left(\frac{A_1}{R_1^2} + \frac{A_2}{R_2^2}\right) - \frac{a}{15}\left(\frac{B_1}{R_1} + \frac{B_2}{R_2}\right) - \frac{ae_3^2 B_c}{30t_c^2}$$

$$k^{(2)}(12,12) = k^{(2)}(11,11)$$

The stiffness matrix $[K^{(3)}]$ is

$k^{(3)}(1,1)$	$k^{(3)}(1,2)$	$k^{(3)}(1,3)$	$k^{(3)}(1,4)$	$k^{(3)}(1,5)$	$k^{(3)}(1,6)$	$k^{(3)}(1,7)$	$k^{(3)}(1,8)$	$k^{(3)}(1,9)$	$k^{(3)}(1,10)$
$k^{(3)}(2,1)$	$k^{(3)}(2,2)$	$k^{(3)}(2,3)$	$k^{(3)}(2,4)$	$k^{(3)}(2,5)$	$k^{(3)}(2,6)$	$k^{(3)}(2,7)$	$k^{(3)}(2,8)$	$k^{(3)}(2,9)$	$k^{(3)}(2,10)$
$k^{(3)}(3,1)$	$k^{(3)}(3,2)$	$k^{(3)}(3,3)$	$k^{(3)}(3,4)$	$k^{(3)}(3,5)$	$k^{(3)}(3,6)$	$k^{(3)}(3,7)$	$k^{(3)}(3,8)$	$k^{(3)}(3,9)$	$k^{(3)}(3,10)$
$k^{(3)}(4,1)$	$k^{(3)}(4,2)$	$k^{(3)}(4,3)$	$k^{(3)}(4,4)$	$k^{(3)}(4,5)$	$k^{(3)}(4,6)$	$k^{(3)}(4,7)$	$k^{(3)}(4,8)$	$k^{(3)}(4,9)$	$k^{(3)}(4,10)$
$k^{(3)}(5,1)$	$k^{(3)}(5,2)$	$k^{(3)}(5,3)$	$k^{(3)}(5,4)$	$k^{(3)}(5,5)$	$k^{(3)}(5,6)$	$k^{(3)}(5,7)$	$k^{(3)}(5,8)$	$k^{(3)}(5,9)$	$k^{(3)}(5,10)$
$k^{(3)}(6,1)$	$k^{(3)}(6,2)$	$k^{(3)}(6,3)$	$k^{(3)}(6,4)$	$k^{(3)}(6,5)$	$k^{(3)}(6,6)$	$k^{(3)}(6,7)$	$k^{(3)}(6,8)$	$k^{(3)}(6,9)$	$k^{(3)}(6,10)$
$k^{(3)}(7,1)$	$k^{(3)}(7,2)$	$k^{(3)}(7,3)$	$k^{(3)}(7,4)$	$k^{(3)}(7,5)$	$k^{(3)}(7,6)$	$k^{(3)}(7,7)$	$k^{(3)}(7,8)$	$k^{(3)}(7,9)$	$k^{(3)}(7,10)$
$k^{(3)}(8,1)$	$k^{(3)}(8,2)$	$k^{(3)}(8,3)$	$k^{(3)}(8,4)$	$k^{(3)}(8,5)$	$k^{(3)}(8,6)$	$k^{(3)}(8,7)$	$k^{(3)}(8,8)$	$k^{(3)}(8,9)$	$k^{(3)}(8,10)$
$k^{(3)}(9,1)$	$k^{(3)}(9,2)$	$k^{(3)}(9,3)$	$k^{(3)}(9,4)$	$k^{(3)}(9,5)$	$k^{(3)}(9,6)$	$k^{(3)}(9,7)$	$k^{(3)}(9,8)$	$k^{(3)}(9,9)$	$k^{(3)}(9,10)$
$k^{(3)}(10,1)$	$k^{(3)}(10,2)$	$k^{(3)}(10,3)$	$k^{(3)}(10,4)$	$k^{(3)}(10,5)$	$k^{(3)}(10,6)$	$k^{(3)}(10,7)$	$k^{(3)}(10,8)$	$k^{(3)}(10,9)$	$k^{(3)}(10,10)$
$k^{(3)}(11,1)$	$k^{(3)}(11,2)$	$k^{(3)}(11,3)$	$k^{(3)}(11,4)$	$k^{(3)}(11,5)$	$k^{(3)}(11,6)$	$k^{(3)}(11,7)$	$k^{(3)}(11,8)$	$k^{(3)}(11,9)$	$k^{(3)}(11,10)$
$k^{(3)}(12,1)$	$k^{(3)}(12,2)$	$k^{(3)}(12,3)$	$k^{(3)}(12,4)$	$k^{(3)}(12,5)$	$k^{(3)}(12,6)$	$k^{(3)}(12,7)$	$k^{(3)}(12,8)$	$k^{(3)}(12,9)$	$k^{(3)}(12,10)$

(B.2)

where

$$k^{(3)}(1,1) = -\frac{54}{35a^2}\left(A_1 + \frac{B_1}{R_1}\right)$$

$$k^{(3)}(1,2) = -2\,k^{(3)}(1,1)$$

$$k^{(3)}(1,3) = -\frac{12}{35a}\left(A_1 + \frac{B_1}{R_1}\right)$$

$$k^{(3)}(1,4) = k^{(3)}(1,3)$$

$$k^{(3)}(1,5) = k^{(3)}(1,1)$$

$$k^{(3)}(1,6) = - k^{(3)}(1,3)$$

$$k^{(3)}(1,7) = - k^{(3)}(1,3)$$

$$k^{(3)}(1,8) = - \frac{3}{35} \left(A_1 + \frac{B_1}{R_1} \right)$$

$$k^{(3)}(1,9) = - \frac{1}{3} k^{(3)}(1,8)$$

$$k^{(3)}(1,10) = k^{(3)}(1,8)$$

$$k^{(3)}(2,1) = - k^{(3)}(1,1)$$

$$k^{(3)}(2,2) = 2\, k^{(3)}(1,1)$$

$$k^{(3)}(2,3) = - k^{(3)}(1,3)$$

$$k^{(3)}(2,4) = - k^{(3)}(1,3)$$

$$k^{(3)}(2,5) = - k^{(3)}(1,1)$$

$$k^{(3)}(2,6) = k^{(3)}(1,3)$$

$$k^{(3)}(2,7) = k^{(3)}(1,3)$$

$$k^{(3)}(2,8) = - k^{(3)}(1,8)$$

$$k^{(3)}(2,9) = \frac{1}{3} k^{(3)}(1,8)$$

$$k^{(3)}(2,10) = - k^{(3)}(1,8)$$

$$k^{(3)}(3,1) = \frac{1}{2} k^{(3)}(1,3)$$

$$k^{(3)}(3,2) = - k^{(3)}(1,3)$$

$$k^{(3)}(3,3) = 2 k^{(3)}(1,8)$$

$$k^{(3)}(3,4) = - \frac{1}{3} k^{(3)}(1,8)$$

$$k^{(3)}(3,5) = \frac{1}{2} k^{(3)}(1,3)$$

$$k^{(3)}(3,6) = - 2 k^{(3)}(1,8)$$

$$k^{(3)}(3,7) = \frac{1}{3} k^{(3)}(1,8)$$

$$k^{(3)}(3,8) = \frac{2a}{35} \left(A_1 + \frac{B_1}{R_1} \right)$$

$$k^{(3)}(3,9) = - \frac{1}{3} k^{(3)}(3,8)$$

$$k^{(3)}(3,10) = - \frac{1}{6} k^{(3)}(3,8)$$

$$k^{(3)}(4,1) = \frac{1}{2} k^{(3)}(1,3)$$

$$k^{(3)}(4,2) = - k^{(3)}(1,3)$$

$$k^{(3)}(4,3) = - \frac{1}{3} k^{(3)}(1,8)$$

$$k^{(3)}(4,4) = 2 k^{(3)}(1,8)$$

$$k^{(3)}(4,5) = \frac{1}{2} k^{(3)}(1,3)$$

$$k^{(3)}(4,6) = \frac{1}{3} k^{(3)}(1,8)$$

$$k^{(3)}(4,7) = -2\, k^{(3)}(1,8)$$

$$k^{(3)}(4,8) = -\frac{1}{6} k^{(3)}(3,8)$$

$$k^{(3)}(4,9) = -\frac{1}{3} k^{(3)}(3,8)$$

$$k^{(3)}(4,10) = k^{(3)}(3,8)$$

$$k^{(3)}(5,1) = -\frac{54}{35a^2}\left(A_2 + \frac{B_2}{R_2}\right)$$

$$k^{(3)}(5,2) = -2\, k^{(3)}(5,1)$$

$$k^{(3)}(5,3) = -\frac{12}{35a}\left(A_2 + \frac{B_2}{R_2}\right)$$

$$k^{(3)}(5,4) = k^{(3)}(5,3)$$

$$k^{(3)}(5,5) = k^{(3)}(5,1)$$

$$k^{(3)}(5,6) = -k^{(3)}(5,3)$$

$$k^{(3)}(5,7) = -k^{(3)}(5,3)$$

$$k^{(3)}(5,8) = -\frac{3}{35}\left(A_2 + \frac{B_2}{R_2}\right)$$

$$k^{(3)}(5,9) = -\frac{1}{3} k^{(3)}(5,8)$$

$$k^{(3)}(5,10) = k^{(3)}(5,8)$$

$$k^{(3)}(6.1) = - k^{(3)}(5,1)$$

$$k^{(3)}(6,2) = 2\, k^{(3)}(5,1)$$

$$k^{(3)}(6,3) = - k^{(3)}(5,3)$$

$$k^{(3)}(6,4) = - k^{(3)}(5,3)$$

$$k^{(3)}(6,5) = - k^{(3)}(5,1)$$

$$k^{(3)}(6,6) = k^{(3)}(5,3)$$

$$k^{(3)}(6,7) = k^{(3)}(5,3)$$

$$k^{(3)}(6,8) = - k^{(3)}(5,8)$$

$$k^{(3)}(6,9) = \frac{1}{3} k^{(3)}(5,8)$$

$$k^{(3)}(6,10) = - k^{(3)}(5,8)$$

$$k^{(3)}(7,1) = \frac{1}{2} k^{(3)}(5,3)$$

$$k^{(3)}(7,2) = - k^{(3)}(5,3)$$

$$k^{(3)}(7,3) = 2\, k^{(3)}(5,8)$$

$$k^{(3)}(7,4) = - \frac{1}{3} k^{(3)}(5,8)$$

$$k^{(3)}(7,5) = \frac{1}{2} k^{(3)}(5,3)$$

$$k^{(3)}(7,6) = - 2\, k^{(3)}(5,8)$$

$$k^{(3)}(7,7) = \frac{1}{3} k^{(3)}(5,8)$$

$$k^{(3)}(7,8) = \frac{2a}{35}\left(A_2 + \frac{B_2}{R_2}\right)$$

$$k^{(3)}(7,9) = -\frac{1}{3}k^{(3)}(7,8)$$

$$k^{(3)}(7,10) = -\frac{1}{6}k^{(3)}(7,8)$$

$$k^{(3)}(8,1) = \frac{1}{2}k^{(3)}(5,3)$$

$$k^{(3)}(8,2) = -k^{(3)}(5,3)$$

$$k^{(3)}(8,3) = -\frac{1}{3}k^{(3)}(5,8)$$

$$k^{(3)}(8,4) = 2\,k^{(3)}(5,8)$$

$$k^{(3)}(8,5) = \frac{1}{2}k^{(3)}(5,3)$$

$$k^{(3)}(8,6) = \frac{1}{3}k^{(3)}(5,8)$$

$$k^{(3)}(8,7) = -2\,k^{(3)}(5,8)$$

$$k^{(3)}(8,8) = -\frac{1}{6}k^{(3)}(7,8)$$

$$k^{(3)}(8,9) = -\frac{1}{3}k^{(3)}(7,8)$$

$$k^{(3)}(8,10) = k^{(3)}(7,8)$$

$$k^{(3)}(9,1) = \frac{3}{5a}\left(\frac{A_1}{R_1} + \frac{A_2}{R_2}\right)$$

$$k^{(3)}(9,2) = -2\,k^{(3)}(9,1)$$

$$k^{(3)}(9,3) = -\frac{1}{35}\left(\frac{A_1}{R_1}+\frac{A_2}{R_2}\right)$$

$$k^{(3)}(9,4) = -8\,k^{(3)}(9,3)$$

$$k^{(3)}(9,5) = k^{(3)}(9,1)$$

$$k^{(3)}(9,6) = -k^{(3)}(9,3)$$

$$k^{(3)}(9,7) = 8\,k^{(3)}(9,3)$$

$$k^{(3)}(9,8) = \frac{43a}{420}\left(\frac{A_1}{R_1}+\frac{A_2}{R_2}\right)$$

$$k^{(3)}(9,9) = -\frac{14}{43}\,k^{(3)}(9,8)$$

$$k^{(3)}(9,10) = \frac{13}{43}\,k^{(3)}(9,8)$$

$$k^{(3)}(10,1) = k^{(3)}(9,1)$$

$$k^{(3)}(10,2) = -2\,k^{(3)}(9,1)$$

$$k^{(3)}(10,3) = -8\,k^{(3)}(9,3)$$

$$k^{(3)}(10,4) = k^{(3)}(9,3)$$

$$k^{(3)}(10,5) = k^{(3)}(9,1)$$

$$k^{(3)}(10,6) = 8\,k^{(3)}(9,3)$$

$$k^{(3)}(10,7) = -k^{(3)}(9,3)$$

$$k^{(3)}(10,8) = \frac{13}{43}\,k^{(3)}(9,8)$$

$$k^{(3)}(10,9) = -\frac{14}{43}k^{(3)}(9,8)$$

$$k^{(3)}(10,10) = k^{(3)}(9,8)$$

$$k^{(3)}(11,1) = -\frac{9}{2}k^{(3)}(9,3)$$

$$k^{(3)}(11,2) = 9\,k^{(3)}(9,3)$$

$$k^{(3)}(11,3) = \frac{6}{43}k^{(3)}(9,8)$$

$$k^{(3)}(11,4) = \frac{18}{43}k^{(3)}(9,8)$$

$$k^{(3)}(11,5) = -\frac{9}{2}k^{(3)}(9,3)$$

$$k^{(3)}(11,6) = -\frac{6}{43}k^{(3)}(9,8)$$

$$k^{(3)}(11,7) = -\frac{18}{43}k^{(3)}(9,8)$$

$$k^{(3)}(11,8) = \frac{a^2}{120}\left(\frac{A_1}{R_1}+\frac{A_2}{R_2}\right)+\frac{B}{3}$$

$$k^{(3)}(11,9) = -\frac{a^2}{420}\left(\frac{A_1}{R_1}+\frac{A_2}{R_2}\right)$$

$$k^{(3)}(11,10) = -\frac{5}{2}k^{(3)}(11,9)$$

$$k^{(3)}(12,1) = \frac{9}{2}k^{(3)}(9,3)$$

$$k^{(3)}(12,2) = -9\,k^{(3)}(9,3)$$

$$k^{(3)}(12,3) = -\frac{18}{43}k^{(3)}(9,8)$$

$$k^{(3)}(12,4) = -\frac{6}{43}k^{(3)}(9,8)$$

$$k^{(3)}(12,5) = \frac{9}{2} k^{(3)}(9,3)$$

$$k^{(3)}(12,6) = \frac{18}{43} k^{(3)}(9,8)$$

$$k^{(3)}(12,7) = \frac{6}{43} k^{(3)}(9,8)$$

$$k^{(3)}(12,8) = \frac{5}{2} k^{(3)}(11,9)$$

$$k^{(3)}(12,9) = - k^{(3)}(11,9)$$

$$k^{(3)}(12,10) = - k^{(3)}(11,8)$$

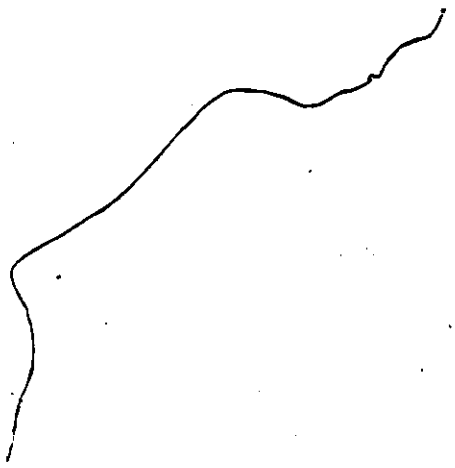

The stiffness matrix $[K^{(4)}]$ is

$k^{(4)}(1,1)$	$k^{(4)}(1,2)$	$k^{(4)}(1,3)$	$k^{(4)}(1,4)$	$k^{(4)}(1,5)$	$k^{(4)}(1,6)$	$k^{(4)}(1,7)$	$k^{(4)}(1,8)$	$k^{(4)}(1,9)$	$k^{(4)}(1,10)$
	$k^{(4)}(2,2)$	$k^{(4)}(2,3)$	$k^{(4)}(2,4)$	$k^{(4)}(2,5)$	$k^{(4)}(2,6)$	$k^{(4)}(2,7)$	$k^{(4)}(2,8)$	$k^{(4)}(2,9)$	$k^{(4)}(2,10)$
		$k^{(4)}(3,3)$	$k^{(4)}(3,4)$	$k^{(4)}(3,5)$	$k^{(4)}(3,6)$	$k^{(4)}(3,7)$	$k^{(4)}(3,8)$	$k^{(4)}(3,9)$	$k^{(4)}(3,10)$
			$k^{(4)}(4,4)$	$k^{(4)}(4,5)$	$k^{(4)}(4,6)$	$k^{(4)}(4,7)$	$k^{(4)}(4,8)$	$k^{(4)}(4,9)$	$k^{(4)}(4,10)$
				$k^{(4)}(5,5)$	$k^{(4)}(5,6)$	$k^{(4)}(5,7)$	$k^{(4)}(5,8)$	$k^{(4)}(5,9)$	$k^{(4)}(5,10)$
		(SYMMETRIC)			$k^{(4)}(6,6)$	$k^{(4)}(6,7)$	$k^{(4)}(6,8)$	$k^{(4)}(6,9)$	$k^{(4)}(6,10)$
						$k^{(4)}(7,7)$	$k^{(4)}(7,8)$	$k^{(4)}(7,9)$	$k^{(4)}(7,10)$
							$k^{(4)}(8,8)$	$k^{(4)}(8,9)$	$k^{(4)}(8,10)$
								$k^{(4)}(9,9)$	$k^{(4)}(9,10)$
									$k^{(4)}(10,10)$

(B.3)

where

$$k^{(4)}(1,1) = \frac{18A}{35a^3}$$

$$k^{(4)}(1,2) = -2\,k^{(4)}(1,1)$$

$$k^{(4)}(1,3) = \frac{9A}{70a^2}$$

$$k^{(4)}(1,4) = k^{(4)}(1,3)$$

$$k^{(4)}(1,5) = k^{(4)}(1,1)$$

$$k^{(4)}(1,6) = - k^{(4)}(1,3)$$

$$k^{(4)}(1,7) = - k^{(4)}(1,3)$$

$$k^{(4)}(1,8) = \frac{3A}{140a}$$

$$k^{(4)}(1,9) = 0$$

$$k^{(4)}(1,10) = k^{(4)}(1,8)$$

$$k^{(4)}(2,2) = 4\, k^{(4)}(1,1)$$

$$k^{(4)}(2,3) = - 2\, k^{(4)}(1,3)$$

$$k^{(4)}(2,4) = - 2\, k^{(4)}(1,3)$$

$$k^{(4)}(2,5) = - 2\, k^{(4)}(1,1)$$

$$k^{(4)}(2,6) = 2\, k^{(4)}(1,3)$$

$$k^{(4)}(2,7) = 2\, k^{(4)}(1,3)$$

$$k^{(4)}(2,8) = - 2\, k^{(4)}(1,8)$$

$$k^{(4)}(2,9) = 0$$

$$k^{(4)}(2,10) = - 2\, k^{(4)}(1,8)$$

$$k^{(4)}(3,3) = 4\, k^{(4)}(1,8)$$

$$k^{(4)}(3,4) = 0$$

$$k^{(4)}(3,5) = k^{(4)}(1,3)$$

$$k^{(4)}(3,6) = -4\,k^{(4)}(1,8)$$

$$k^{(4)}(3,7) = 0$$

$$k^{(4)}(3,8) = -\frac{A}{280}$$

$$k^{(4)}(3,9) = -2\,k^{(4)}(3,8)$$

$$k^{(4)}(3,10) = -k^{(4)}(3,8)$$

$$k^{(4)}(4,4) = 4\,k^{(4)}(1,8)$$

$$k^{(4)}(4,5) = k^{(4)}(1,3)$$

$$k^{(4)}(4,6) = 0$$

$$k^{(4)}(4,7) = -4\,k^{(4)}(1,8)$$

$$k^{(4)}(4,8) = -k^{(4)}(3,8)$$

$$k^{(4)}(4,9) = -2\,k^{(4)}(3,8)$$

$$k^{(4)}(4,10) = k^{(4)}(3,8)$$

$$k^{(4)}(5,5) = k^{(4)}(1,1)$$

$$k^{(4)}(5,6) = -k^{(4)}(1,3)$$

$$k^{(4)}(5,7) = -k^{(4)}(1,3)$$

$$k^{(4)}(5,8) = k^{(4)}(1,8)$$

$$k^{(4)}(5,9) = 0$$

$$k^{(4)}(5,10) = k^{(4)}(1,8)$$

$$k^{(4)}(6,6) = 4\, k^{(4)}(1,8)$$

$$k^{(4)}(6,7) = 0$$

$$k^{(4)}(6,8) = -\, k^{(4)}(3,8)$$

$$k^{(4)}(6,9) = 2\, k^{(4)}(3,8)$$

$$k^{(4)}(6,10) = k^{(4)}(3,8)$$

$$k^{(4)}(7,7) = 4\, k^{(4)}(1,8)$$

$$k^{(4)}(7,8) = k^{(4)}(3,8)$$

$$k^{(4)}(7,9) = 2\, k^{(4)}(3,8)$$

$$k^{(4)}(7,10) = -\, k^{(4)}(3,8)$$

$$k^{(4)}(8,8) = \frac{aA}{70}$$

$$k^{(4)}(8,9) = -\frac{1}{4}\, k^{(4)}(8,8)$$

$$k^{(4)}(8,10) = \frac{1}{12}\, k^{(4)}(8,8)$$

$$k^{(4)}(9,9) = \frac{1}{3}\, k^{(4)}(8,8)$$

$$k^{(4)}(9,10) = -\frac{1}{4}\, k^{(4)}(8,8)$$

$$k^{(4)}(10,10) = k^{(4)}(8,8)$$

The mass matrix $[M^{(2)}]$ is

$m^{(2)}(1,1)$	$m^{(2)}(1,2)$	$m^{(2)}(1,3)$	$m^{(2)}(1,4)$	$m^{(2)}(1,5)$	$m^{(2)}(1,6)$	$m^{(2)}(1,7)$	$m^{(2)}(1,8)$	$m^{(2)}(1,9)$	$m^{(2)}(1,10)$	$m^{(2)}(1,11)$	$m^{(2)}(1,12)$
	$m^{(2)}(2,2)$	$m^{(2)}(2,3)$	$m^{(2)}(2,4)$	$m^{(2)}(2,5)$	$m^{(2)}(2,6)$	$m^{(2)}(2,7)$	$m^{(2)}(2,8)$	$m^{(2)}(2,9)$	$m^{(2)}(2,10)$	$m^{(2)}(2,11)$	$m^{(2)}(2,12)$
		$m^{(2)}(3,3)$	$m^{(2)}(3,4)$	$m^{(2)}(3,5)$	$m^{(2)}(3,6)$	$m^{(2)}(3,7)$	$m^{(2)}(3,8)$	$m^{(2)}(3,9)$	$m^{(2)}(3,10)$	$m^{(2)}(3,11)$	$m^{(2)}(3,12)$
			$m^{(2)}(4,4)$	$m^{(2)}(4,5)$	$m^{(2)}(4,6)$	$m^{(2)}(4,7)$	$m^{(2)}(4,8)$	$m^{(2)}(4,9)$	$m^{(2)}(4,10)$	$m^{(2)}(4,11)$	$m^{(2)}(4,12)$
				$m^{(2)}(5,5)$	$m^{(2)}(5,6)$	$m^{(2)}(5,7)$	$m^{(2)}(5,8)$	$m^{(2)}(5,9)$	$m^{(2)}(5,10)$	$m^{(2)}(5,11)$	$m^{(2)}(5,12)$
	(SYMMETRIC)				$m^{(2)}(6,6)$	$m^{(2)}(6,7)$	$m^{(2)}(6,8)$	$m^{(2)}(6,9)$	$m^{(2)}(6,10)$	$m^{(2)}(6,11)$	$m^{(2)}(6,12)$
						$m^{(2)}(7,7)$	$m^{(2)}(7,8)$	$m^{(2)}(7,9)$	$m^{(2)}(7,10)$	$m^{(2)}(7,11)$	$m^{(2)}(7,12)$
							$m^{(2)}(8,8)$	$m^{(2)}(8,9)$	$m^{(2)}(8,10)$	$m^{(2)}(8,11)$	$m^{(2)}(8,12)$
								$m^{(2)}(9,9)$	$m^{(2)}(9,10)$	$m^{(2)}(9,11)$	$m^{(2)}(9,12)$
									$m^{(2)}(10,10)$	$m^{(2)}(10,11)$	$m^{(2)}(10,12)$
										$m^{(2)}(11,11)$	$m^{(2)}(11,12)$
											$m^{(2)}(12,12)$

(B.4)

where

$$m^{(2)}(1,1) = \frac{13aQ_1}{35} + \frac{13aQ_c}{140} + \frac{6I_1}{5aR_1^2} + \frac{13aI_c}{35t_c^2} + \frac{26aJ_1}{35R_1} - \frac{13aJ_c}{35t_c}$$

$$m^{(2)}(1,2) = \frac{9aQ_1}{70} + \frac{9aQ_c}{280} - \frac{6I_1}{5aR_1^2} + \frac{9aI_c}{70t_c^2} + \frac{9aJ_1}{35R_1} - \frac{9aJ_c}{70t_c}$$

$$m^{(2)}(1,3) = \frac{11a^2Q_1}{210} + \frac{11a^2Q_c}{840} + \frac{I_1}{10R_1^2} + \frac{11a^2I_c}{210t_c^2} + \frac{11a^2J_1}{105R_1} - \frac{11a^2J_c}{210t_c}$$

$$m^{(2)}(1,4) = -\frac{13a^2Q_1}{420} - \frac{13a^2Q_c}{1680} + \frac{I_1}{10R_1^2} - \frac{13a^2I_c}{420t_c^2} - \frac{13a^2J_1}{210R_1} + \frac{13a^2J_c}{420t_c}$$

$$m^{(2)}(1,5) = \frac{13aQ_c}{140} - \frac{13aI_c}{35t_c^2}$$

$$m^{(2)}(1,6) = \frac{9aQ_c}{280} - \frac{9aI_c}{70t_c^2}$$

$$m^{(2)}(1,7) = \frac{11a^2Q_c}{840} - \frac{11a^2I_c}{210t_c^2}$$

$$m^{(2)}(1,8) = -\frac{13a^2Q_c}{1680} + \frac{13a^2I_c}{420t_c^2}$$

$$m^{(2)}(1,9) = \frac{(h_1 - h_2)Q_c}{8} - \frac{6I_1}{5aR_1} + \frac{(h_1 + h_2)I_c}{2t_c^2} + \frac{J_1}{2} - \frac{h_1J_c}{2t_c}$$

$$m^{(2)}(1,10) = -m^{(2)}(1,9)$$

$$m^{(2)}(1,11) = -\frac{a(h_1 - h_2)Q_c}{40} - \frac{I_1}{10R_1} - \frac{a(h_1 + h_2)I_c}{10t_c^2} - \frac{aJ_1}{10} + \frac{ah_1J_c}{10t_c}$$

$$m^{(2)}(1,12) = \frac{a(h_1 - h_2)Q_c}{40} - \frac{I_1}{10R_1} + \frac{a(h_1 + h_2)I_c}{10t_c^2} + \frac{aJ_1}{10} - \frac{ah_1J_c}{10t_c}$$

$$m^{(2)}(2,2) = m^{(2)}(1,1)$$

$$m^{(2)}(2,3) = -m^{(2)}(1,4)$$

$$m^{(2)}(2,4) = -m^{(2)}(1,3)$$

$$m^{(2)}(2,5) = m^{(2)}(1,6)$$

$$m^{(2)}(2,6) = m^{(2)}(1,5)$$

$$m^{(2)}(2,7) = -m^{(2)}(1,8)$$

$$m^{(2)}(2,8) = -m^{(2)}(1,7)$$

$$m^{(2)}(2,9) = \frac{(h_1 - h_2)Q_c}{8} + \frac{6I_1}{5aR_1} + \frac{(h_1 + h_2)I_c}{2t_c^2} + \frac{J_1}{2} - \frac{h_1 J_c}{2t_c}$$

$$m^{(2)}(2,10) = -m^{(2)}(2,9)$$

$$m^{(2)}(2,11) = -m^{(2)}(1,11)$$

$$m^{(2)}(2,12) = -m^{(2)}(1,12)$$

$$m^{(2)}(3,3) = \frac{a^3 Q_1}{105} + \frac{a^3 Q_c}{420} + \frac{2aI_1}{15R_1^2} + \frac{a^3 I_c}{105t_c^2} + \frac{2a^3 J_1}{105R_1} - \frac{a^3 J_c}{105t_c}$$

$$m^{(2)}(3,4) = -\frac{a^3 Q_1}{140} - \frac{a^3 Q_c}{560} - \frac{aI_1}{30R_1^2} - \frac{a^3 I_c}{140t_c^2} - \frac{a^3 J_1}{70R_1} + \frac{a^3 J_c}{140t_c}$$

$$m^{(2)}(3,5) = m^{(2)}(1,7)$$

$$m^{(2)}(3,6) = -m^{(2)}(1,8)$$

$$m^{(2)}(3,7) = \frac{a^3 Q_c}{420} - \frac{a^3 I_c}{105t_c^2}$$

$$m^{(2)}(3,8) = -\frac{a^3 Q_c}{560} + \frac{a^3 I_c}{140t_c^2}$$

$$m^{(2)}(3,9) = m^{(2)}(1,12)$$

$$m^{(2)}(3,10) = -m^{(2)}(1,12)$$

$$m^{(2)}(3,11) = -\frac{2aI_1}{15R_1}$$

$$m^{(2)}(3,12) = \frac{a^2(h_1 - h_2)Q_c}{240} + \frac{aI_1}{30R_1} + \frac{a^2(h_1 + h_2)I_c}{60t_c^2} + \frac{a^2J_1}{60} - \frac{a^2h_1J_c}{60t_c}$$

$$m^{(2)}(4,4) = m^{(2)}(3,3)$$

$$m^{(2)}(4,5) = m^{(2)}(1,8)$$

$$m^{(2)}(4,6) = -m^{(2)}(1,7)$$

$$m^{(2)}(4,7) = m^{(2)}(3,8)$$

$$m^{(2)}(4,8) = m^{(2)}(3,7)$$

$$m^{(2)}(4,9) = m^{(2)}(1,11)$$

$$m^{(2)}(4,10) = -m^{(2)}(1,11)$$

$$m^{(2)}(4,11) = -\frac{a^2(h_1 - h_2)Q_c}{240} + \frac{aI_1}{30R_1} - \frac{a^2(h_1 + h_2)I_c}{60t_c^2} - \frac{a^2J_1}{60} + \frac{a^2h_1J_c}{60t_c}$$

$$m^{(2)}(4,12) = m^{(2)}(3,11)$$

$$m^{(2)}(5,5) = \frac{13aQ_2}{35} + \frac{13aQ_c}{140} + \frac{6I_2}{5aR_2^2} + \frac{13aI_c}{35t_c^2} + \frac{26aJ_2}{35R_2} + \frac{13aJ_c}{35t_c}$$

$$m^{(2)}(5,6) = \frac{9aQ_2}{70} + \frac{9aQ_c}{280} - \frac{6I_2}{5aR_2^2} + \frac{9aI_c}{70t_c^2} + \frac{9aJ_2}{35R_2} + \frac{9aJ_c}{70t_c}$$

$$m^{(2)}(5,7) = \frac{11a^2Q_2}{210} + \frac{11a^2Q_c}{840} + \frac{I_2}{10R_2^2} + \frac{11a^2I_c}{210t_c^2} + \frac{11a^2J_2}{105R_2} + \frac{11a^2J_c}{210t_c}$$

$$m^{(2)}(5,8) = -\frac{13a^2Q_2}{420} - \frac{13a^2Q_c}{1680} + \frac{I_2}{10R_2^2} - \frac{13a^2I_c}{420t_c^2} - \frac{13a^2J_2}{210R_2} - \frac{13a^2J_c}{420t_c}$$

$$m^{(2)}(5,9) = \frac{(h_2 - h_2)Q_c}{8} - \frac{6I_2}{5aR_2} - \frac{(h_1 + h_2)I_c}{2t_c^2} + \frac{J_2}{2} - \frac{h_2J_c}{2t_c}$$

$$m^{(2)}(5,10) = -m^{(2)}(5,9)$$

$$m^{(2)}(5,11) = -\frac{a(h_1 - h_2)Q_c}{40} - \frac{I_2}{10R_2} + \frac{a(h_1 + h_2)I_c}{10t_c^2} - \frac{aJ_2}{10} + \frac{ah_2J_c}{10t_c}$$

$$m^{(2)}(5,12) = \frac{a(h_1 - h_2)Q_c}{40} - \frac{I_2}{10R_2} - \frac{a(h_1 + h_2)I_c}{10t_c^2} + \frac{aJ_2}{10} - \frac{ah_2J_c}{10t_c}$$

$$m^{(2)}(6,6) = m^{(2)}(5,5)$$

$$m^{(2)}(6,7) = -m^{(2)}(5,8)$$

$$m^{(2)}(6,8) = -m^{(2)}(5,7)$$

$$m^{(2)}(6,9) = \frac{(h_1 - h_2)Q_c}{8} + \frac{6I_2}{5aR_2} - \frac{(h_1 + h_2)I_c}{2t_c^2} + \frac{J_2}{2} - \frac{h_2J_c}{2t_c}$$

$$m^{(2)}(6,10) = -m^{(2)}(6,9)$$

$$m^{(2)}(6,11) = -m^{(2)}(5,11)$$

$$m^{(2)}(6,12) = -m^{(2)}(5,12)$$

$$m^{(2)}(7,7) = \frac{a^3Q_2}{105} + \frac{a^3Q_c}{420} + \frac{2aI_2}{15R_2^2} + \frac{a^3I_c}{105t_c^2} + \frac{2a^3J_2}{105R_2} + \frac{a^3J_c}{105t_c}$$

$$m^{(2)}(7,8) = -\frac{a^3Q_2}{140} - \frac{a^3Q_c}{560} - \frac{aI_2}{30R_2^2} - \frac{a^3I_c}{140t_c^2} - \frac{a^3J_2}{70R_2} - \frac{a^3J_c}{140t_c}$$

$$m^{(2)}(7,9) = m^{(2)}(5,12)$$

$$m^{(2)}(7,10) = -m^{(2)}(5,12)$$

$$m^{(2)}(7,11) = -\frac{2aI_2}{15R_2}$$

$$m^{(2)}(7,12) = \frac{a^2(h_1 - h_2)Q_c}{240} + \frac{aI_2}{30R_2} - \frac{a^2(h_1 + h_2)I_c}{60t_c^2} + \frac{a^2J_2}{60} - \frac{a^2h_2J_c}{60t_c}$$

$$m^{(2)}(8,8) = m^{(2)}(7,7)$$

$$m^{(2)}(8,9) = m^{(2)}(5,11)$$

$$m^{(2)}(8,10) = -m^{(2)}(5,11)$$

$$m^{(2)}(8,11) = -\frac{a^2(h_1 - h_2)Q_c}{240} + \frac{aI_2}{30R_2} + \frac{a^2(h_1 + h_2)I_c}{60t_c^2} - \frac{a^2J_2}{60} + \frac{a^2h_2J_c}{60t_c}$$

$$m^{(2)}(8,12) = m^{(2)}(7,11)$$

$$m^{(2)}(9,9) = \frac{13aQ_1}{35} + \frac{13aQ_2}{35} + \left(\frac{13a}{35} + \frac{3(h_1 - h_2)^2}{10a}\right)Q_c + \frac{6I_1}{5a} + \frac{6I_2}{5a}$$

$$+ \frac{6(h_1 + h_2)^2I_c}{5at_c^2} - \frac{6(h_1^2 - h_2^2)J_c}{5at_c}$$

$$m^{(2)}(9,10) = \frac{9aQ_1}{70} + \frac{9aQ_2}{70} + \left(\frac{9a}{70} - \frac{3(h_1 - h_2)^2}{10a}\right)Q_c - \frac{6I_1}{5a} - \frac{6I_2}{5a}$$

$$- \frac{6(h_1 + h_2)^2I_c}{5at_c^2} + \frac{6(h_1^2 - h_2^2)J_c}{5at_c}$$

$$m^{(2)}(9,11) = \frac{11a^2Q_1}{210} + \frac{11a^2Q_2}{210} + \left(\frac{11a^2}{210} + \frac{(h_1 - h_2)^2}{40}\right)Q_c + \frac{I_1}{10} + \frac{I_2}{10}$$

$$+ \frac{(h_1 + h_2)^2 I_c}{10t_c^2} - \frac{(h_1^2 - h_2^2)J_c}{10t_c}$$

$$m^{(2)}(9,12) = -\frac{13a^2Q_1}{420} - \frac{13a^2Q_2}{420} - \left(\frac{13a^2}{420} - \frac{(h_1 - h_2)^2}{40}\right)Q_c + \frac{I_1}{10} + \frac{I_2}{10}$$

$$+ \frac{(h_1 + h_2)^2 I_c}{10t_c^2} - \frac{(h_1^2 - h_2^2)J_c}{10t_c}$$

$$m^{(2)}(10,10) = m^{(2)}(9,9)$$

$$m^{(2)}(10,11) = -m^{(2)}(9,12)$$

$$m^{(2)}(10,12) = -m^{(2)}(9,11)$$

$$m^{(2)}(11,11) = \frac{a^3Q_1}{105} + \frac{a^3Q_2}{105} + \left(\frac{a^3}{105} + \frac{a(h_1 - h_2)^2}{30}\right)Q_c + \frac{2aI_1}{15} + \frac{2aI_2}{15}$$

$$+ \frac{2a(h_1 + h_2)^2 I_c}{15t_c^2} - \frac{2a(h_1^2 - h_2^2)J_c}{15t_c}$$

$$m^{(2)}(11,12) = -\frac{a^3Q_1}{140} - \frac{a^3Q_2}{140} - \left(\frac{a^3}{140} + \frac{a(h_1 - h_2)^2}{120}\right)Q_c - \frac{aI_1}{30} - \frac{aI_2}{30}$$

$$- \frac{a(h_1 + h_2)^2 I_c}{30t_c^2} + \frac{a(h_1^2 - h_2^2)J_c}{30t_c}$$

$$m^{(2)}(12,12) = m^{(2)}(11,11)$$

VITA AUCTORIS

1957 Born in Pematang Siantar, Indonesia, on September 15.

1978 In June, finished the Secondary High School at St. Basil The Great College High School, Toronto. In September, enrolled in the Faculty of Engineering, University of Windsor, Windsor, Ontario.

1982 In May, graduated from The University of Windsor, with the degree of Bachelor of Applied Science in Civil Engineering and enrolled at The University of Windsor as a candidate for the degree of Master of Applied Science in Civil Engineering.